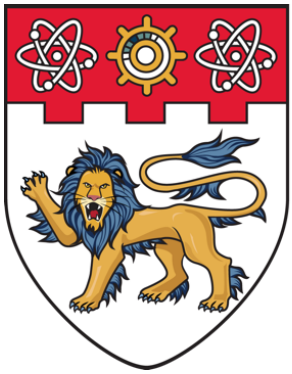

NANYANG TECHNOLOGICAL UNIVERSITY

SINGAPORE

PART I: COBALT-CATALYZED C–H BENZYLATION OF ARENES

PART II: HYPERVALENT IODINE-MEDIATED REARRANGEMENT OF PROPARGYLIC ALCOHOLS

LASKAR ROSHAYED ALI

SCHOOL OF PHYSICAL AND MATHEMATICAL SCIENCES

2021

PART I: COBALT-CATALYZED C–H BENZYLATION OF ARENES

PART II: HYPERVALENT IODINE-MEDIATED REARRANGEMENT OF PROPARGYLIC ALCOHOLS

LASKAR ROSHAYED ALI

SCHOOL OF PHYSICAL AND MATHEMATICAL SCIENCES

A thesis submitted to the Nanyang Technological University in partial fulfilment of the requirement for the degree of Doctor of Philosophy

2021

Dedicated to my grandparents

and

my teacher late Dr. Dinabandhu Kundu

Statement of Originality

I hereby certify that the work embodied in this thesis is the result of original research done by me except where otherwise stated in this thesis. The thesis work has not been submitted for a degree or professional qualification to any other university or institution. I declare that this thesis is written by myself and is free of plagiarism and of sufficient grammatical clarity to be examined. I confirm that the investigations were conducted in accord with the ethics policies and integrity standards of Nanyang Technological University and that the research data are presented honestly and without prejudice.

21 June 2021

. . . . . .

Date

. . . . . .

Laskar Roshayed Ali

Supervisor Declaration Statement

I have reviewed the content and presentation style of this thesis and declare it of sufficient grammatical clarity to be examined. To the best of my knowledge, the thesis is free of plagiarism and the research and writing are those of the candidate's except as acknowledged in the Author Attribution Statement. I confirm that the investigations were conducted in accord with the ethics policies and integrity standards of Nanyang Technological University and that the research data are presented honestly and without prejudice.

[21 June 2021]

. . . . . .

Date

. . . . . .

Shunsuke Chiba

Authorship Attribution Statement

*This thesis contains material from (1 number) paper(s) published in the following peer-reviewed journal(s) / from papers accepted at conferences in which I am listed as an author.

Chapter 2 is published as Laskar, R. A., Yoshikai, N. Cobalt-Catalyzed N–H Imine-Directed Arene C–H Benzylation with Benzyl Phosphates. *The Journal of Organic Chemistry* **2019**, *84*, 13172-13178**.** DOI: 10.1021/acs.joc.9b01775.

The contributions of the co-authors are as follows:

- Prof. Yoshikai given the project and edited manuscript drafts.
- The laboratory work, analysis of data, and preparation of SI was done my me.

Chapter 4 is submitted as Laskar, R. A., Ding, W., Yoshikai, N. Iodo(III)-Meyer–Schuster Rearrangement of Propargylic Alcohols Promoted by Benziodoxole Triflate (under revision in *Organic Letters*).

The contributions of the co-authors are as follows:

- Prof. Yoshikai given the project and edited manuscript drafts, and corrected supporting information.
- Dr. Ding Wei found the initial result of the project and characterized the model product by NMR spectroscopy and X-ray crystallography. He also performed the ^{18}O labeling experiment and helped me to optimize the reaction conditions.
- I did exploration of the substrate scope, data analysis, manuscript as well as SI draft preparation.

[8 January 2021]

. . . . . .

Date

. . . . . .

[Laskar Roshayed Ali]

Abstract

1,1-Diarylmethanes represent as integral structural moieties that are present in pharmaceutical and biologically active molecules. Thus, the synthetic community has been continuously searching for an efficient and practical method to access these scaffolds. In this regard, a synthetic protocol utilizing directing-group assisted arene C–H functionalization represents an attractive alternative to traditional methods because of the atom- and step-economy of the process as well as controllable regioselectivity. Particularly, C–H benzylation using benzylic electrophile has been well explored using either precious 4d/5d-transition metal-based catalytic system or earth-abundant and cheap 3d-transition metal-based system. Among the first-row transition metals, cobalt-based catalytic systems showed the capabilities to emulate the reactivity of its higher congener congeners as well as distinct reactivity.

With the above background, Chapter 1 describes a brief review of a different kind of C–H functionalization reactions that have been achieved using low-valent cobalt-based systems. Building on this background, Chapter 2 is mainly focused on what are the traditional approaches to access diarylmethanes and how we used the directed C–H functionalization approach using a low-valent cobalt system to synthesize diarylmethanes. In our developed synthetic protocol, we used benzylic phosphates and pivalophenone N–H imines as starting materials, and a cobalt salt-ligand-Grignard reagent based catalytic system to successfully prepare diarylmethane derivatives under room-temperature conditions.

Chapter 3 and Chapter 4 of the thesis deal with completely different chemistry. In Chapter 3, a glimpse of the recent development of cyclic hypervalent iodine reagents and their applications in synthetic organic chemistry is described with special focus on the heteroaryl- and vinyl-benziodoxol(on)es. Benziodoxol(on)es (BX) are generally

bench-stable polyvalent iodine compounds bearing 5-membered heterocyclic scaffolds where the iodine atom is part of the ring. Some of this type of compounds have already proved to serve as useful group transfer reagents, and much effort has been devoted to the development of new BX-type reagents to expand the scope of transferable groups, including aryl and vinyl groups. Chapter 4 shows how we synthesized a novel class of vinyl-benziodoxole derivatives starting from easily accessible propargylic alcohols and benziodoxole triflate using the concept of century-old Meyer-Schuster rearrangement. These vinyl-BXs are air-stable, easy to handle, and have already proven to act as enone building blocks for traditional cross-coupling reactions.

Acknowledgments

I would like to express my deepest gratitude to my previous supervisor, Associate Professor Naohiko Yoshikai for his valuable guidance, moral support throughout the journey, and his patience on the corrections, from manuscript draft to the thesis.

I wish to extend my thanks to my current supervisor Professor Shunsuke Chiba for his kind help and support in the last phase of my Ph.D. In addition, I want to thank my TAC member Prof. Liu Xuewei and Prof. Ge Shaozhong for their help and support. Furthermore, I have borrowed chemicals many times from Prof. Chiba's lab, mainly from Dhika, Derek, and Wang Bin, and it helped me a lot. Thank you very much, Prof. Chiba and his group members. I am also thankful to all of Dr. Yoshikai's group members for their discussion, help, and friendship over this time, especially to Dr. Xu Wengang for the mentorship in my first year of Ph.D. and Dr. Ding for helping me with the hypervalent iodine project. I also wish to extend my thanks to all the staff in CBC central facility, mainly to Ee-Ling Goh in the NMR laboratory and Wen-Wei Zhu in the Mass spectrometry laboratory. I would like to thank NTU for providing me the four-year scholarship to facilitate me to finish my Ph.D. study in world-class university.

Lastly, I would like to give my deepest gratitude to my parents, Mohasin Laskar and Runa Layala Laskar, and my siblings, Rustam and Meherunnesa for their love and support.

Table of Contents

Abstract 1

Acknowledgements 3

Table of Contents 4

List of Abbreviations 6

Chapter 1 Low-Valent Cobalt-Catalyzed C–H Functionalization **9**

1.1 Introduction 9

1.1.1 Hydroarylation of Alkynes 15

1.1.2 Hydroarylation of Olefins 18

1.1.3 C–H/Electrophile Coupling 21

1.1.4 Hydroacylation Reaction 24

1.2. References 28

Chapter 2 Cobalt-Catalyzed, N−H Imine-Directed Arene C−H Benzylation with Benzyl Phosphates **31**

2.1 Introduction 32

2.1.1 Friedel-Crafts Benzylation 32

2.1.2 Transition Metal Catalyzed Cross-Coupling Reaction 34

2.1.3 Cross-Electrophile Coupling 35

2.1.4 Direct C–H Benzylation of Arenes 37

2.1.5 Design of the Work 39

2.2 Result And Discussion 41

2.3 Conclusion 51

2.4 Experimental Section 51

2.5 References 63

Chapter 3 Synthesis and Application of Aryl-, Heteroaryl-, and Vinyl-BX Reagents 65

3.1 Introduction 65

3.2 Aryl- and Heteroaryl-BX 66

3.2.1 Synthesis of Aryl-BX and Heteroaryl-BX 66

3.2.2 Synthetic Application of Heteroaryl-BX 70

3.3 Vinyl-BX 73

3.3.1 Synthesis of Vinyl-BX 73

3.3.2 Synthetic Application of Vinyl-BX 76

3.4 Future Outlook 80

3.5 References 81

Chapter 4 Iodo(III)-Meyer-Schuster Rearrangement of Propargylic Alcohols Promoted by Benziodoxole Triflate 83

4.1 Introduction 83

4.1.2 Design of the Work 93

4.2 Result and Discussion 94

4.3 Conclusion 100

4.4 Experimental Section 101

4.5 References 128

List of Publication 131

List of Abbreviations

δ	chemical shift (ppm)
°C	degree centigrade
Ac	acetyl
Ar	aryl (substituted aromatic ring)
aq	aqueous
br	broad
Bn	benzyl
Boc	*tert*-butyloxycarbonyl
*t*Bu	*tert*-butyl
cod	1,5-cyclooctadiene
coe	cyclooctene
Cp*	1,2,3,4,5-pentamethylcyclopentadienyl
Cy	cyclohexyl
d	doublet
dd	doublet of doublet
dt	doublet of triplet
dppe	1,2-bis(diphenylphosphino)ethane
dppf	1,1'-bis(diphenylphosphino)ferrocene
dppp	1,3-bis(diphenylphosphino)propane
ESI	electrospray ionization
eq /equiv.	equivalent
EtOAc	ethyl acetate
Et	ethyl

g	gram
h	hour
H	hydrogen
HRMS	high resolution mass spectrometry
Hz	hertz
J	coupling constants
m	multiple
m/z	mass per charge ratio
M	concentration (mol/L)
M^+	parent ion peak (mass spectrum)
Me	methyl
mg	milligram
MHz	mega hertz
min	minute
mL	milliliter
mmol	millimole
m.p.	melting point
NMR	nuclear magnetic resonance
PMP	*p*-methoxylphenyl
ppm	parts per million
q	quartet
s	singlet
sat	saturated
rt/r.t.	room temperature
t	triplet

td	triplet of doublet
Tf	trifluoromethyl
THF	tetrahydrofuran
TLC	thin layer chromatography
TMS	trimethylsilyl
Ts	*p*-toluenesulfonyl
p-TSA	*p*-toluenesulfonic acid
vol	volume

Chapter 1. Low-Valent Cobalt-Catalyzed C–H Functionalization

1.1 Introduction

Transition metal-catalyzed cross-coupling reactions between organic electrophiles and organometallic nucleophiles are among the most widely used methods to construct carbon-carbon bonds.[1] Nevertheless, the requirement for pre-functionalized starting materials as well as the generation of stoichiometric waste byproducts represent serious limitations of the cross-coupling reaction. To address these issues related to the cross-coupling reaction extensive efforts have been devoted on the development of transition metal-catalyzed C–H bond activation, which would offer a step and atom-economical alternative approach for carbon-carbon bond formation from readily accessible, unfunctionalized starting materials. Two of the major challenges associated with this strategy are a) high bond dissociation energies of most of the C–H bonds and b) site-selective activation of a specific C–H bond over other C–H bonds in a given molecule. One of the most widely employed approaches to achieve efficient and site-selective C–H activations is the installation of, a heteroatom directing group, which would assist a transition metal catalyst to activate the proximal C–H bond to form a five- or six-membered metallacycle intermediate. One of the early example of directing group assisted C–H functionalization was reported by Murahashi.[2] Thus, using Co_2CO_8 as catalyst phthalimidines were synthesized form Schiff bases utilizing concept of cyclometallation (Scheme 1.1a). Later on Murai and coworkers reported a ruthenium-catalyzed directed alkylation of aromatic ketones with olefins such as vinyl silane (Scheme 1.1b).[3] Since then, numerous C–C and C–heteroatom bond-forming reactions C–H activation have been developed. Despite the significant

progress, the majority of directed C–H functionalization reaction have relied on precious second- and third-row transition metals.

Scheme 1.1. Early examples of directed C–H functionalization

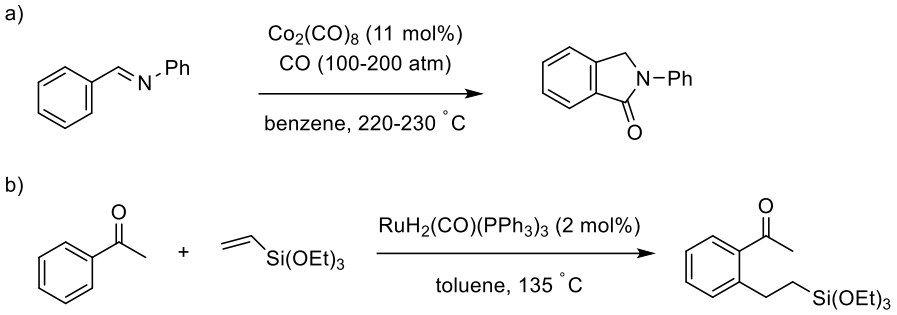

In the following some representative examples of second and third-row transition metal-catalyzed directed C–H functionalization are given. Genet et al. reported directed *ortho*-alkylation of aromatic ketones involving ruthenium-based catalytic system.[4] A catalytic system comprised of $[Ru(p\text{-cymene})Cl_2\}_2]_2$, triphenyl phosphine ligand and formate salt effectively catalyzed ortho-C–H functionalization of ketone to furnish hydroarylated products in excellent yields (Scheme 1.2a). In 2013, Ackermann and coworkers utilized similar catalytic system to perform hydroarylation of heteroarenes with olefins using pyridine and pyrimidyl directing group (Scheme 1.2b). [5]

Scheme 1.2. Ruthenium catalyzed directed C–H functionalization

a)

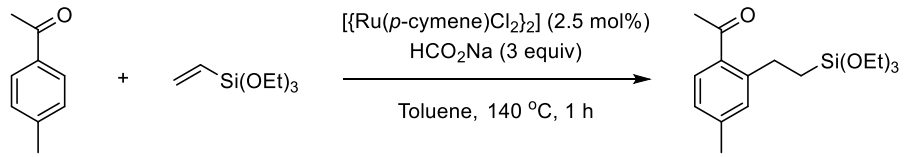

b)

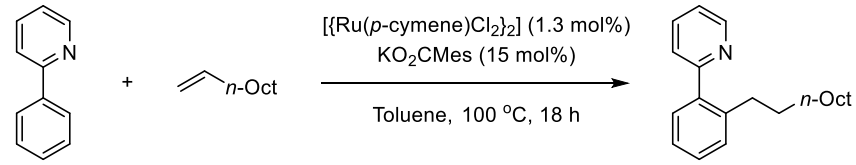

On the other hand, Jun et al. first reported imine directed-ortho alkylation of aromatic ketimine with activated olefin using Wilkinson's catalyst (Scheme 1.3a).[6] Recently, Chatani et al. reported a Rh-catalyzed alkylation of styrene derivative using a bidentate 8-aminoquinoline directing group (Scheme 1.3b).[7] The catalytic system comprised of a Rh(I) precatalyst and pivalic acid promoted the ortho-alkylation of benzamide derivatives with tolerance to various functional groups such as methoxy, fluoro, acetate, and trifluoromethyl to give the linear hydroarylation product. The presence of the amide N–H and the quinoline nitrogen atom proved crucial for the alkylation.

Scheme 1.3. Rh-catalyzed hydroarylation of olefins

a)

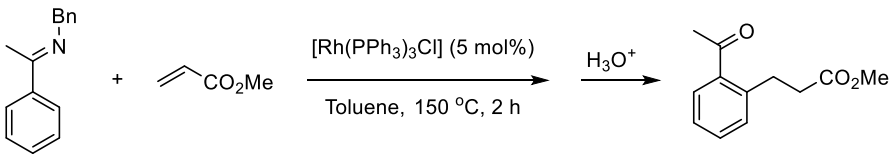

b)

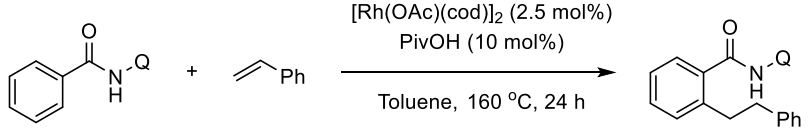

In light of the directed hydroarylation reaction, third-row transition metal iridium showed good capability to promote C–H functionalization reactions. Iridium(I) complexes have emerged as competent rare metal catalysts for the chelation-assisted olefin hydroarylation. In 2012, Shibata and coworkers reported C-2 selective alkylation of indole with styrenes using cationic Ir-diphosphine catalysts (Scheme 1.4).[8] Interestingly, the linear/branched selectivity of the reaction was controlled by the choice of the N-protecting group on the indole substrate and the supporting diphosphine ligand. A preliminary result of an enantioselective variant of the branched-selective hydroarylation was also reported, albeit with a moderate ee value.

Scheme 1.4. Ir(I)-catalyzed hydroarylation of indoles

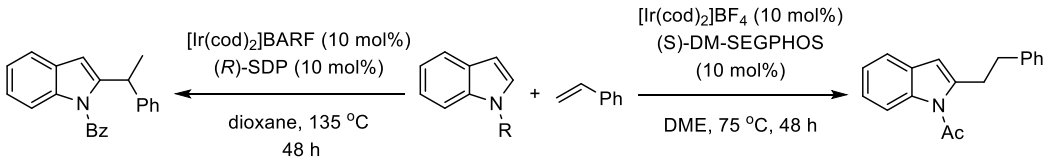

Bower and coworkers achieved branched-selective hydrorylation of 1-alkenes with *N*, *N*-diethylbenzamide based on a "cooperative destabilization" strategy (Scheme 1.5).[9] Analysis of a putative catalytic cycle promoted them to hypothesize that a diphosphine ligand of a wider bite angle and lower electro-donating ability would facilitate the reductive elimination step leading to a branched product. Along this hypothesis, a novel polyfluorinated diphosphine, d^Fppb, was identified as an effective ligand to promate the amide-directed hydroarylation of general 1-alenes with high branched selectivity (>25:1 branched:linear). The scope of the new catalytic system was extended to acetanilides.

Scheme 1.5. Branched-selective hydroarylation using Ir-catalyst

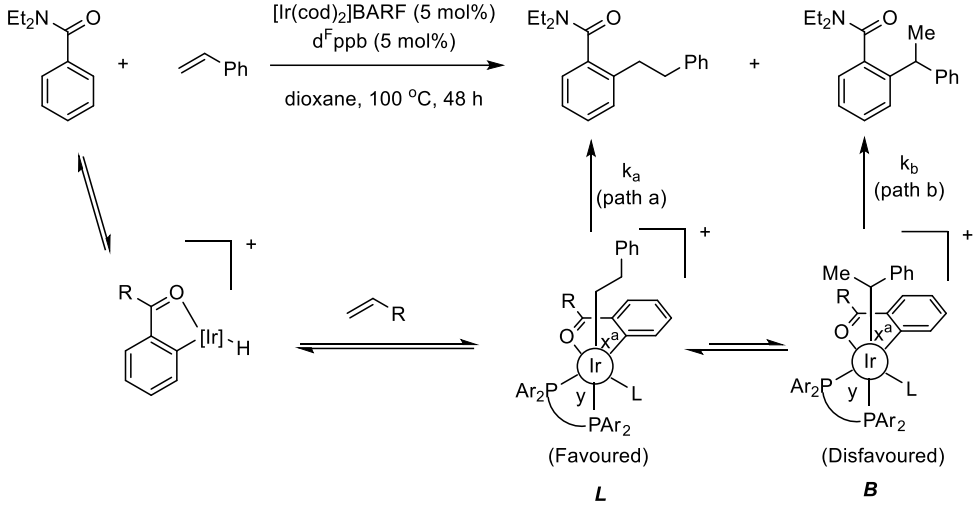

In 2015, Nishimura et al. reported iridium-catalyzed branched-selective hydroarylation of vinyl ethers with 2-arylpyridines (Scheme 1.6). [10] The reaction was achieved using a cationic iridium catalyst generated from $[IrCl(cod)]_2$ and $NaBAr^F$ under relatively mild conditions. Mechanistic experiments revealed that the branched selectivity originated from preferential reductive elimination of a branched alkyliridium intermediate rather than linear alkyliridium intermediate.

Scheme 1.6. Ir-catalyzed hydroarylation of vinyl ether

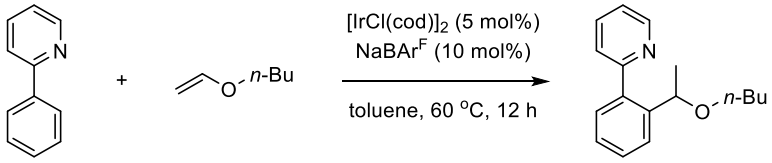

Given this background, the development of the C–H functionalization catalyzed by first row transition metals is highly desirable. Among the first row transition metals, cobalt has gradually become the choice for directed C–H functionalization. [11]In an early study, Klein and coworkers reported cyclometallation reaction of azobenzene with

$Co(Me)(PMe_3)_4$ under mild reaction conditions (Scheme 1.7a).[12] The plausible reaction pathway includes oxidative addition of *ortho*-C–H bond with assistant to azo group followed by reductive elimination of methane. After that, several other cobalt complexes showed the capabilities of cyclometallation of $C(sp^2)$–H and $C(sp^3)$–H bonds with different directing groups. Kisch reported *ortho*-alkenylation of azobenzene derivatives using $Co(H)(N_2)(PPh_3)_3$ or $CoH_3(PPh_3)_3$ catalysts demonstrating further indication of potential utility of cobalt in C–H functionalization reaction (Scheme 1.7b).[13]

Scheme 1.7. Azo-group assisted cyclometallation with cobalt complex

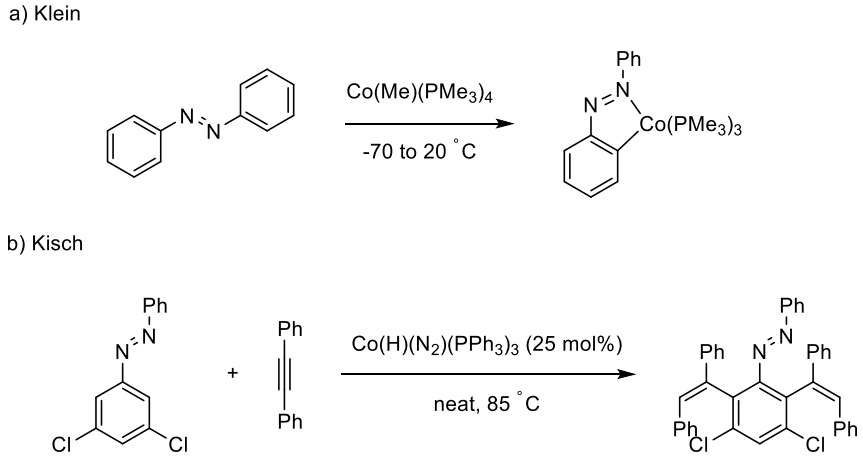

Inspired by above seminal works, Yoshikai group have hypothesized two catalytic cycles for low-valent cobalt-catalyzed directed C–H functionalization of arenes (cycle A) and another for cross-coupling between an electrophile and C–H bond (cycle B) (Scheme 1.8).[14] For catalytic cycle **A**, an in-situ generated organocobalt species $Co(R)L_n$ (**1**) would undergo oxidative addition of ortho C–H bond to generate a cobaltacycle species **2**. Next, migratory insertion of alkyne or alkene would takes

place to species **2**, followed by reductive elimination of diorganocobalt species **3** to give hydroarylation product and regeneration of **1**.

In catalytic cycle **B**, the first step is same as cycle **A**, but in the second step reductive elimination would take place to generate a new low-valent metallacycle **4**. Finally an electrophile would be intercepted by the species **4** to give a C–C coupling product and a cobalt halide species **5**. At last, transmetalation between an organometallic reagent R–M and the species **5** would regenerate species the **1**. Based on the above hypothesis Yoshikai and coworkers have developed a series of cobat-catalyzed C–H functionalizations. In addition, Nakamura, Ackermann and others also made significant contribution to this field.

Scheme 1.8. Hypothetical catalytic cycles for hydroarylation (cycle A) and C–H/electrophile coupling (cycle B).

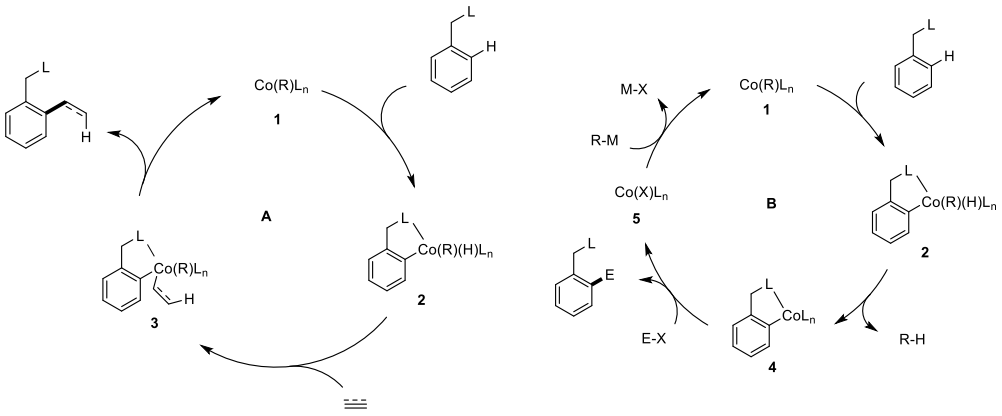

1.1.1 Hydroarylation of Alkynes

In 2010, first example of low-valent cobalt-catalyzed hydroarylation reaction was reported by Yoshikai et al. In this work, a ternary catalytic system consisting of a cobalt salt, a phosphine ligand and a Grignard reagent promoted hydroarylation reaction internal alkyne to 2-phenyl pyridine with high efficiency (Scheme 1.9a).[15] This reaction

complements the use of Wilkinson catalyst in this kind of transformation demonstrating reactivity of Rh(I) can be emulate by cobalt catalyst with proper tuning.[16] Later the same group extended the scope of hydroarylation reaction to wide range of substrates. For example, a catalytic system consists of $CoBr_2$, 2-(diphenylphosphinoethyl)pyridine (pyphos), and neopentyl magnesium bromide catalyzed addition of *N*-pyrimidylindole with a range of internal alkynes at room temperature (Scheme 1.9b).[17] In addition to 2-phenylpyridine and indole, low-valent cobalt-based catalytic system promoted hydroarylation of alkynes with azole was also reported by Yoshikai and coworkers. Thus, *in situ* generated active catalyst from cobalt salt, ligand and $Me_3SiMgCl$ furnished C2-alkenylations of azole in syn-selective fashion (Scheme 1.9c).[18]

Scheme 1.9. Co-catalyzed hydroarylation of internal alkyne with 2-phenyl pyridine, indole and azole

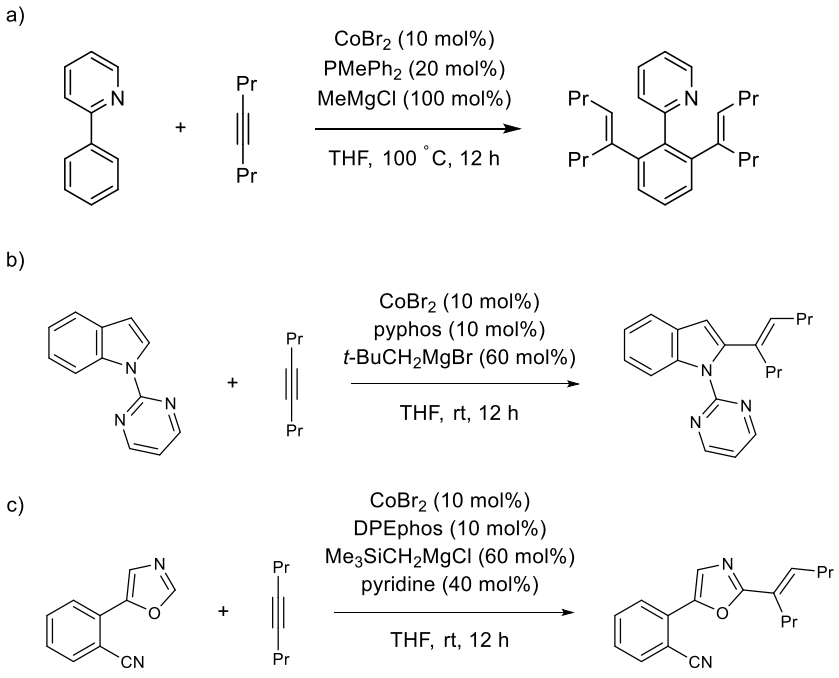

Furthermore, aryl ketimine derived from acetophenone and para-anisidine was successfully underwent ortho-hydroarylation reaction with diarylalkyne using $CoBr_2$,

$P(3\text{-}ClC_6H_4)_3$, *t*$BuCH_2MgBr$ based catalytic system under room temperature (Scheme 1.9b).[19] Interestingly, *ortho*-hydroarylation reaction was also amenable to unsymmetrical alkyne in regioselective manner where C–C bond formation was taken place between ketimine and less hindered acetylenic carbon. In their subsequent work, Yoshikai et al. extended the scope for *ortho*-alkenylation reaction to wide range of substrates including aryl adimines,[20] and α,β-unsaturated ketimines.[21] A plausible catalytic cycle for imine directed hydroarylation was proposed based on the mechanistic investigation (Scheme 1.10). At first, neopentylmagnesium bromide would act as reductant to generate catalytically active low-valent cobalt species, subsequently alkyne coordination to metal center in reversible manner, followed by rate limiting oxidative addition of *ortho*-C–H bond. Subsequently, alkyne insertion into Co–H bond and reductive elimination would produce *ortho*-alkenylation product. Notably, Petit et al. also achieved ortho-hydroarylation with aryl ketimine and alkyne using $Co(PMe_3)_4$ complex as catalyst under microwave conditions and they have proposed alternative ligand to ligand transfer mechanism for this reactions.[22]

Scheme 1.10. Proposed catalytic cycle for hydroarylation of ketimine

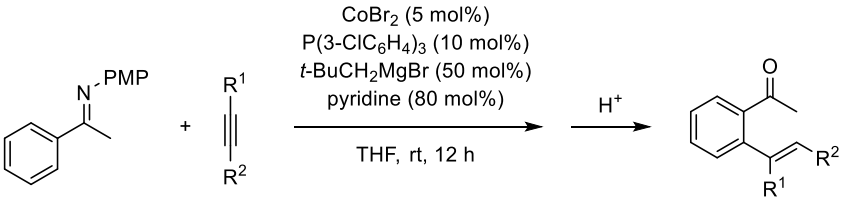

Mechanism

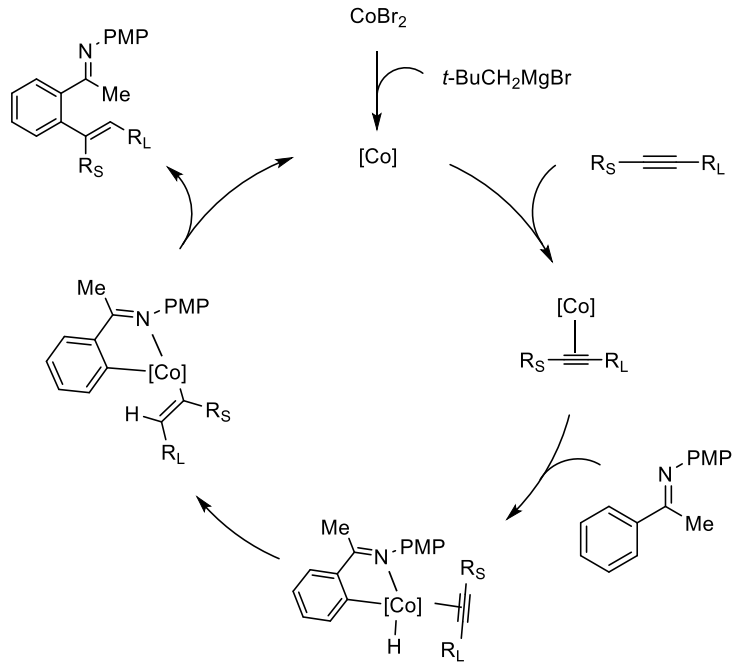

1.1.2. Hydroarylation of Olefins

On the basis of high efficiency of alkyne hydroarylation, Yoshikai and Nakamura group independently achieved hydroarylation of challenging alkenes using low-valent cobalt-catalyzed C–H bond functionalization strategy. Nakamura group used $Co(acac)_3$ as catalytic precursor, CyMgCl as Grignard reagent, DMPU as additive to carry out linear selective *ortho*-alkylation of benzamide derivative under ambient reaction conditions (Scheme 1.11a).[23] At the same time Yoshikai and coworkers developed a method for hydroarylation of styrene with 2-phenylpyridine under regioselective manner. Importantly, *ortho*-C–H alkylation of 2-arylpyridine was achieved in linear or branched selective fashion by ligand control manner. While under optimized reaction conditions Co-NHC-based catalytic system promoted ligand

selective product whereas Co-PCy_3-based system afforded branched selective product (Scheme 1.11b). [24] In a study performed by Fu and coworkers examined the detailed mechanism of the this ligand-controlled regioselectivity by DFT methods.[25] The proposed mechanism by Yoshikai et al. was well matched with Fu's computational analysis. The study carried out by Fu et al. revealed that styrene is not coordinated to cobalt center during the reactions and reductive elimination step is the rate determining step for this reaction. More interestingly, they found that the ligand-controlled regioselectivity is primarily attributable too the steric effect of the ligands.

Scheme 1.11. Low-valent Co-catalyzed hydroarylation with olefins

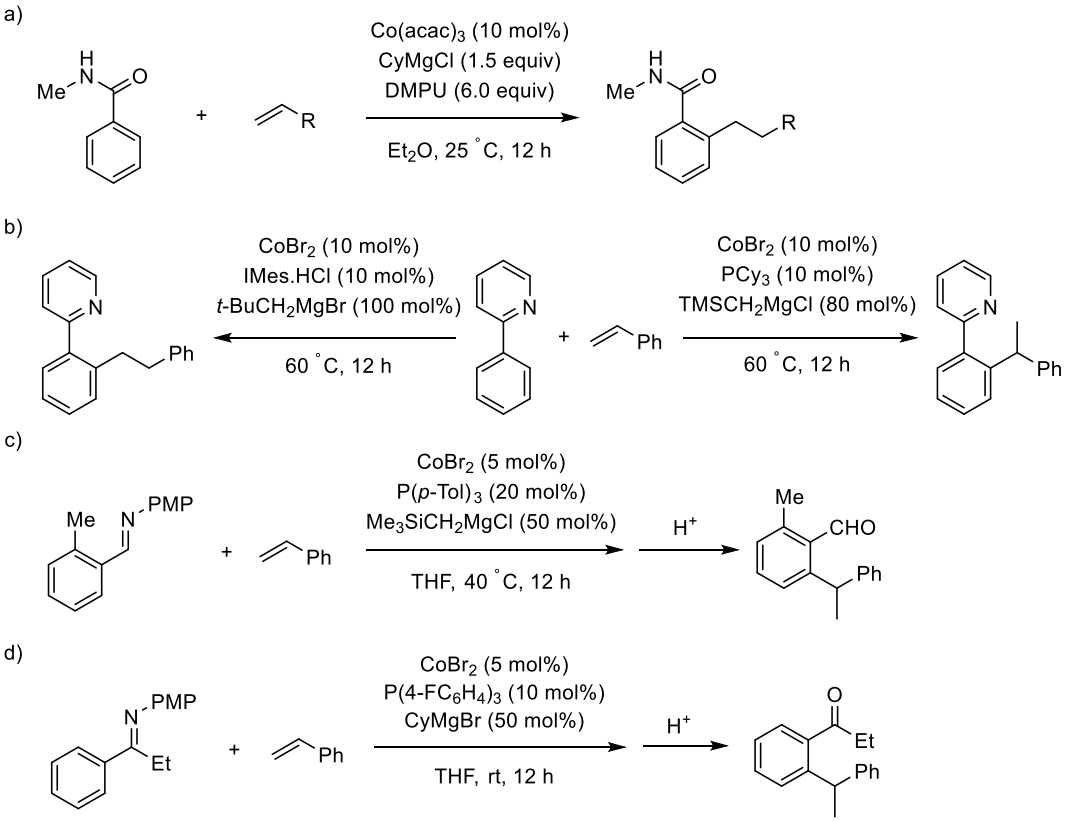

In addition to 2-phenylpyridine derivatives, the substrate scope of branched-selective hydroarylation reaction was extended to aldimines and ketimines. For example, in the presence of $CoBr_2$, P(*p*-Tol)$_3$ and Me_3SiCH_2MgCl, aryl aldimines were

successfully coupled with styrene derivatives to afford 1,1-diaryethanes (Scheme 1.11c).[26] In case of aryl ketimines, the branched-selective reaction was achieved using an analogoues cobalt/phosphine catalyst in combination with cyclohexylmagnesium (Scheme 1.11d).[27]

Scheme 1.12. Aldimine-directed hydroarylation with indole using cobalt catalysis

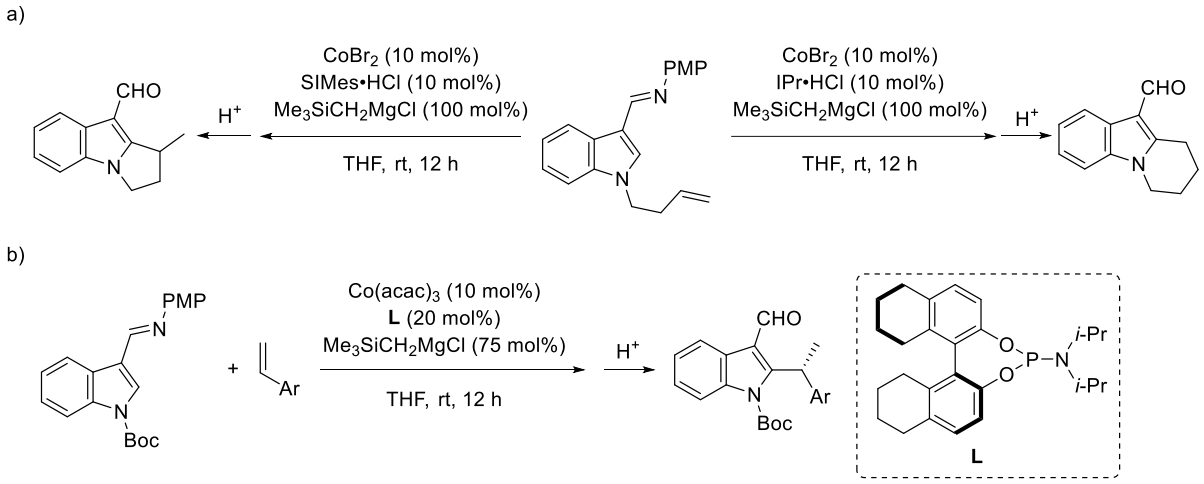

Yoshikai and coworkers further extended the scope of hydroarylation to heterocyclic system. For example, a Co-NHC-based catalytic system catalyzed the intramolecular C2-alkylation of alkene tethered indole with aldimine directing group (Scheme 1.12a).[28] Importantly, Co-IPr catalyst promoted regioselective cyclization of N-homoallylindole to a tetrahydropyridoindole derivative whereas a Co-SIMes catalyst furnished selective formation of dihydropyrroloindole. In their subsequent work, Yoshikai et al. developed an enantioselective protocol for aldimine directed addition of styrene with indoles using cobalt-phosphoramidite catalyst (Scheme 1.12b).[29]

1.1.3. C–H/Electrophile Coupling

Initial reports of C–H functionalization utilizing low-valent cobalt chemistry was revolved around hydroarylation reaction. In 2012, Ackermann and coworkers demonstrated C–H arylation reaction using organic electrophile via C–O bond cleavage. A catalytic system consisting of $Co(acac)_2$, IMes.HCl and CyMgCl facilitated arylation reaction of 2-arylpyridine derivative with aryl halides, carbamates, aryl sulfamates (Scheme 1.13a).[30] The reaction was also applicable to *N*-pyridylindoles. In another important work, Ackermann group extended the scope of C–H arylation to benzamide substrates using similar Co-NHC-CyMgCl type catalytic systems (Scheme 1.13b).[31] In the same year, Yoshikai group accomplished C–H arylation reaction of aryl ketimines with aryl chloride using Co-NHC-*t*$BuCH_2MgBr$ based catalytic system at room temperature (Scheme 1.13c). [32]

Scheme 1.13. Cobalt-catalyzed directed C–H arylation of 2-arylpyridines, amides, and ketimines

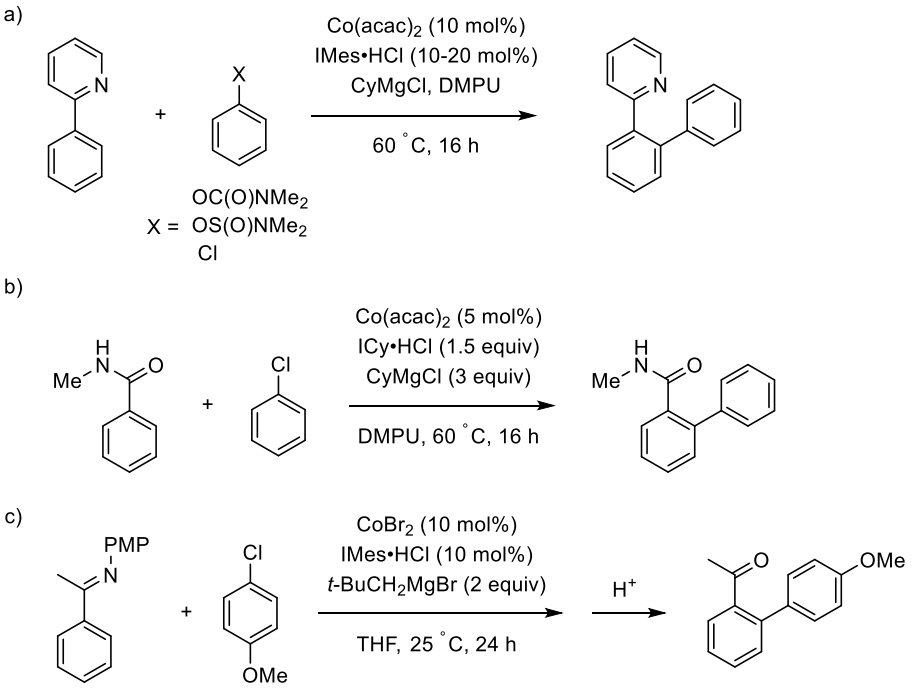

Following the success of *ortho*-C–H arylation using cobalt-NHC precursor based catalytic system, Yoshikai group demonstrated ortho-alkylation of aryl ketimines with primary and secondary alkyl halides. Interestingly, both alkyl chlorides and alkyl bromides were employed as electrophile coupling partner for this reaction (Scheme 1.14).[33] Mechanistic experiments on this reaction using radical clock and stereochemistry probes led to a proposed catalytic cycle shown in Scheme 1.14. An organocobalt species generated from the cobalt precatalyst and the Grignard undergoes cyclometallation of the aryl imine from a cobaltacycle species and an alkane (R–H). The cobaltacycle species then undergoes single electron transfer (SET) to the alkyl halide to generate an oxidized cobaltacycle and an alkyl radical, followed by a C–C coupling to form the alkylated product and a cobalt halide species.

Scheme 1.14. Imine directed C–H alkylation using cobalt catalysis

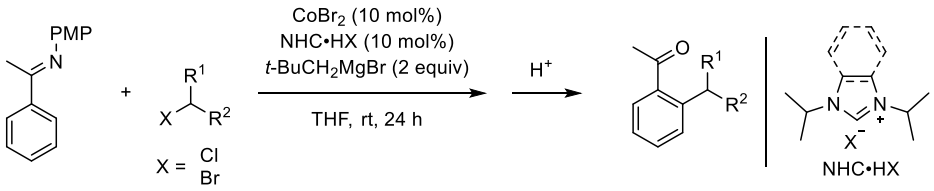

Catalytic cycle

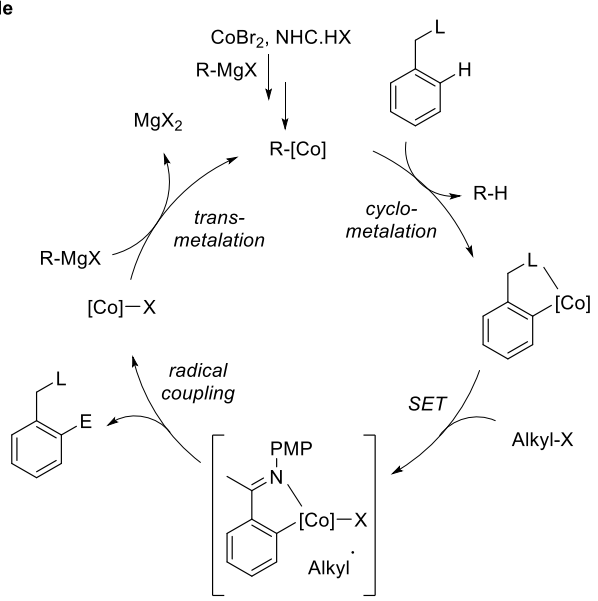

Low-valent cobalt catalyzed hydroarylation reactions were not restricted to alkyne or alkene, Yoshikai group demonstrated *ortho*-C–H functionalization of 2-arylpyridines with N-aryl aziridines using a catalytic system comprised of $CoCl_2$ (5 mol%), IPr.HCl (5 mol%) and *t*$BuCH_2MgBr$ (1.8 equiv) under mild reaction conditions, affording regioselective ring opening product (Scheme 1.15a).[34] Using a similar catalytic system with a higher catalyst loading at an elevated temperature, 2-arylpyridines also took part in the addition reaction of aryl aldimines (Scheme 1.15b).[35]

Scheme 1.15. Cobalt-catalyzed addition of aziridines and aldimines with 2-arylpyridine

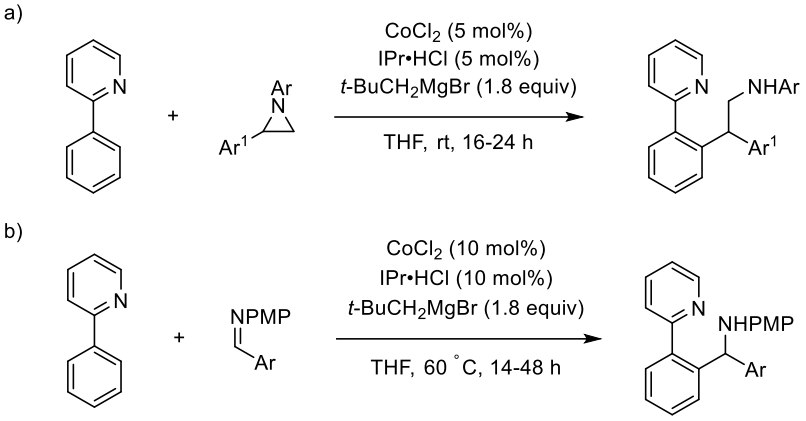

In addition to directing group-assisted C–H functionalization, low-valent cobalt system is also capable to perform selective regio- and stereo-selective C–H functionalization without the assistance of directing group. For example, a number of research paper featuring C–H hydroacylation with low-valent cobalt system is reported in literature. In the following section, example of both directed- and non-directed hydroacylation reaction is discussed.

1.1.4. Hydroacylation reaction

Despite significant progress in low-valent cobalt-catalyzed C–H functionalization by Yoshikai group and others, hydroacylation reaction involving cobalt is somewhat less developed. One of the early example of Co-catalyzed hydroacylation reaction was reported by Brookhart in 1997. They accomplished intermolecular hydroacylation of olefins such as vinylsilane with aldehydes using a $Cp^*Co(I)$-based catalytic system (Scheme 1.16a).[36] Recently, Dong group reported hydroacylation of 1,3-dienes with aromatic and aliphatic aldehydes under cobalt catalysis. A catalytic system comprised of cobalt complex bearing modified dppp ligand, metallic In and $InBr_3$ enabled *Z*-selective hydroacylation of dienes in a1,4-addition manner (Scheme 1.16b).[37] Later, Yoshikai et al. reported that an analogous

catalytic system promotes hydroacylative dimerization of alkyl allenes to afford dialkylidine ketones with high regioselectivity (up to >20:1) (Scheme 1.16c).[38] Note that the latter two reactions do not involve direct C–H activation on cobalt.

Scheme 1.16. Cobalt-catalyzed hydroacylation of aldehydes and aldimines with olefins

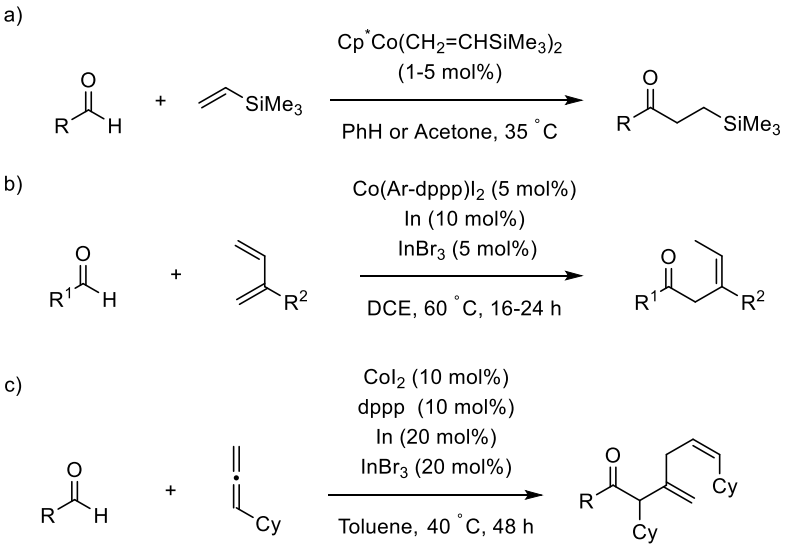

Yoshikai and co-workers also reported linear-selective C–H hydroacylation of nonactivated olefins and styrenes with chelating benzaldimines under low-valent cobalt-diphosphine catalysis (Scheme 1.17).[39] Based on the mechanistic investigation, a probable reaction pathway for this reaction was proposed. First, $CoBr_2$ would be reduced with Zn dust to generate a catalytically active Co(I) species **I**. Next, the species **I** would undergo picolyl-assisted oxidative addition of the imidoyl C–H bond to generate an intermediate **II**. Finally, migratory insertion of the olefin to Co–H bond and reductive elimination of the resulting intermediate **III** would produce the active catalyst and produce the desired hydroacylated product and regenerate the active catalyst.

Scheme 1.17. Picolyl-directed hydroacylation of olefins

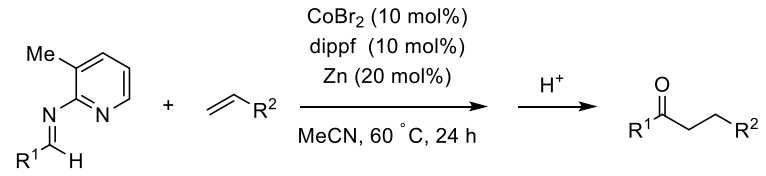

Proposed catalytic cycle

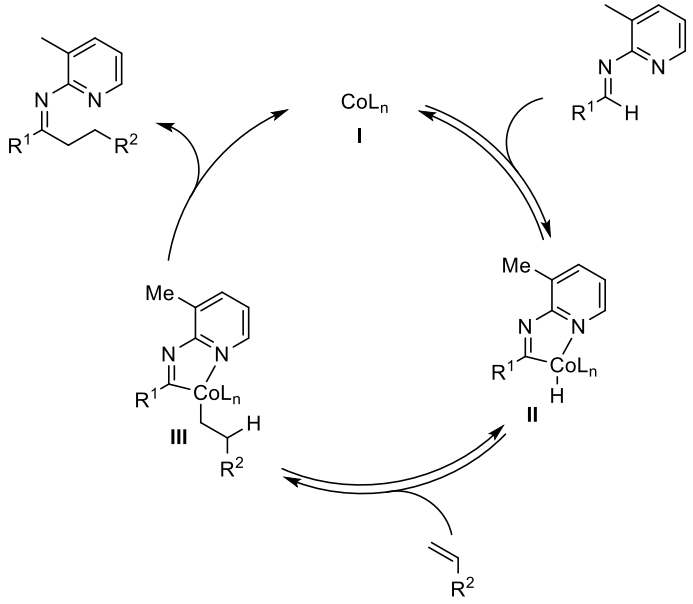

Besides intermolecular hydroacylation, Yoshikai also group described enantioselective intramolecular hydroacyalation using Co-chiral diphosphine ligand based catalytic systems. For example, a reaction protocol employing $CoBr_2$, (*R*,*R*)-Ph-BPE and indium promoted hydroacylation of 2-acylbenzaldehydes to afford enantioenriched phthalides (Scheme 1.18a).[40] Alkenylbenzaldehydes were also found to undergo intramolecular enantioselective hydroacylation under a catalytic system consisting of $CoCl_2$, (*R*,*R*)-BDPP and zinc to give indanones. In their later work, Yoshikai group further extended the scope of enantioselective intramolecular hydroacylation reaction to trisubstituted alkenes for the synthesis of 2,3-disubstituted indanones with high diastereo- and enantioselectivities (Scheme 1.18b).[41]

Scheme 1.18. Cobalt-catalyzed enantioselective intramolecular hydroacylation

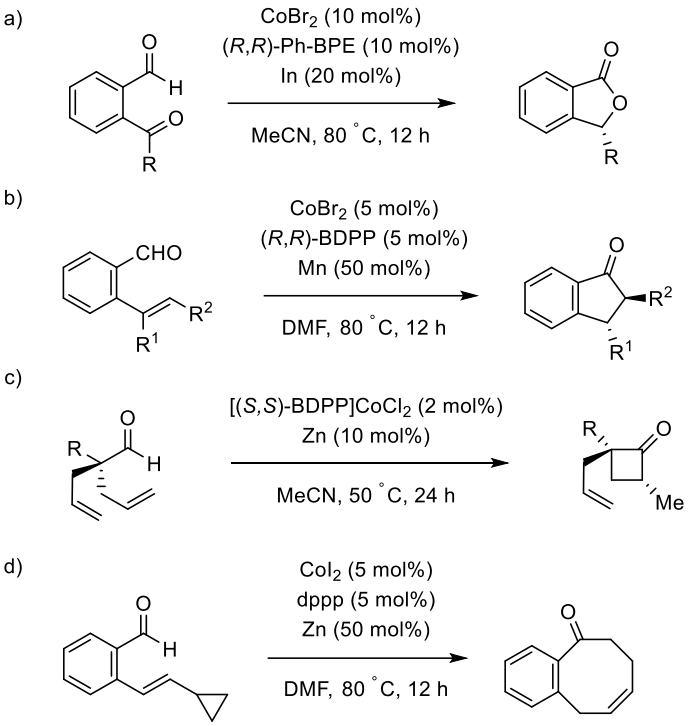

Dong and coworkers also demonstrated cobalt-catalyzed intramolecular hydroacylation to prepare enantioriched cyclobutanones from α-aryl dienyl aldehydes using a catalyst generated from [(S,S)-BDPP]$CoCl_2$ and zinc dust (Scheme 1.18c).[42] In 2020, Yoshikai et al. extended the scope of cobalt-catalyzed intramolecular hydroacylation to cyclopropylvinyl benzaldehydes (Scheme 1.18d).[43] A cobalt-diphosphine-based catalytic system promoted ring opening cyclization of cyclopropylvinyl benzaldehydes via β-carbon elimination to furnish benzocyclooctadienones.

1.2. References

1. (a) Johansson Seechurn, C. C. C.; Kitching, M. O.; Colacot, T. J.; Snieckus, V., *Angew. Chem. Int. Ed.* **2012,** *51* (21), 5062-5085; (b) Frisch, A. C.; Beller, M., *Angew. Chem. Int. Ed.* **2005,** *44* (5), 674-688.

2. Murahashi, S., *J. Am. Chem. Soc.* **1955,** *77* (23), 6403-6404.

3. Murai, S.; Kakiuchi, F.; Sekine, S.; Tanaka, Y.; Kamatani, A.; Sonoda, M.; Chatani, N., *Nature* **1993,** *366* (6455), 529-531.

4. Martinez, R.; Chevalier, R.; Darses, S.; Genet, J.-P. *Angew. Chem. Int. Ed.* **2006**, *45*, 8232.

5. Schinkel, M.; Marek, I.; Ackermann, L. *Angew. Chem., Int. Ed.* **2013**, *52*, 3977−3980.

6. Lim, S.-G.; Ahn, J.-A.; Jun, C.-H. *Org. Lett.* **2004**, *6*, 4687.

7. Shibata, K.; Yamaguchi, T.; Chatani, N. *Org. Lett.* **2015,** *17*, 3584-3587.

8. S. Pan, N. Ryu, T. Shibata, *J. Am. Chem. Soc.* **2012**, *134*, 17474.

9. Crisenza, G. E. M.; Sokolova, O. O.; Bower, J. F. *Angew. Chem. Int. Ed.* **2015,** *54*, 14866-14870.

10. Ebe, Y.; Nishimura, T. *J. Am. Chem. Soc.* **2015,** *137*, 5899-5902.

11. Moselage, M.; Li, J.; Ackermann, L., *ACS Catalysis* **2016,** *6* (2), 498-525.

12. Klein, H. F.; Helwig, M.; Koch, U.; Florke, U.; Haupt, H. J. *Z. Naturforsch. B* **1993**, 48, *778-784*.

13. Halbritter, G.; Knoch, F.; Wolski, A.; Kisch, H., *Angewandte Chemie International Edition in English* **1994,** *33* (15-16), 1603-1605.

14. Gao, K.; Yoshikai, N., *Acc. Chem. Res.* **2014,** *47* (4), 1208-1219.

15. Gao, K.; Lee, P.-S.; Fujita, T.; Yoshikai, N., *J. Am. Chem. Soc.* **2010,** *132* (35), 12249-12251.

16. Lim, Y.-G.; Lee, K.-H.; Koo, B. T.; Kang, J.-B., *Tetrahedron Lett.* **2001,** *42* (43), 7609-7612.

17. Ding, Z.; Yoshikai, N., *Angew. Chem. Int. Ed.* **2012,** *51* (19), 4698-4701.

18. Ding, Z.; Yoshikai, N. *Org. Lett.* **2010**, *12*, 4180−4183.

19. Lee, P.-S.; Fujita, T.; Yoshikai, N., *J. Am. Chem. Soc.* **2011,** *133* (43), 17283-17295.

20. Yamakawa, T.; Yoshikai, N., *Tetrahedron* **2013,** *69* (22), 4459-4465.

21. Yamakawa, T.; Yoshikai, N., *Org. Lett.* **2013,** *15* (1), 196-199.

22. Fallon, B. J.; Derat, E.; Amatore, M.; Aubert, C.; Chemla, F.; Ferreira, F.; Perez-Luna, A.; Petit, M., *J. Am. Chem. Soc.* **2015,** *137* (7), 2448-2451.

23. Ilies, L.; Chen, Q.; Zeng, X.; Nakamura, E., *J. Am. Chem. Soc.* **2011,** *133* (14), 5221-5223.

24. Gao, K.; Yoshikai, N., *J. Am. Chem. Soc.* **2011,** *133* (3), 400-402.

25. Yang, Z.; Yu, H.; Fu, Y. *Chem. - Eur. J.* **2013**, *19*, 12093.

26. Lee, P.-S.; Yoshikai, N., *Angew. Chem. Int. Ed.* **2013,** *52* (4), 1240-1244.

27. Dong, J.; Lee, P.-S.; Yoshikai, N., *Chem. Lett.* **2013,** *42* (10), 1140-1142.

28. Ding, Z.; Yoshikai, N. *Angew. Chem., Int. Ed.* **2013**, *52*, 8574−8578.

29. Lee, P.-S.; Yoshikai, N. *Org. Lett.* **2015**, *17*, 22-25.

30. Punji, B.; Song, W.; Shevchenko, G. A.; Ackermann, L., *Chemistry – A European Journal* **2013,** *19* (32), 10605-10610.

31. Li, J.; Ackermann, L., *Chem. Eur. J.* **2015**, 21, 5718-5722.

32. Gao, K.; Lee, P.-S.; Long, C.; Yoshikai, N., *Org. Lett.* **2012,** *14* (16), 4234-4237.

33. Gao, K.; Yoshikai, N., *J. Am. Chem. Soc.* **2013,** *135* (25), 9279-9282.

34. Gao, K.; Paira, R.; Yoshikai, N., *Adv. Synth. Catal.* **2014,** *356* (7), 1486-1490.

35. Gao, K.; Yoshikai, N., *Chem. Commun.* **2012,** *48* (36), 4305-4307.

36. Lenges, C. P.; Brookhart, M., *J. Am. Chem. Soc.* **1997,** *119* (13), 3165-3166.

37. Chen, Q.-A.; Kim, D. K.; Dong, V. M., *J. Am. Chem. Soc.* **2014,** *136* (10), 3772-3775.

38. Ding, W.; Ho, Y. K. T.; Okuda, Y.; Wijaya, C. K.; Tan, Z. H.; Yoshikai, N., *Org. Lett.* **2019,** *21* (15), 6173-6178.

39. Yang, J.; Seto, Y. W.; Yoshikai, N., *ACS Catalysis* **2015,** *5* (5), 3054-3057.

40. Yang, J.; Yoshikai, N., *J. Am. Chem. Soc.* **2014,** *136* (48), 16748-16751.

41. Yang, J.; Rérat, A.; Lim, Y. J.; Gosmini, C.; Yoshikai, N., *Angew. Chem. Int. Ed.* **2017,** *56* (9), 2449-2453.

42. Kim, D. K.; Riedel, J.; Kim, R. S.; Dong, V. M., *J. Am. Chem. Soc.* **2017,** *139*, 10208.

43. Yang, J.; Mori, Y.; Yamanaka, M.; Yoshikai, N., *Chemistry – A European Journal* **2020,** *26* (37), 8302-8307.

Chapter 2. Cobalt-Catalyzed, N−H Imine-Directed Arene C−H Benzylation with Benzyl Phosphates

Adapted with permission from (Laskar, R. A.; Yoshikai, N. *J. Org. Chem.* **2019**, *84*, 13172-13178.)

Copyright (2019) American Chemical Society

2.1. Introduction

1,1-Diarylalkanes, 1,1-diarylmethanes in particular, serve as important building blocks in many pharmaceuticals and biologically active organic compounds (Scheme 2.1). Thus, synthetic protocols to access 1,1-diaryl methane scaffolds from readily available starting materials have been of immense interest for synthetic organic chemists. Representative approaches to produce 1,1-diarylmethane derivatives include Friedel-Crafts-type reaction of electron-rich arenes using benzyl electrophiles, and transition-metal catalyzed cross-coupling reaction between benzyl electrophiles and arylmetal reagents or between aryl electrophiles and benzylmetal reagents. More recently, alternative approaches such as cross-electrophile coupling between aryl- and benzyl electrophiles, and direct benzylation of arenes via C–H activation have emerged. In following subsections, general feature and representative examples of each of these approaches are described.

Scheme 2.1. Biologically active compounds containing 1,1-diarylalkane scaffolds

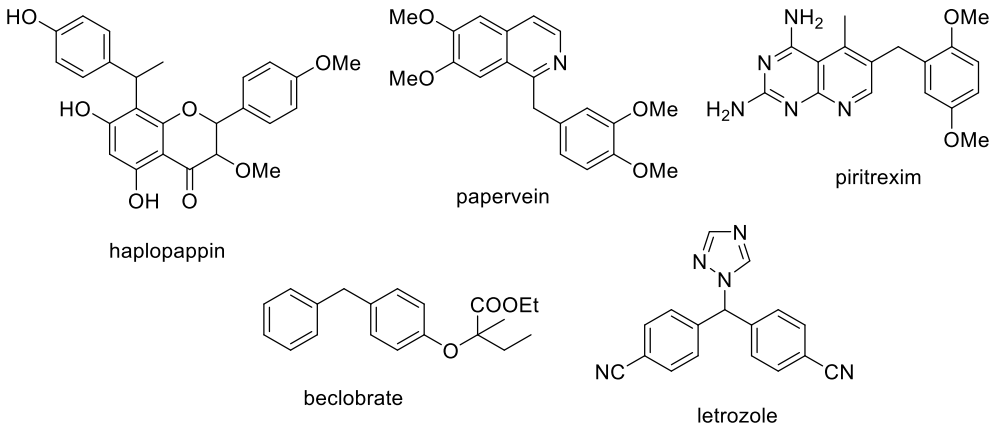

2.1.1. Friedel-Crafts Benzylation

The Friedel-Crafts-type benzylation of aromatic and heteroaromatic compounds has been achieved using Lewis acid catalysts. For example, Wang et al. achieved

benzylation of different arenes with benzyl methyl ether using $FeCl_3$ catalyst (Scheme 2.2a).[1] In 2011, Bode et al. reported benzylation of electron-poor arenes containing nitrile, trifluoromethyl, nitro, ester group using benzylic hydroxamate electrophile and stoichiometric amount of $BF_3.OEt_2$ promoter (Scheme 2.2.b).[2] It is hypothesized that success for this transformation lies on the reversible formation of benzyl cation from benzyl hydroxamate by $BF_3.OEt_2$.

Scheme 2.2. Friedel-Crafts type benzylation with benzyl electrophile

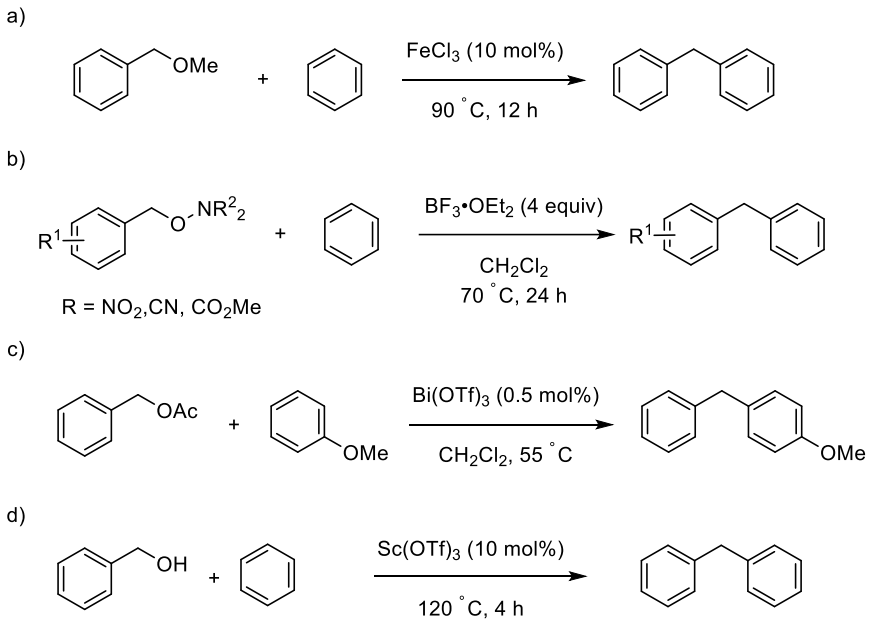

Later, Rueping et al. disclosed $Bi(OTf)_3$-catalyzed benzylation of arenes using 1-phenyl ethanol as benzylating source (Scheme 2.2c).[3] Interestingly, air and moisture sensitive bismuth salts was used in low catalyst loading. Use of benzyl alcohol as benzylic source in Friedel-Crafts benzylation offers attractive alternative compared to other benzylic electrophile. It would eliminate the prefunctionalization step and produce water as side product, which is environment friendly in nature. In 1997, Fukuzawa et al. reported

$Sc(OTf)_3$ catalyzed benzylation using benzyl alcohol as benzylation source (Scheme 2.2d).[4]

2.1.2. Transition Metal-Catalyzed Cross-Coupling Reaction

Transition metal-catalyzed cross-coupling reactions offer efficient and straightforward method to access 1,1-diarymethane scaffolds. For example, Suzuki-Miyaura cross-coupling of benzyl bromide and phenyl boronic acid using $Pd(PPh_3)_4$ catalyst was developed by Georghiou et al. (Scheme 2.3a).[5] Phopase and coworkers described a protocol for ligand-free Suzuki cross-coupling between benzylic halides and aryl boronic acids under mild conditions (Scheme 2.3b).[6] Palladium chloride was used in low catalyst loading to synthesize diarylmethanes at room temperature in an acetone/ water mixed solvent system. Bifold and chemo-selective benzylation was also achieved using this reaction conditions. McLaughlin utilized benzylic phosphates as coupling partners to aryl boronic acids, where palladium acetate in combination with triphenylphosphine promoted the Suzuki-Miyaura coupling to afford the desired diarylmethanes in high yield (Scheme 2.3c).[7]

Scheme 2.3. Synthesis of 1,1-diarylmethane by Suzuki-Miyaura cross-coupling

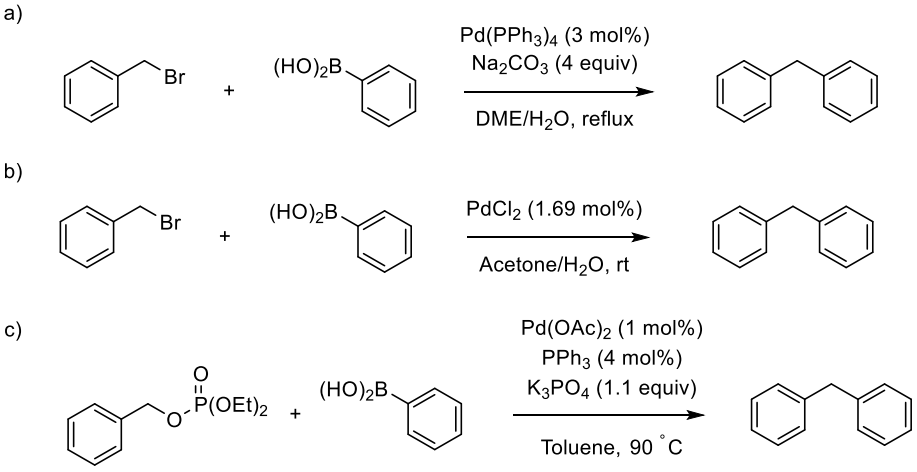

Access to diarylmethane scaffold using Stille coupling strategy is rare. In 2005, Taylor and co-workers reported using cross-coupling of benzyl halides and aryltin reagents using a newly synthesized air stable Pd(II) complex (Scheme 2.4a). [8] First-row transition metal copper has also been used for cross-coupling of arylmagnesium reagent and benzyl phosphates by Knochel group (Scheme 2.4b).[9] A catalytic system comprised on copper(I) chloride, triethylphosphite and tetrabutylammonium iodide promoted the reaction to afford various diarylmethanes in excellent yield. In 2009, Bedford and coworkers used Fe-phosphine complex-based catalytic system to perform Negeshi coupling of benzyl halides and phosphates with aryl Grignard reagents (Scheme 2.4c). [10]

Scheme 2.4. Transition metal-catalyzed cross-coupling for the synthesis of 1,1-diarymethanes

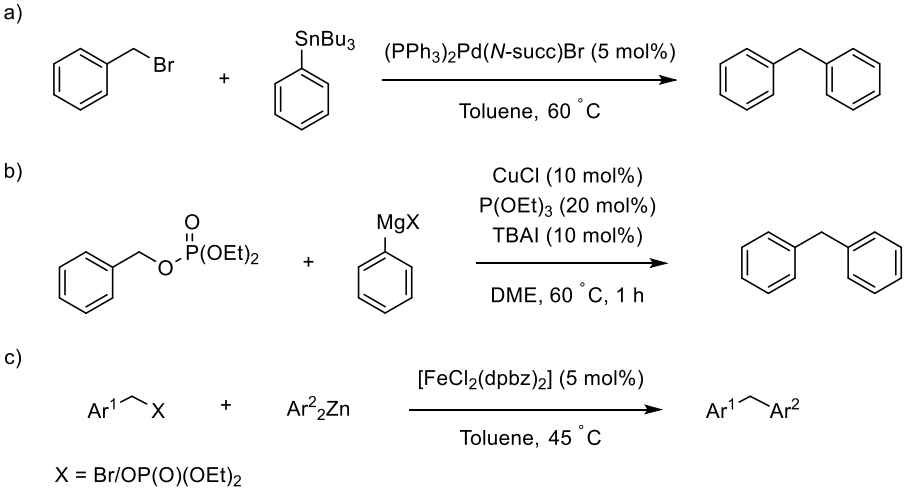

2.1.3. Cross-Electrophile Coupling

A coupling reaction between two different electrophiles called cross-electrophile coupling. It offers step economical approach to access desired product over

traditional cross-coupling reaction, although selective coupling between two substrates is challenging and generation of homo-coupled side product is frequent. Weix group reported Co(Pc) and Ni-based co-catalytic system for selective cross-electrophile coupling between benzyl mesylates and aryl halide to generate diarylmethanes (Scheme 2.5a). [11] Key feature of this report is the generation benzyl radical from benzyl mesylate using Co(Pc) and coupling of benzyl radical with $(L)Ni^{II}(Ar)X$ to form desired product over bibenzyl formation. One of the early examples of nickel-catalyzed cross electrophile coupling reaction was reported by Sun et al. using magnesium reductant (Scheme 2.5b).[12] This strategy offers ambient reaction conditions for various benzyl chlorides and aryl chlorides. Gosmini and coworkers reported diarylmethane synthesis by using cobalt-based catalytic system (Scheme 2.5c).[13] A catalytic system using cobalt bromide as pre-catalyst and stoichiometric manganese as reductant delivered cross-electrophile coupling of benzylic chlorides and aryl halides at room temperature.

Scheme 2.5. Benzylation using cross-electrophile coupling strategy

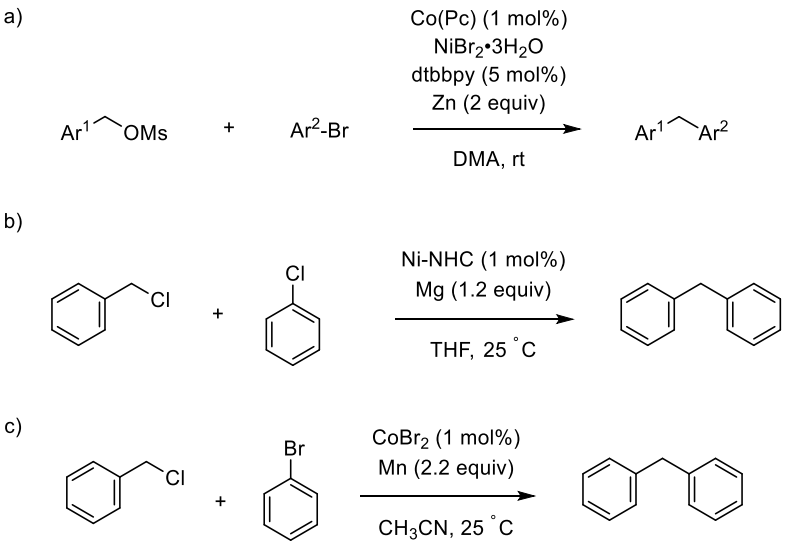

2.1.4. Direct C–H Benzylation of Arenes

Late transition metals are frequently used for the synthesis of diarylmethane derivatives via direct C–H benzylation approach. For example, Ackermann et al. demonstrated C–H benzylation of arenes directed by nitrogen based directing groups (Scheme 2.6a). [14] A ruthenium complex, bulky carboxylic acid based catalytic system was used to perform benzylation of oxazolines, pyridines and pyrazole derivatives using benzylic chloride at high temperature. Bach group accomplished directing group assisted ortho-selective C–H benzylation reaction of 2-arylpyrroles with using Pd(II)-based reaction system (Scheme 2.6b).[15] In 2017, Loh et al. employed $Cp^*Rh(III)$ salt as precatalyst, Cu(II) acetate as stoichiometric oxidant and AgF activator for benzylation of N-(2-pyrimidyl)indoles with benzyltriethoxysilane (Scheme 2.6c).[16] A wide range of indole derivatives bearing electron-donating and electron-withdrawing groups underwent smooth participation in the reaction.

Scheme 2.6. Directed C–H benzylation with benzyl electrophiles

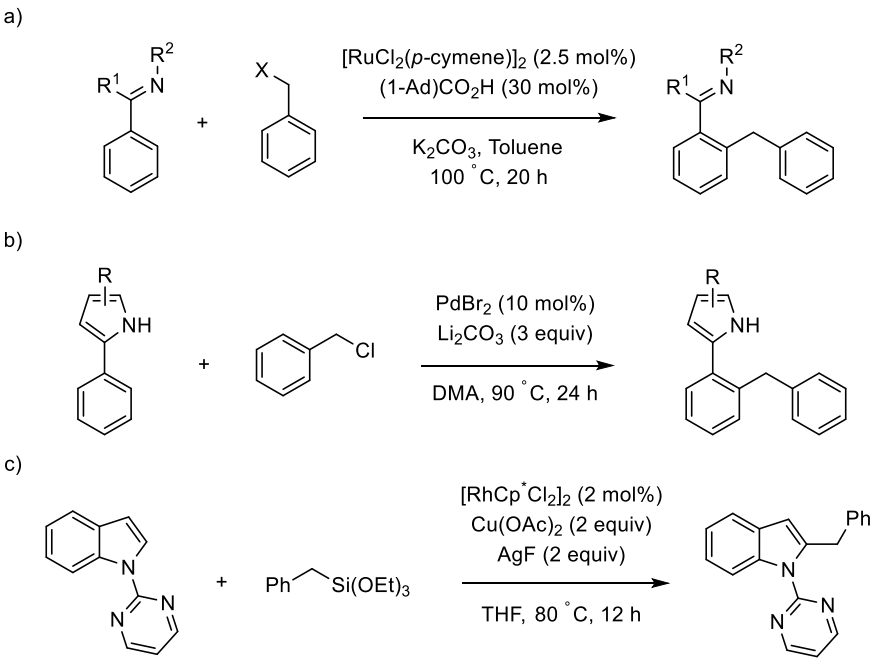

While most of the C–H benzylation protocols are accompanied by use of precious late transition metals, some group reported first-row transition-metal-based catalytic system to achieve the synthesis of diarymethanes. For example, Ackermann group developed a Fe-dppe-PhMgBr-based catalytic system to perform C–H benzylation of benzamide bearing bidentate directing group (Scheme 2.7a). [17] On the other hand, Chatani and co-workers utilized 8-aminoquinoline directing group to carry out *ortho*-C–H benzylation of benzamides using nickel-based catalytic system (Scheme 2.7b). [18] Thus, a catalytic system comprising of nickel triflate, triphenyl phosphine and sodium carbonate promoted benzylation of benzamides. Ackermann et al. also utilized low-valent cobalt-based catalytic system to carry out benzylation reaction Thus, a combination of $Co(acac)_2$ as pre-catalyst, NHC precursor as ligand, Grignard reagent as reductant afforded benzylation reaction of N-(2-pyrimidyl)indole with benzylic phosphate electrophile (Scheme 2.7c).[19] Later in 2015, our group reported *ortho*-benzylation of aryl imines using cobalt-pyphos based catalytic system with benzyl phosphate electrophile to furnish diarylmethane scaffolds (Scheme 2.7d).[20] A broad range of functional group containing imines underwent *ortho*-benzylation in moderate to good yields at room temperature. In mechanistic study, it turned out that addition of radical scavenger TEMPO completely shuts the desired benzylation reaction indicating radical nature of reaction system.

Scheme 2.7. First-row transition metal-catalyzed C–H benzylation reaction

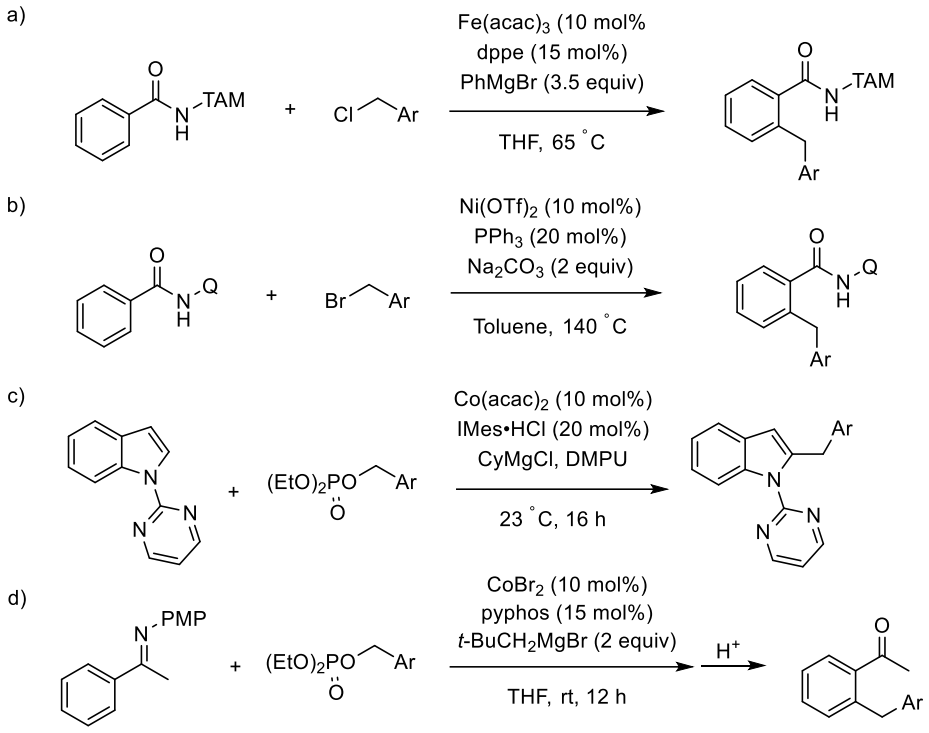

2.1.5. Design of the Work

In light of the above background, we intended to expand the scope of low-valent cobalt catalysis of the C–H/electrophile coupling reaction. In our previous studies involving low-valent cobalt chemistry, we explored the scope of hydroarylation, arylation, alkylation, and alkenylation reaction of substrates such as 2-arylpyridines, N-pyrimidylindoles, aryl ketimines and aryl aldimines. The use of these directing groups in C–H functionalization reaction often possesses several limitations. For example, the removal of pyridyl directing group in the functionalized 2-arylpyridine cannot be removed. Also, the synthesis of aryl N-PMP imines from bulky ketones is nontrivial. In search for a new powerful directing group that can address some of the problems related to traditional directing groups as well as unlock unprecedented reactivity patterns, we found that an N–H imine derived from benzonitrile and organolithium or -magnesium reagent can serve as a robust directing group in low-valent cobalt-catalyzed C–H functionalization reaction. Previously using rhodium-based catalytic

system, Miura and coworkers[21] described oxidative coupling of benzophenone N–H imine and internal alkyne to afford isoquinoline derivatives, whereas Cramer et al.[22] utilized benzophenone N–H imines for enantioselective (3+2) annulation with internal alkynes. In 2016, our group accomplished four-fold *ortho*-alkylation of benzophenone N–H imine with vinyl silane using a ternary catalytic system consisting of $Co(acac)_2$, $P(3\text{-}FC_6H_4)_3$, *t*-$BuCH_2MgBr$, and pyridine (Scheme 2.8a).[23] In addition, we also described N–H imine-directed hydroarylation reaction of pivalophenone N–H imines with broad range of olefins, affording mono-alkylation products in high yield. Furthermore, pivalophenone N–H imines also served as good substrates for cobalt-catalyzed directed C–H alkylation reaction. A catalytic system comprised of $CoBr_2$, NHC preligand in combination with *t*-$BuCH_2MgBr$ successfully promoted the *ortho*-alkylation of imines with alkyl bromides at room temperature (Scheme 2.8b).[24] Importantly, the pivaloyl N–H imine could be readily converted to a cyano group under peroxide photolysis or aerobic copper catalysis. In 2018, we developed Co-NHC catalytic system-promoted ortho-alkenylation reaction of pivalophenone N–H imines with alkenyl phosphates (Scheme 2.8c).[25] These previous studies have prompted us to explore N–H imine-directed *ortho*-C–H benzylation under cobalt catalysis, which would afford diarylmethane derivatives bearing potentially useful N–H imine functionality (Scheme 2.8d).

Scheme 2.8. N–H directed Co-catalyzed C–H functionalization

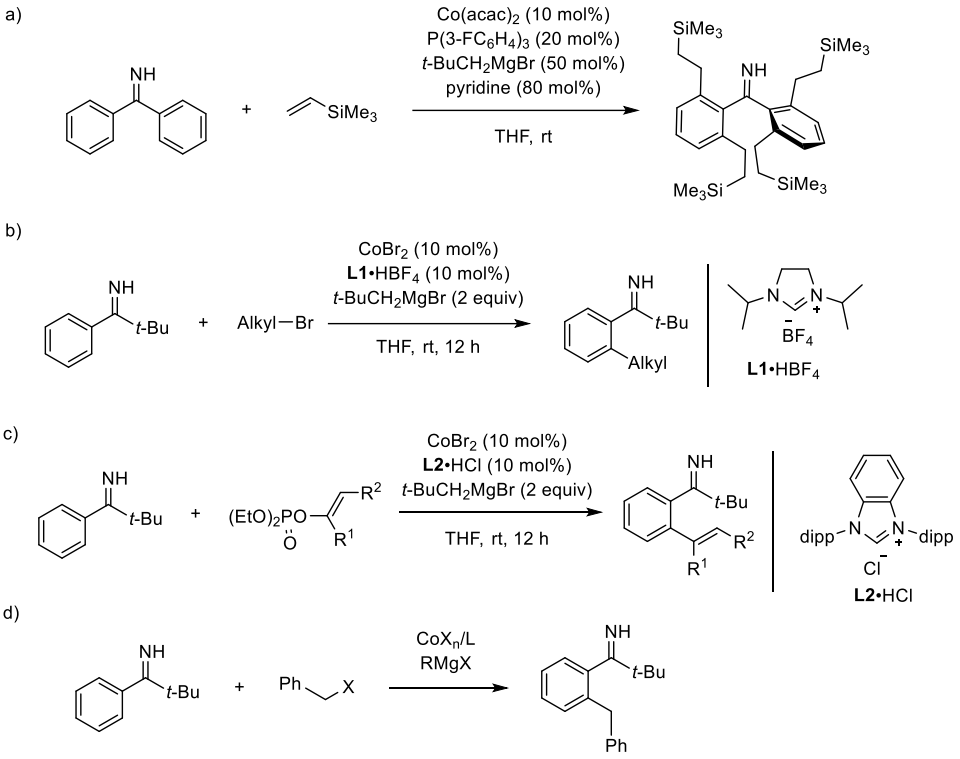

2.2. Result and Discussion

We initiated the present study by optimizing reaction conditions between pivalophenone N–H imine (**1a**) and benzyl diethyl phosphate (**2a**). At first, we have screened effective ligand to selectively perform *ortho*-benzylation reaction using $CoBr_2$ as precatalyst and *t*-$BuCH_2MgBr$ (Table 2.1). Use of NHC precursors such as IMes.HCl and IPr.HCl afforded desired product in 14% and 17% yield respectively (Table 2.1, entry 1 and 2). No particular improvement was observed using other NHC preligands (entry 3-8). Use of monodentate phosphine ligand such as PPh_3 and PCy_3-based led to similar outcome (entry 9 and 10). Bidentate phosphine ligand with different bite angle showed poor reactivity under present reaction conditions (entry 11-13). Moreover, nitrogen-based bidentate phosphine ligand such as 2,2'-bipyridine and 1,10-phenanthroline did not improved the yield (entry 14 and 15). Fortunately, a bidentate

ligand containing phosphine and pyridyl scaffold such as 2-(2-(diphenylphosphanyl)-ethyl)pyridine (pyphos) promoted to benzylation reaction to give 21% yield (entry 16).

Table 2.1. Optimization of reaction conditions[a]

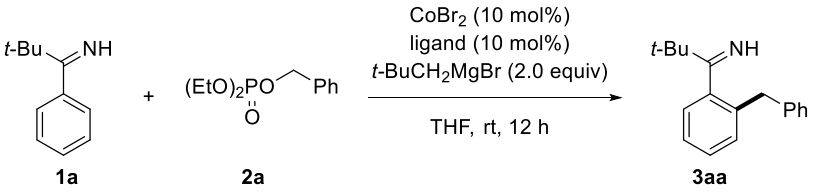

1a **2a** **3aa**

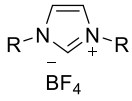

L1•HBF_4 (R = *i*-Pr)
L2•HBF_4 (R = *t*-Bu)
L3•HBF_4 (R = *i*-Pr)

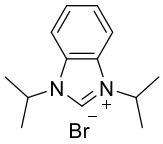

L4•HBr

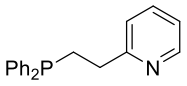

pyphos

Entry	Ligand	Conv.	Yield (%)[b]
1	IMes•HCl	54	14
2	IPr•HCl	55	17
3	SIMes•HCl	42	11
4	SIPr•HCl	58	16
5	**L1**•HBF_4	64	16
6	**L2**•HBF_4	37	10
7	**L3**•HBF_4	69	18
8	**L4**•HBr	59	15
9	PPh_3	70	11
10	PCy_3	83	18
11	dppe	30	7
12	dppbz	48	4
13	XantPhos	40	6
14	phen	88	13
15	bpy	56	10
16	**pyphos**	**55**	**21**

[a] 0.1 mmol of **1a**, 0.2 mmol of **2a**, and 0.2 mmol of *t*-$BuCH_2MgBr$ were used. [b] Determined by GC.

Employing pyphos as optimized ligand, we checked the reactivity of different cobalt source and Grignard reagent in our reaction system (Table 2.2). Use of $CoCl_2$ and CoI_2 as cobalt precursor in combination with pyphos ligand and *t*-$BuCH_2MgBr$ as Grignard reagent improved the reaction efficiency, affording desired product in 36% and 31% yield respectively (entry 1 and 2). Other cobalt precursors such as $Co(OAc)_2$ and $Co(acac)_2$ showed similar reactivity to the present conditions (entry 2 and 4). Finally, $Co(acac)_3$ in combination with *t*-$BuCH_2MgBr$ reagent and pyphos ligand afforded the *ortho*-benzylation product in 40% yield. Next, we turned our attention to use various Grignard reagent to our reaction system. Unfortunately, *i*-PrMgBr, Me_3SiCH_2MgCl, and PhMgBr did not promoted benzylation reaction instead diminish the yield (entry 6-10).

Table 2.2. Screening of cobalt salt and Grignard reagent[a]

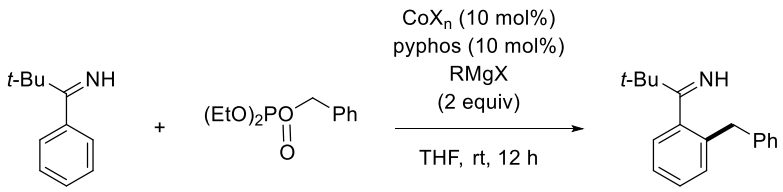

1a **2a** **3aa**

Entry	CoX_n	RMgX	Conv.	Yield (%)
1	$CoCl_2$	*t*-$BuCH_2MgBr$	60	36
2	CoI_2	*t*-$BuCH_2MgBr$	55	31
3	$Co(acac)_2$	*t*-$BuCH_2MgBr$	61	38
4	$Co(OAc)_2$	*t*-$BuCH_2MgBr$	65	39
5	**$Co(acac)_3$**	***t*-$BuCH_2MgBr$**	**70**	**40**
6	$Co(acac)_3$	*i*-PrMgBr	42	2
7	$Co(acac)_3$	$TMSCH_2MgCl$	21	4
8	$Co(acac)_3$	$CyCH_2MgBr$	41	5
9	$Co(acac)_3$	CyHeptMgBr	30	2
10	$Co(acac)_3$	PhMgBr	30	4

[a] 0.1 mmol of **1a**, 0.2 mmol of **2a**, and 0.2 mmol of *t*-BuCH$_2$MgBr were used. [b] Determined by GC.

After screening the cobalt salt, ligand and Grignard reagent, we attempted to optimize the stoichiometric ratio of benzylic phosphate (**2a**) and *t*-BuCH$_2$MgBr (Table 2.3). Lowering of Grignard reagent from 2.0 equiv to 1.6 equiv resulted lowering of yield from 40% to 28%. (Table 2.3, entry 1). Using 2.4 equiv of *t*-BuCH$_2$MgBr in combination with 2.0 equiv of benzylic phosphate afforded the best yield of 51% (entry 2). Further increase in the Grignard amount diminished the desired product formation (entry 3). Other reaction conditions with low amount of benzylic phosphate with different amount of Grignard reagent did not improved the yield.

Table 2.3. Change in stoichiometric ratio of benzylic phosphate and Grignard reagent[a]

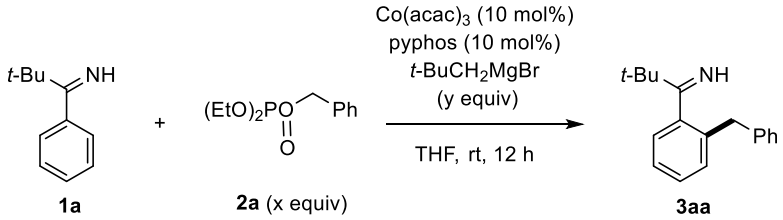

1a **2a** (x equiv) **3aa**

Entry	x	y	Conv.	Yield (%)[b]
1	2.0	1.6	45	28
2	**2.0**	**2.4**	**78**	**50 (51)[c]**
3	2.0	2.8	37	17
4	1.5	1.8	40	18
5	1.5	2.0	74	46
6	1.5	2.4	76	50

[a] 0.1 mmol of **1a**, 0.01 mmol of $Co(acac)_3$, and 0.01 mmol of pyphos was used. [b] Determined by GC. [c] Isolated for 0.4 mmol scale-reaction.

With our best reaction conditions for benzylation reaction, we explored the scope of pivalophenone imine for C–H benzylation reaction (Table 2.4). A number of para-substituted imines took part in the reaction to afford desired products **3ba**-**3ha** in 40-65% of yields, demonstrating the tolerance of functional group such as tert-butyl, methoxy as well as trifluoromethoxy to present reaction system. Probable cross-coupling side product was not observed in case of chloro-substituted imine. Notably, the model reaction between imine **1a** and benzyl phosphate **2a** can be scaled up to 4 mmol with higher yield (58%) compared to small-scale reaction (51%). N–H Imines containing meta-methyl and meta-chloro substituents smoothly promoted regioselective benzylation at sterically less hindered *ortho*-position, giving corresponding products **3ia** and **3ka** respectively. On the contrary, meta-fluorinated imine was benzylated in adjacent to fluorine atom, indicating secondary directing effect might be operated. To our optimized reaction conditions ortho-methyl substituted N–H imine did not take part in our C–H benzylation reactions. In addition, benzophenone N–H imine was also tested with our reaction system, it afforded mono-benzylated product in low yield.

Table 2.4. Scope of pivalophenone N–H imines[a]

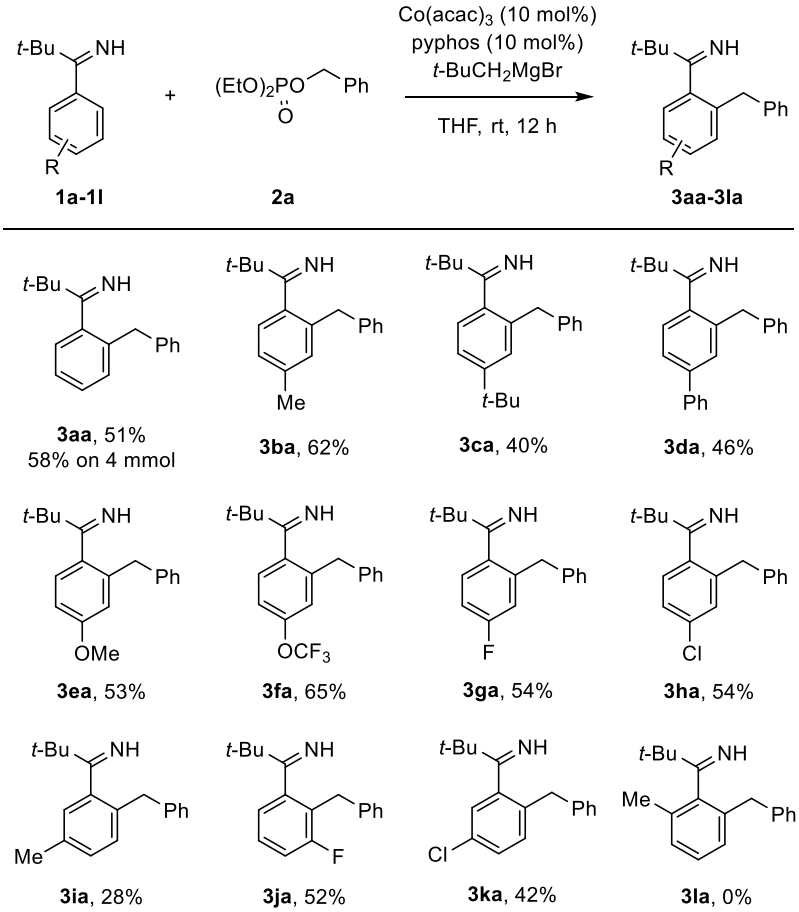

[a] 0.2 mmol of **1**, 0.4 mmol of **2a**, and 0.48 mmol of *t*-BuCH$_2$MgBr were used.

Next, we used pivalophenone N–H imine **1a** as the reaction partner to explore the scope of benzyl phosphates (Table 2.5). Para-substituted benzyl phosphates underwent benzylation reaction to afford corresponding diarylmethane in moderate yields (**3ab**-**3ad**). Phosphates derived from meta-substituted benzyl alcohols bearing methyl, methoxy, chloro and fluoro group furnished the desired product in lower yields (**3af**-**3ai**). Interestingly, *ortho*-chloro substituted benzyl phosphate also amenable to benzylation reaction affording desired product in 29% yield.

Table 2.5. Scope of benzyl phosphates[a]

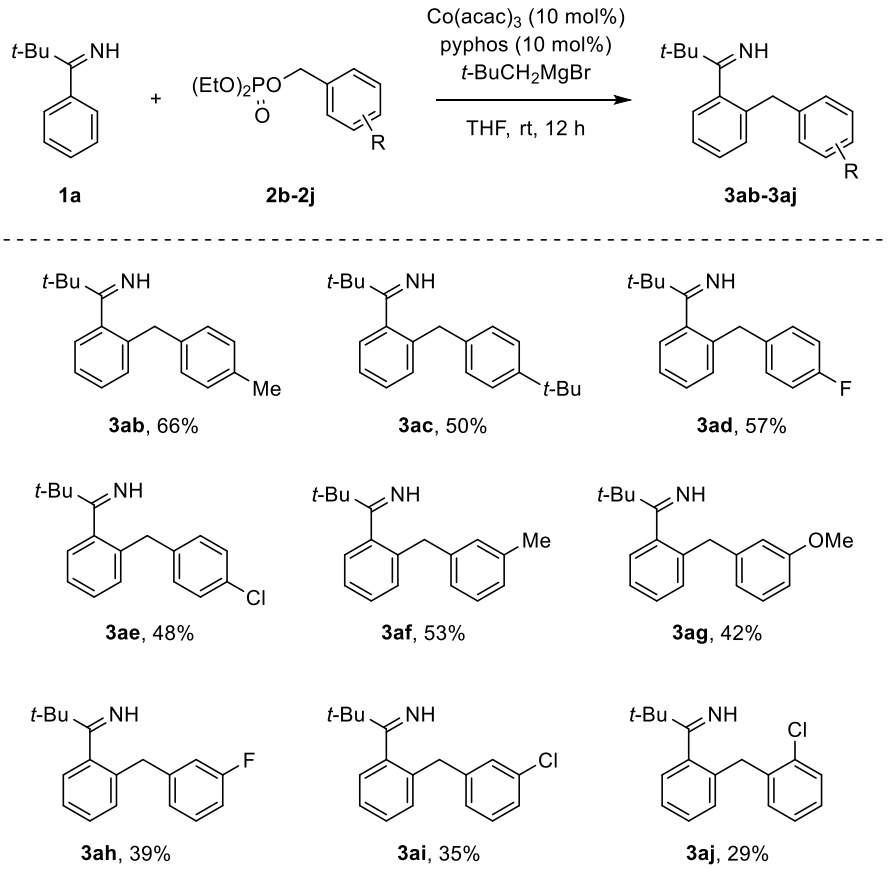

[a] 0.2 mmol of **1**, 0.4 mmol of **2a**, and 0.48 mmol of *t*-BuCH$_2$MgBr were used.

To shed some light on the mechanism, we performed a series of control experiments. First, benzylation reaction was conducted in the presence of free radical scavenger, TEMPO, afforded desired product in 45% yield (Scheme 2.9a). It indicates the mechanism of *ortho*-benzylation in current system is different from that of the previously developed C–H benzylation of N-aryl imines, where the reaction was completely inhibited by TEMPO.[20] In addition, we have conducted a parallel reaction of **1a** and its deuterated counterpart **1a**-d_5 with **2a**, which indicated no kinetic isotope effect (Figure 2.1), strongly suggesting that C–H activation step is not the rate limiting step. Secondly, a competition reaction employing electronically distinct imines with benzyl phosphate resulted predominance formation of **3ga** over **3ba**, implying more facile C–H bond activation of electro-poor ring (Scheme 2.9b). A competition reaction

of *para*-substituted benzyl phosphates **2c** and **2d** with imine **1a** preferentially afforded the product with the electro-deficient phosphate (Scheme 2.9c). In addition, we also investigated the background reaction between benzyl phosphate with Grignard reagent, which resulted in the formation of cross-coupling and homo-coupling products (Scheme 2.9d). Notably, in the absence of the cobalt catalyst, the cross-coupling product formed as the major product.

Scheme 2.9. Control experiments

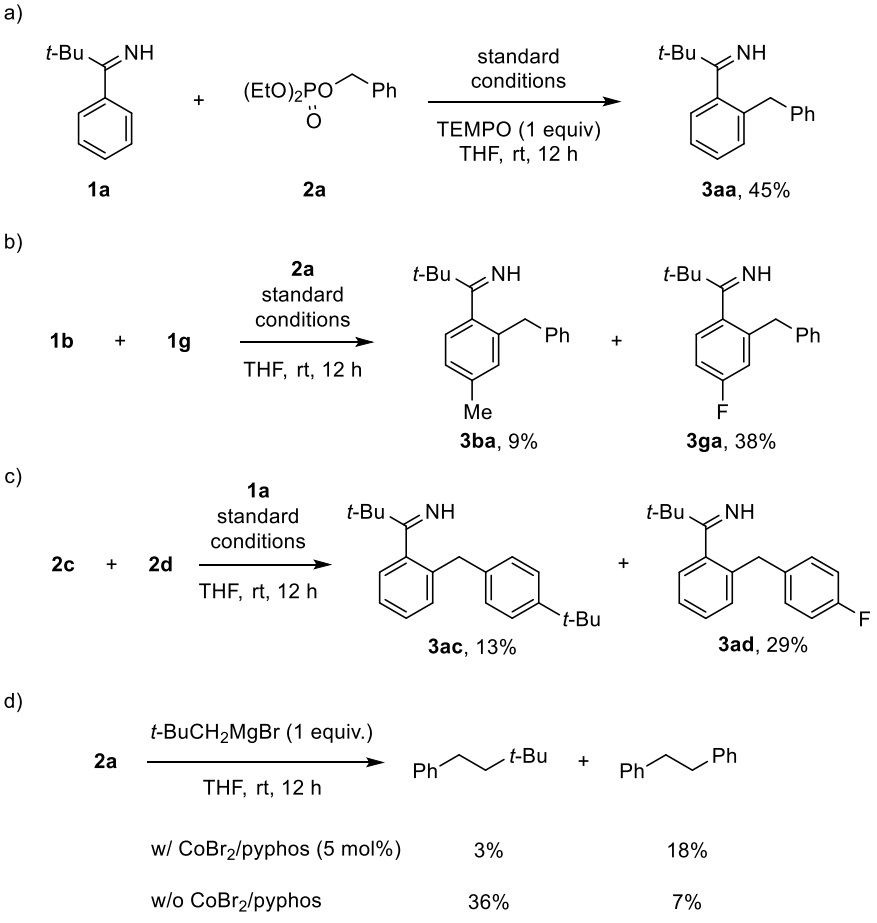

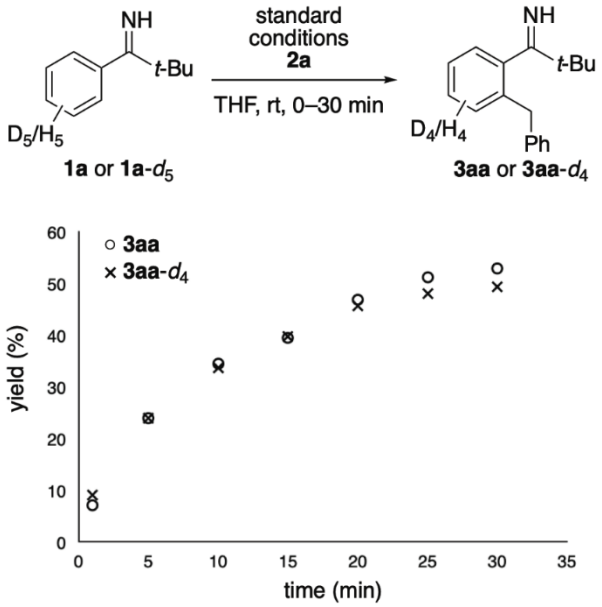

Figure 2.1. Comparison of reactivity **1a** and **1a**-d_5 toward benzylation reactions

We propose a plausible catalytic cycle for the present C–H benzylation reaction based on the mechanistic investigation (Scheme 2.10). First, *t*-BuCH_2MgBr would reduce the Co(acac)$_3$-pyphos to generate active catalytic species **A**. Next, cyclocobaltation of magnesium alkylideneamide 1.MgBr, resulted from deprotonation of N–H imine with *t*-BuCH_2MgBr would form intermediate **B**. The cyclometalated intermediate **B** would then undergo oxidative addition with benzyl phosphate **2** followed by reductive elimination would furnish the product **3**.MgBr. Catalytically active alkyl cobalt species **A** would then regenerate through transmetalation between intermediate **D** and Grignard reagent. From the control experiment with TEMPO, we hypothesize that two electron mechanism for oxidative addition or an single electron transfer type mechanism via intermediate **C'** could be operated here.

Scheme 2.10. Proposed catalytic cycle

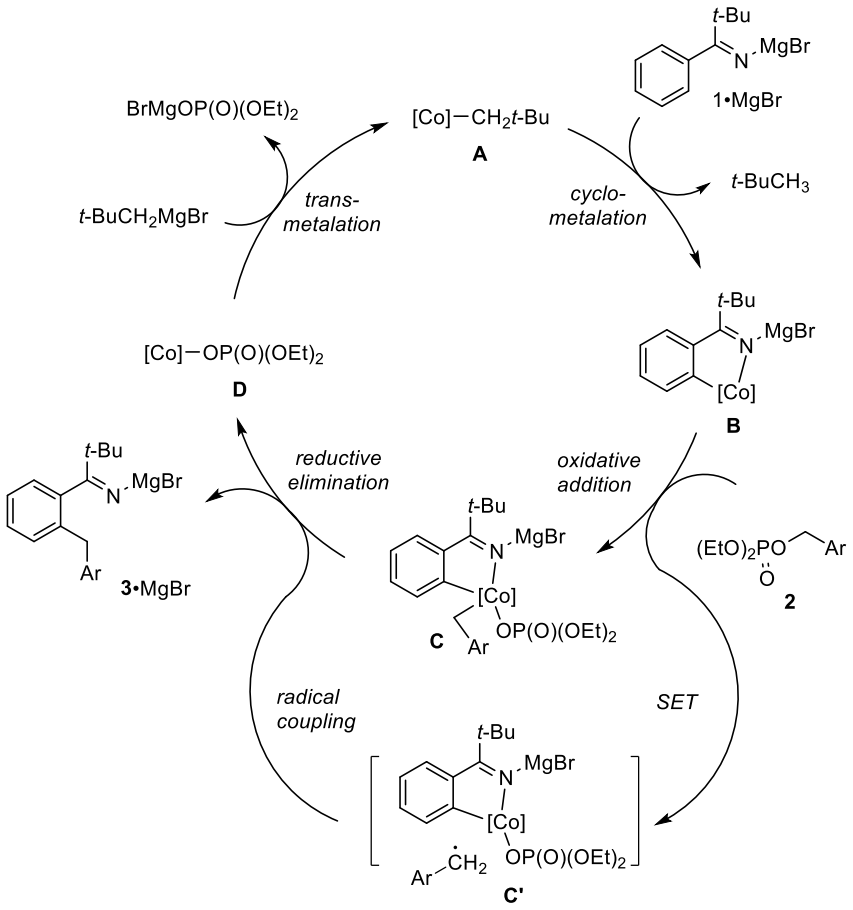

Finally, we performed transformation of the imine functional group of the benzylated product using copper-catalyzed aerobic oxidation conditions, which resulted in oxidation of the benzylic position to form a diketone compound **4** (Scheme 2.11).[26] This was contrary to our expectation of imine to nitrile conversion (see **5**), which was observed for *ortho*-alkylated and arylated pivalophenone imines.[24] The formation of compound **4** instead of **5** can be rationalized by analogous benzylic oxygenation reaction proposed by Chiba, where an in situ generated iminylcopper(II) species get oxidized by O_2, followed by benzyl-to-N 1,5-hydrogen transfer and interception of the benzyl radical by a peroxycopper(II) species.

Scheme 2.11. Aerobic C–H oxygenation using copper catalyst

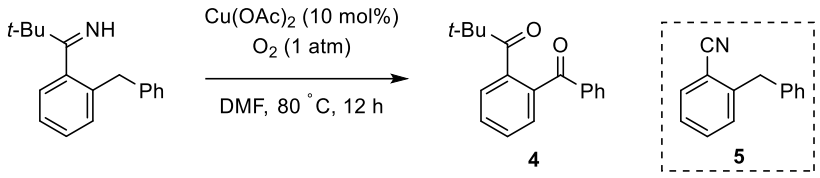

2.3. Conclusion

In conclusion, we have accomplished cobalt-catalyzed directed *ortho*-C–H benzylation of pivalophenone N–H imine with benzyl phosphates. The reaction offers broad range of functional group tolerance for both pivalophenone imine and benzyl phosphate, furnishing the desired diarylmethane derivatives at room temperature. In addition, the benzylated proved to undergo benzylic C–H oxygenation to afford a 1,2-diacylbenzene derivative.

2.4. Experimental Section

Preparation of N–H Imines: General Procedure. An oven-dried Schlenk flask (100 mL) equipped with a stir bar was charged with aryl nitrile (20 mmol), CuBr (58 mg, 0.4 mmol), and THF (20 mL) under N_2 atmosphere. To the mixture was added *tert*-butylmagnesium chloride (11 mL, 2 M in THF, 22 mmol), and the reaction mixture was stirred at 80 °C for 16 h. The resulting solution was cooled in an ice bath and quenched with methanol (20 mL). After stirring for 10 min, the ice bath was removed and the mixture was stirred for additional 1 h. The volatile materials were evaporated under reduced pressure. The residue was diluted with Et_2O (50 mL) and filtered thorough Celite. The resulting filtrate was concentrated under reduced pressure, and the crude oil was purified with Kugelrohr distillation to afford the desired N–H imine as light yellow oil. Except **1c**, the N–H imines (**1a**,[27] **1b**,[28] **1d**,[28] **1e**,[29] **1f-g**,[28] **1h**,[30] **1i**,[28] **1j-1k**[30] & **1l**[31])

are known compounds and their spectral data showed good agreement with the literature data.

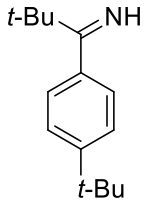

1-(4-(*tert*-Butyl)phenyl)-2,2-dimethylpropan-1-imine (1c). ^{1}H NMR (300 MHz, $CDCl_3$) δ 9.13 (brs, 1H), 7.34 (d, *J* = 8.1 Hz, 2H), 7.14 (d, *J* = 7.5 Hz, 2H), 1.32 (s, 9H), 1.25 (s, 9H); ^{13}C NMR (75 MHz, $CDCl_3$) δ 190.5, 151.0, 139.5, 126.3, 124.9, 34.7, 31.4, 28.7; HRMS (ESI) Calcd for $C_{15}H_{24}N$ $[M + H]^+$ 218.1909, found 218.1911.

Preparation of Benzyl Phosphates. Benzyl phosphates were prepared from the corresponding benzyl alcohols and diethyl chlorophosphates according to the literature procedure[32] and purified using silica gel chromatography. Except **2j**, the benzyl phosphates (**2a**,[32] **2b**,[32] **2c**,[33] **2d**,[34] **2e**,[32] and **2f-i**,[33]) are known compounds and their spectral data showed good agreement with the literature data.

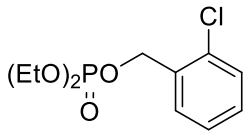

2-Chlorobenzyl diethyl phosphate (2j). ^{1}H NMR (300 MHz, $CDCl_3$) δ 7.53-7.50 (m, 1H), 7.38-7.33 (m, 1H), 7.30-7.24 (m, 2H), 5.17 (d, *J* = 7.2 Hz, 2H), 4.17-4.07 (m, 4H), 1.32 (t, *J* = 7.2 Hz, 6H); ^{13}C NMR (75 MHz, $CDCl_3$) δ 134.0 (d, $^{2}J_{C\text{-}P}$ = 7.8 Hz), 133.0, 129.7, 129.6, 129.4, 127.0, 66.2 (d, $^{2}J_{C\text{-}P}$ = 4.9 Hz), 64.1 (d, $^{2}J_{C\text{-}P}$ = 5.8 Hz), 16.2 (d, $^{3}J_{C\text{-}P}$ = 6.6 Hz); ^{31}P (121 MHz, $CDCl_3$) δ -0.4; HRMS (ESI) Calcd for $C_{11}H_{17}ClO_4P$ $[M + H]^+$ 279.0553, found 279.0565.

General Procedure for C–H Benzylation. A dry 10 mL Schlenk tube equipped with a stir bar was charged with $Co(acac)_3$ (14.3 mg, 0.040 mmol) and 2-(2-(diphenylphosphanyl)ethyl)pyridine (pyphos, 11.7 mg, 0.040 mmol), and THF (1.0 mL) under N_2 atmosphere. The resulting solution was cooled in an ice bath, followed by dropwise addition of *t*-$BuCH_2MgBr$ (1.0 M in THF, 0.96 mL, 0.96 mmol). After stirring for 30 min, N–H imine (0.40 mmol) and benzyl phosphate (0.80 mmol) were added sequentially. The reaction mixture was allowed to warm to room temperature and stirred for 12 h. The resulting mixture was filtered through a short pad of silica gel while washing with EtOAc (10 mL x 3). The filtrate was concentrated under reduced pressure, and the residue was purified by silica gel chromatography (eluent: hexane/EtOAc/NEt_3 = 50/1/1) to afford the benzylation product.

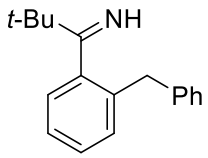

1-(2-Benzylphenyl)-2,2-dimethylpropan-1-imine (3aa). R_f 0.50 (hexane/EtOAc = 4/1); ^{1}H NMR (500 MHz, $CDCl_3$) δ 9.21 (brs, 1H), 7.26-7.10 (m, 8H), 7.06 (dd, *J* = 1 Hz, 1H), 3.86 (s, 2H), 1.22 (s, 9H); ^{13}C NMR (125 MHz, $CDCl_3$) δ 190.1, 141.6, 140.8, 137.0, 130.5, 129.1, 128.6, 127.9, 126.32, 126.26, 125.6, 40.6, 39.5, 28.8; HRMS (ESI) Calcd for $C_{18}H_{22}N$ $[M + H]^+$ 252.1752, found 252.1747.

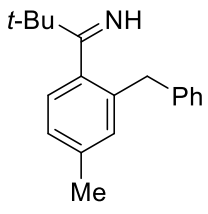

1-(2-Benzyl-4-methylphenyl)-2,2-dimethylpropan-1-imine (3ba). Light yellow oil (66 mg, 62%); R_f 0.50 (hexane/EtOAc = 4/1); ^{1}H NMR (400 MHz, $CDCl_3$) δ 8.87 (brs, 1H), 7.26 - 7.23 (m, 2H), 7.18-7.09 (m, 3H), 6.95-6.91(m, 3H), 3.82 (s, 2H), 2.25(s, 3H), 1.20 (s, 9H); ^{13}C NMR (100 MHz, $CDCl_3$) δ 190.3, 141.0, 139.0, 137.6, 136.8, 131.1, 129.1, 128.6, 126.33, 126.28, 126.22, 40.7, 39.5, 28.9, 21.3; HRMS (ESI) Calcd for $C_{19}H_{24}N$ $[M + H]^+$ 266.1909, found 266.1915.

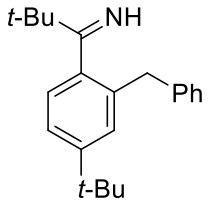

1-(2-Benzyl-4-(*tert*-butyl)phenyl)-2,2-dimethylpropan-1-imine (3ca). Light yellow oil (49 mg, 40%); R_f 0.55 (hexane/EtOAc = 4/1); ^{1}H NMR (400 MHz, $CDCl_3$) δ 9.19 (brs, 1H), 7.29-7.25 (m, 2H), 7.20-7.18 (m, 3H), 7.12 (d, J = 7.2 Hz, 2H), 7.01 (d, J = 8 Hz, 1H), 3.89 (s, 2H), 1.26 (s, 9H), 1.23 (s, 9H); ^{13}C NMR (100 MHz, $CDCl_3$) δ 190.3, 150.7, 141.1, 139.0, 129.0, 128.6, 127.7, 126.2, 126.0, 122.5, 40.7, 39.8, 34.6, 31.4, 28.9; HRMS (ESI) Calcd for $C_{22}H_{30}N$ $[M + H]^+$ 308.2378, found 308.2382.

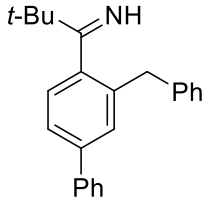

1-(3-Benzyl-[1,1'-biphenyl]-4-yl)-2,2-dimethylpropan-1-imine (3da): Light yellow oil (60 mg, 46%); R_f 0.45 (hexane/EtOAc = 4/1); ^{1}H NMR (500 MHz, $CDCl_3$) δ 9.26 (brs, 1H), 7.54-7.52 (m, 2H), 7.44-7.40 (m, 4H), 7.36-7.28 (m, 3H), 7.23-7.18 (m, 4H), 3.97 (s, 2H), 1.30 (s, 9H); ^{13}C NMR (125 MHz, $CDCl_3$) δ 190.0, 140.8, 140.7, 140.6,

137.5, 129.3, 129.1, 128.9, 128.7, 127.6, 127.2. 126.8, 126.4, 124.4, 40.7, 39.7, 28.9; HRMS (ESI) Calcd for $C_{24}H_{26}N$ $[M + H]^+$ 328.2065, found 328.2059.

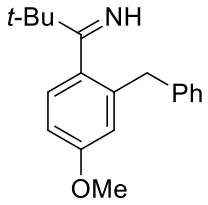

1-(2-Benzyl-4-methoxyphenyl)-2,2-dimethylpropan-1-imine (3ea): Light yellow oil (60 mg, 53%); R_f 0.43 (hexane/EtOAc = 4/1); ^{1}H NMR (300 MHz, $CDCl_3$) δ 9.24 (brs, 1H), 7.31-7.26 (m, 2H), 7.21-7.18 (m, 1H), 7.17-7.13 (m, 2H), 7.03 (d, *J* = 8.4 Hz, 1H), 6.73 (dd, *J* = 8.4, 2.7 Hz, 1H), 6.66 (d, *J* = 2.4 Hz, 1H), 3.87 (s, 2H), 3.73 (s, 3H), 1.24 (s, 9H); ^{13}C NMR (75 MHz, $CDCl_3$) δ 189.9, 159.0, 140.6, 138.8, 134.4, 129.1, 128.6, 127.4, 126.4, 116.0, 110.8, 55.3, 40.8, 39.7, 28.9; HRMS (ESI) Calcd for $C_{19}H_{24}NO$ $[M + H]^+$ 282.1858, found 282.1862.

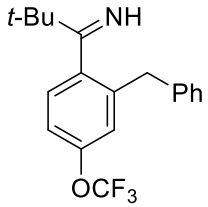

1-(2-Benzyl-4-(trifluoromethoxy)phenyl)-2,2-dimethylpropan-1-imine (3fa): Light yellow oil (87 mg, 65%); R_f 0.43 (hexane/EtOAc = 4/1); ^{1}H NMR (400 MHz, $CDCl_3$) δ 9.37 (brs, 1H), 7.32-7.21 (m, 4H), 7.14-7.11 (m, 3H), 7.06-7.04 (m, 1H), 6.95 (d, *J* = 1.2 Hz, 1H), 3.89 (s, 2H), 1.24 (s, 9H); ^{13}C NMR (100 MHz, $CDCl_3$) δ 190.0, 148.8, 139.7, 129.1, 128.9, 127.8, 126.8, 122.8, 121.8, 119.3, 118.0, 40.8, 39.4, 28.7; ^{19}F NMR (282 MHz, $CDCl_3$) δ -57.8; HRMS (ESI) Calcd for $C_{19}H_{21}F_3NO$ $[M + H]^+$ 336.1575, found 366.1583.

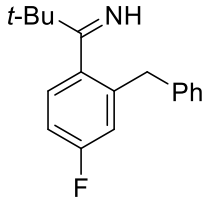

1-(2-Benzyl-4-fluorophenyl)-2,2-dimethylpropan-1-imine (3ga): Light yellow oil (59 mg, 54%); R_f 0.45 (hexane/EtOAc = 4/1); ^{1}H NMR (300 MHz, $CDCl_3$) δ 9.28 (brs, 1H), 7.38-7.20 (m, 3H), 7.13 (d, *J* = 7.2 Hz, 2H), 7.07 (dd, *J* = 8.4, 6 Hz, 1H), 6.89 (td, *J* = 8.4, 2.4 Hz, 1H), 6.80 (dd, *J* = 9.9, 2.4 Hz, 1H), 3.87 (s, 2H), 1.24 (s, 9H); ^{13}C NMR (75 MHz, $CDCl_3$) δ 189.4, 162.2 (d, $^1J_{C\text{-}F}$ = 245.1 Hz), 140.1 (d, $^3J_{C\text{-}F}$ = 7.1 Hz), 139.9, 137.5 (d, $^3J_{C\text{-}F}$ = 3.1 Hz), 129.2, 128.8, 127.9 (d, $^3J_{C\text{-}F}$ = 8.1 Hz), 126.7, 117.1 (d, $^2J_{C\text{-}F}$ = 21.5 Hz), 112.7(d, $^2J_{C\text{-}F}$ = 21.5 Hz), 40.8, 39.5, 28.8; ^{19}F NMR (282 MHz, $CDCl_3$) δ -113.8; HRMS (ESI) Calcd for $C_{18}H_{21}NF$ $[M + H]^+$ 270.1658, found 270.1660.

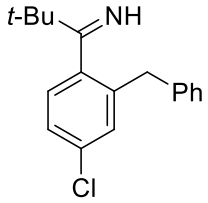

1-(2-Benzyl-4-chlorophenyl)-2,2-dimethylpropan-1-imine (3ha): Light yellow oil (62 mg, 54%); R_f 0.44 (hexane/EtOAc = 4/1); ^{1}H NMR (300 MHz, $CDCl_3$) δ 9.29 (brs, 1H), 7.32-7.22 (m, 3H), 7.20-7.10 (m, 4H), 7.05-7.02 (m, 1H), 3.86 (s, 2H), 1.23 (s, 9H); ^{13}C NMR (75 MHz, $CDCl_3$) δ 189.1, 139.9, 139.8, 139.4, 133.8, 130.4, 129.1, 128.9, 127.7, 126.7, 125.9, 40.8, 39.4, 28.7. HRMS (ESI) Calcd for $C_{18}H_{21}NCl$ $[M + H]^+$ 286.1363, found 286.1357.

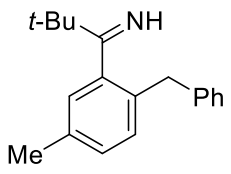

1-(2-Benzyl-5-methylphenyl)-2,2-dimethylpropan-1-imine (3ia); Light yellow oil (30 mg, 28%); R_f 0.65 (hexane/EtOAc = 4/1); ^{1}H NMR (300 MHz, $CDCl_3$) δ 9.21 (brs, 1H,), 7.31-7.27 (m, 2H), 7.23-7.13 (m, 3H), 7.08-7.01 (m, 2H), 6.91 (s, 1H), 3.86 (s, 2H), 2.34 (s, 3H), 1.27 (s, 9H); ^{13}C NMR (75 MHz, $CDCl_3$) δ 190.3 (NH=*C*), 141.7, 141.1, 135.1, 133.9, 130.4, 129.1, 128.7, 128.6, 126.8, 126.3, 40.6, 39.2, 28.9, 21.2; HRMS (ESI) Calcd for $C_{19}H_{24}N$ $[M + H]^+$ 266.1909, found 266.1911.

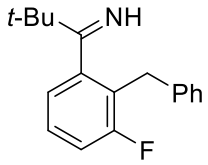

1-(2-Benzyl-5-fluorophenyl)-2,2-dimethylpropan-1-imine (3ja): Light yellow oil (56 mg, 52%); R_f 0.45 (hexane/EtOAc = 4/1); ^{1}H NMR (400 MHz, $CDCl_3$) δ 9.28 (brs, 1H), 7.36-7.32 (m, 3H), 7.3-7.28 (m, 1H), 7.23-7.21 (m, 2H), 7.14 (t, *J* = 8.4 Hz, 1H), 7.00 (d, *J* = 7.6 Hz, 1H), 4.03 (s, 2H), 1.30 (s, 9H); ^{13}C NMR (100 MHz, $CDCl_3$) δ 188.5, 161.8 (d, $^1J_{C\text{-}F}$ = 245.6 Hz), 143.8, 139.8, 128.6, 128.3, 127.6 (d, $^3J_{C\text{-}F}$ = 8.8 Hz), 126.3, 122.2 (d, $^3J_{C\text{-}F}$ = 2.8 Hz), 115.0 (d, $^2J_{C\text{-}F}$ = 22.7 Hz), 40.6, 33.3, 28.8; ^{19}F NMR (282 MHz, $CDCl_3$) δ -113.1; HRMS (ESI) Calcd for $C_{18}H_{21}NF$ $[M + H]^+$ 270.1658, found 270.1651.

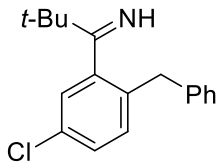

1-(2-Benzyl-5-chlorophenyl)-2,2-dimethylpropan-1-imine (3ka): Light yellow oil (48 mg, 42%); R_f 0.43 (hexane/EtOAc = 4/1); ^{1}H NMR (400 MHz, $CDCl_3$) δ 9.21 (brs, 1H), 7.34-7.29 (m, 2H), 7.26-7.22 (m, 2H), 7.15-7.07 (m, 4H), 3.88 (s, 2H), 1.28 (s, 9H); ^{13}C NMR (100 MHz, $CDCl_3$) δ 188.7, 140.2, 131.9, 131.5, 129.1, 128.8, 128.1,

126.6, 40.7, 39.0, 28.7; HRMS (ESI) Calcd for $C_{18}H_{21}NCl$ $[M + H]^+$ 286.1363, found 286.1357.

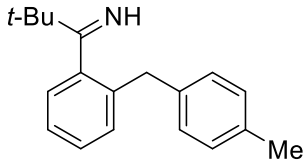

2,2-Dimethyl-1-(2-(4-methylbenzyl)phenyl)propan-1-imine (3ab); Light yellow oil (70 mg, 66%); R_f 0.50 (hexane/EtOAc = 4/1); ^{1}H NMR (300 MHz, $CDCl_3$) δ 9.26 (brs, 1H), 7.25-7.00 (m, 8H), 3.84 (s, 2H), 2.31 (s, 3H), 1.25 (s, 9H); ^{13}C NMR (75 MHz, $CDCl_3$) δ 190.2, 141.7, 137.8, 137.3, 135.8, 130.5, 129.3, 129.0, 127.9, 126.2, 125.5, 40.7, 39.2, 28.9, 21.1; HRMS (ESI) Calcd for $C_{19}H_{24}N$ $[M + H]^+$ 266.1909, found 266.1913.

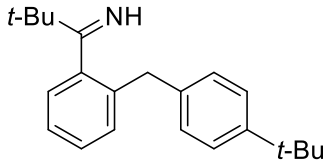

1-(2-(4-(*tert*-Butyl)benzyl)phenyl)-2,2-dimethylpropan-1-imine (3ac): Light yellow oil (62 mg, 50%); R_f 0.53 (hexane/EtOAc = 4/1); ^{1}H NMR (400 MHz, $CDCl_3$) δ 9.22 (brs, 1H), 7.33-7.29 (m, 2H), 7.27-7.23 (m, 1H), 7.21-7.17 (m, 2H), 7.11-7.07 (m, 3H), 3.87 (s, 2H), 1.31 (s, 9H), 1.27(s, 9H); ^{13}C NMR (100 MHz, $CDCl_3$) δ 190.0, 149.1, 141.6, 137.7, 137.2, 130.6, 128.7, 127.9, 126.2, 125.5, 40.6, 39.1, 34.5, 31.5, 28.9; HRMS (ESI) Calcd for $C_{22}H_{30}N$ $[M + H]^+$ 308.2378, found 308.2384.

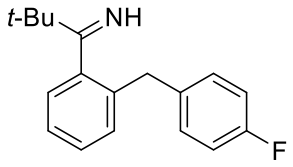

1-(2-(4-Fluorobenzyl)phenyl)-2,2-dimethylpropan-1-imine (3ad): Light yellow oil (62 mg, 57%); R_f 0.43 (hexane/EtOAc = 4/1); ^{1}H NMR (300 MHz, $CDCl_3$) δ 9.16 (brs, 1H), 7.26-7.16 (m, 2H), 7.11-7.07 (m, 4H), 7.00-6.93 (m, 2H), 3.86 (s, 2H), 1.24 (s, 9H); ^{13}C NMR (75 MHz, $CDCl_3$) δ 190.1, 161.6 (d, $^1J_{C\text{-}F}$ = 242.8 Hz), 136.8, 136.5, 136.4, 130.5 (d, $^3J_{C\text{-}F}$ = 7.8 Hz), 128.0, 126.4, 125.8, 115.4 (d, $^2J_{C\text{-}F}$ = 21.1 Hz), 40.7, 38.7, 28.8; ^{19}F NMR (282 MHz, $CDCl_3$) δ -117.0; HRMS (ESI) Calcd for $C_{18}H_{21}NF$ $[M + H]^+$ 270.1658, found 270.1665.

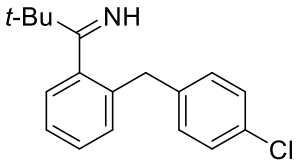

1-(2-(4-Chlorobenzyl)phenyl)-2,2-dimethylpropan-1-imine (3ae): Light yellow oil (55 mg, 48%); R_f 0.47 (hexane/EtOAc = 4/1); ^{1}H NMR (300 MHz, $CDCl_3$) δ 9.26 (brs, 1H), 7.31-7.21 (m, 4H), 7.15-7.10 (m, 4H), 3.90 (s, 2H), 1.29 (s, 9H); ^{13}C NMR (75 MHz, $CDCl_3$) δ 190.0, 141.6, 139.3, 136.4, 132.2, 130.4, 128.7, 128.1, 126.4, 125.8, 40.7, 38.9, 28.8; HRMS (ESI) Calcd for $C_{18}H_{21}NCl$ $[M + H]^+$ 286.1373, found 286.1370.

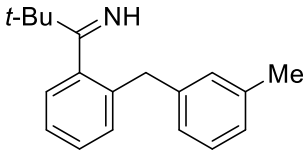

2,2-Dimethyl-1-(2-(3-methylbenzyl)phenyl)propan-1-imine (3af): Light yellow oil (55 mg, 53%); R_f 0.50 (hexane/EtOAc = 4/1); ^{1}H NMR (300 MHz, $CDCl_3$) δ 9.24 (brs, 1H), 7.26-7.09 (m, 5H), 7.02 (d, J = 7.5 Hz, 1H), 6.97-6.93 (m, 2H), 3.87 (s, 2H), 2.32 (s, 3H), 1.27 (s, 9H); ^{13}C NMR (75 MHz, $CDCl_3$) δ 190.1, 141.7, 140.7, 138.2, 137.1,

130.5, 129.9, 128.5, 127.9, 127.1, 126.2, 125.5, 40.6, 39.4, 28.9, 21.6; HRMS (ESI) Calcd for $C_{19}H_{24}N$ $[M + H]^+$ 266.1909, found 266.1912.

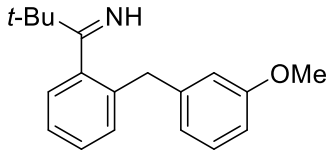

1-(2-(3-Methoxybenzyl)phenyl)-2,2-dimethylpropan-1-imine (3ag): Light yellow oil (47 mg, 42%); R_f 0.33 (hexane/EtOAc = 4/1); ^{1}H NMR (300 MHz, $CDCl_3$) δ 9.28 (brs, 1H), 7.32-7.14 (m, 5H), 6.82-6.75 (m, 3H), 3.93 (s, 2H), 3.83 (s, 3H), 1.31 (s, 9H); ^{13}C NMR (75 MHz, $CDCl_3$) δ 190.1, 159.8, 142.4, 141.7, 136.7, 130.5, 129.6, 127.9, 126.2, 125.6, 121.6, 115.1, 111.5, 55.2, 40.7, 39.5, 28.9; HRMS (ESI) Calcd for $C_{19}H_{24}NO$ $[M + H]^+$ 282.1858, found 282.1859.

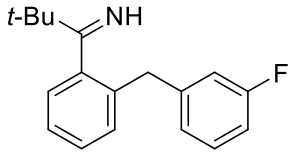

1-(2-(3-Fluorobenzyl)phenyl)-2,2-dimethylpropan-1-imine (3ah): Light yellow oil (42 mg, 39%); R_f 0.43 (hexane/EtOAc = 4/1); ^{1}H NMR (300 MHz, $CDCl_3$) δ 9.36 (brs, 1H), 7.34-7.24 (m, 3H), 7.19-7.15 (m, 2H), 6.98-6.87 (m, 3H), 3.94 (s, 2H), 1.30 (s, 9H); ^{13}C NMR (75 MHz, $CDCl_3$) δ 190.0, 163.1 (d, $^1J_{C\text{-}F}$ = 244.4 Hz), 143.4 (d, $^3J_{C\text{-}F}$ = 7.3 Hz), 136.2, 130.5, 130.0 (d, $^3J_{C\text{-}F}$ = 8.3 Hz), 128.1, 126,5, 125.9, 124.8 (d, $^3J_{C\text{-}F}$ = 2.8 Hz), 116.0 (d, $^2J_{C\text{-}F}$ = 21.2 Hz), 113.3 (d, $^2J_{C\text{-}F}$ = 20.9 Hz), 40.7, 39.2, 28.8; ^{19}F NMR (282 MHz, $CDCl_3$) δ -113.3; HRMS (ESI) Calcd for $C_{18}H_{21}NF$ $[M + H]^+$ 270.1658, found 270.1660.

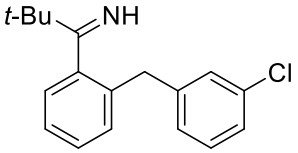

1-(2-(3-Chlorobenzyl)phenyl)-2,2-dimethylpropan-1-imine (3ai): Light yellow oil (40 mg, 35%); R_f 0.43 (hexane/EtOAc = 4/1); ^{1}H NMR (400 MHz, $CDCl_3$) δ 9.18 (brs, 1H), 7.27-7.17 (m, 4H), 7.11 (d, *J* = 8.0 Hz, 3H), 7.01 (d, *J* = 6.4 Hz, 1H), 3.87 (s, 2H), 1.24 (s, 9H); ^{13}C NMR (100 MHz, $CDCl_3$) δ 190.0, 142.9, 141.7, 136.1, 134.4, 130.5, 129.9, 129.2, 128.1, 127.3, 126.6, 126.5, 125.9, 40.7, 39.1, 28.8; HRMS (ESI) Calcd for $C_{18}H_{21}NCl$ $[M + H]^+$ 286.1363, found 286.1369.

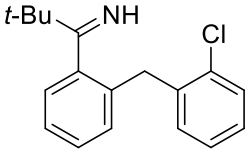

1-(2-(2-Chlorobenzyl)phenyl)-2,2-dimethylpropan-1-imine (3aj): Light yellow oil (34 mg, 29%), R_f 0.51 (hexane/EtOAc = 4/1); ^{1}H NMR (300 MHz, $CDCl_3$) δ 9.32 (brs, 1H), 7.40-7.37 (m, 1H), 7.23-7.10 (m, 5H), 7.03-6.96 (m, 2H), 4.00 (s, 2H), 1.27 (s, 9H); ^{13}C NMR (75 MHz, $CDCl_3$) δ 190.1, 138.3, 135.5, 134.4, 131.1, 129.9, 129.7, 128.0, 127.9, 127.0, 126.4, 125.8, 40.8, 37.0, 28.9; HRMS (ESI) Calcd for $C_{18}H_{21}NCl$ $[M + H]^+$ 286.1363, found 286.1367.

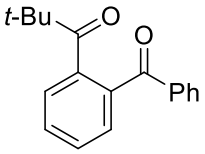

1-(2-Benzoylphenyl)-2,2-dimethylpropan-1-one (4). In a 25 mL Schlenk tube equipped with a stir bar were placed **3aa** (0.6 mmol) and $Cu(OAc)_2$ (11 mg, 0.06 mmol), followed by the addition of DMF (6 mL). An oxygen balloon was attached to the

Schlenk tube, and the reaction mixture was stirred at 80 °C for 12 h. The mixture was concentrated under reduced pressure, and the residue was subjected to silica gel chromatography to afford the title compound as a light yellow oil (48 mg, 30%). R_f 0.33 (hexane/EtOAc = 4/1); ^{1}H NMR (400 MHz, $CDCl_3$) δ 7.78-7.76 (m, 2H), 7.60-7.53 (m, 3H), 7.48-7.42 (m, 4H), 1.30 (s, 9H); ^{13}C NMR (100 MHz, $CDCl_3$) δ 213.7, 196.7, 137.5, 137.2, 132.9, 131.0, 130.9, 130.2, 128.5, 128.3, 126.3, 44.7, 27.9; HRMS (ESI) Calcd for $C_{18}H_{19}O_2$ $[M + H]^+$ 267.1385, found 267.1383.

2.5. References

1. Wang, B.-Q.; Xiang, S.-K.; Sun, Z.-P.; Guan, B.-T.; Hu, P.; Zhao, K.-Q.; Shi, Z.-J., *Tetrahedron Lett.* **2008,** *49* (27), 4310-4312.

2. Schäfer, G.; Bode, J. W., *Angew. Chem. Int. Ed.* **2011,** *50* (46), 10913-10916.

3. Rueping, M.; Nachtsheim, B. J.; Ieawsuwan, W., *Adv. Synth. Catal.* **2006,** *348* (9), 1033-1037.

4. *Synlett* **1996**, 557.

5. Chowdhury, S.; Georghiou, P. E., *Tetrahedron Lett.* **1999,** *40* (43), 7599-7603.

6. Bandgar, B. P.; Bettigeri, S. V.; Phopase, J., *Tetrahedron Lett.* **2004,** *45* (37), 6959-6962.

7. McLaughlin, M., *Org. Lett.* **2005,** *7* (22), 4875-4878.

8. Crawforth, C. M.; Burling, S.; Fairlamb, I. J. S.; Kapdi, A. R.; Taylor, R. J. K.; Whitwood, A. C., *Tetrahedron* **2005,** *61* (41), 9736-9751.

9. Kofink, C. C.; Knochel, P., *Org. Lett.* **2006,** *8* (18), 4121-4124.

10. Bedford, R. B.; Huwe, M.; Wilkinson, M. C., *Chem. Commun.* **2009,** (5), 600-602.

11. Ackerman, L. K. G.; Anka-Lufford, L. L.; Naodovic, M.; Weix, D. J., *Chemical Science* **2015,** *6* (2), 1115-1119.

12. Zhang, J.; Lu, G.; Xu, J.; Sun, H.; Shen, Q., *Org. Lett.* **2016,** *18* (12), 2860-2863.

13. Pal, S.; Chowdhury, S.; Rozwadowski, E.; Auffrant, A.; Gosmini, C., *Adv. Synth. Catal.* **2016,** *358* (15), 2431-2435.

14. Ackermann, L.; Novák, P., *Org. Lett.* **2009,** *11* (21), 4966-4969.

15. Wiest, J. M.; Pöthig, A.; Bach, T., *Org. Lett.* **2016,** *18* (4), 852-855.

16. Lu, M.-Z.; Wang, C.-Q.; Song, S.-J.; Loh, T.-P., *Organic Chemistry Frontiers* **2017,** *4* (2), 303-307.

17. Cera, G.; Haven, T.; Ackermann, L., *Angew. Chem. Int. Ed.* **2016,** *55* (4), 1484-1488.

18. Aihara, Y.; Wuelbern, J.; Chatani, N., *Bull. Chem. Soc. Jpn.* **2015,** *88* (3), 438-446.

19. Song, W.; Ackermann, L., *Angew. Chem. Int. Ed.* **2012,** *51* (33), 8251-8254.

20. Xu, W.; Paira, R.; Yoshikai, N., *Org. Lett.* **2015,** *17* (17), 4192-4195.

21. Fukutani, T.; Umeda, N.; Hirano, K.; Satoh, T.; Miura, M., *Chem. Commun.* **2009,** (34), 5141-5143.

22. Tran, D. N.; Cramer, N., *Angew. Chem. Int. Ed.* **2011,** *50* (47), 11098-11102.

23. Xu, W.; Yoshikai, N., *Angew. Chem. Int. Ed.* **2016,** *55* (41), 12731-12735.

24. Xu, W.; Yoshikai, N., *Chemical Science* **2017,** *8* (8), 5299-5304.

25. Xu, W.; Yoshikai, N., *Beilstein Journal of Organic Chemistry* **2018,** *14*, 709-715.

26. Zhang, L.; Ang, G. Y.; Chiba, S., *Org. Lett.* **2010,** *12* (16), 3682-3685.

27. Weiberth, F. J.; Hall, S. S., *J. Org. Chem.* **1978,** *52*, 3901-3904.

28. Xu, W.; Yoshikai, N., *Chem. Sci.* **2017,** *8* (8), 5299-5304.

29. He, R.; Huang, Z.-T.; Zheng, Q.-Y.; Wang, C., *Angew. Chem., Int. Ed.* **2014,** *53* (19), 4950-3.

30. Xu, W.; Pek, J. H.; Yoshikai, N., *Asian J. Org. Chem.* **2018,** *7*, 1351-1354.

31. Xu, W.; Yoshikai, N., *ChemSusChem* **2019,** *12*.

32. McLaughlin, M., *Org. Lett.* **2005,** *7* (22), 4875-8.

33. Xu, W.; Paira, R.; Yoshikai, N., *Org. Lett.* **2015,** *17* (17), 4192-5.

34. Trost, B. M.; Czabaniuk, L. C., *J. Am. Chem. Soc.* **2012,** *134* (13), 5778-81.

Chapter 3: Synthesis and Application of Aryl-, Heteroaryl-, and Vinyl-BX Reagents

3.1. Introduction

Polyvalent iodine compounds have found numerous applications in organic synthesis. [1] The oxidizing properties of iodine-(III) and iodine-(V) derivatives have been extensively exploited in oxidative organic transformations. For example, Dess-Martin periodinane (DMP)[2] and 2-iodoxy-benzoic acid (IBX)[3] have been widely used for selective oxidation of alcohols under mild conditions. Meanwhile, iodine(III) compounds have proved to serve as group-transfer agents for C–C and C–heteroatom bond-forming reactions. Thus, the weak three-center four-electron bonding (X–I–X) of such compounds makes them facile donors of the ligand X via X–I bond cleavage (Scheme 3.1). On the other hand, the intrinsic weakness of the hypervalent iodine bonds make some iodine(III) compounds unstable and even practically inaccessible. In this context, cyclic hypervalent iodine reagents have received significant attention for their high stability, ease of handling, and tunable reactivity owing to the rigid benziodoxol(on)es (BX) backbone.[4] In particular, Togni's reagent[5] and ethynylbenziodoxol(on)e (EBX)[6] have been extensively used for the transfer of trifluoromethyl and alkynyl groups respectively. Benziodoxol(on)e-based reagents have also been used for the transfer of azide, cyano and halogen group. Thus, the development new type of benziodoxol(on)es derivatives holds significant promise in synthetic methodology. In the following section, synthesis and application of aryl-, heteroaryl-, and vinylbenxiodoxol(on)es are discussed.

Scheme 3.1. Structure of benziodoxol(on)es and hypervalent iodine bond

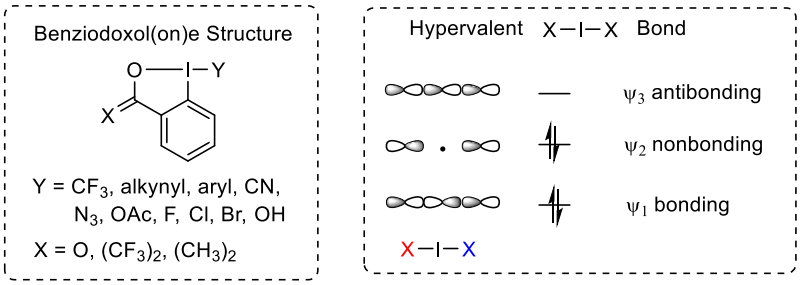

3.2. Aryl- and Heteroaryl-BX

3.2.1. Synthesis of Aryl-BX and Heteroaryl-BX

One of the early examples of phenyl-benziodoxolone (Ph-BX) synthesis was reported by Olofsson et al (Scheme 3.2).[7] Thus, 2-iodobenzoic acid was oxidized using meta-chloroperbenzoic acid, followed by treatment with trifluoromethanesulfonic acid and benzene to afford a diaryliodonium triflate. Finally, cyclization of the diaryliodonium triflate was conducted using 25% aq. ammonia to form the desired Ph-BX. Despite the high efficiency and operational simplicity only the parent Ph-BX was synthesized by this method.

Scheme 3.2. Synthesis of Ph-VBX from 2-iodobenzoic acid

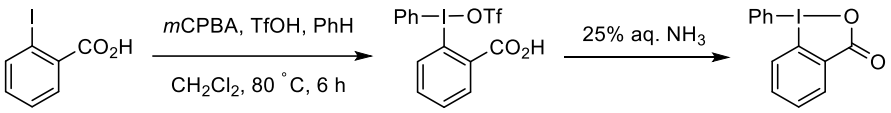

Later, Zhdankin et al. reported a more general synthetic approach to various aryl-benziodoxolones starting from 2-iodobenzoic acid.[8] Thus, 2-iodobenzoic acid was oxidized with oxone, followed by treatment with H_2SO_4 and arenes to afford a variety of electron-rich aryl-benziodoxolones in 40-94% yields (Scheme 3.3). This protocol tolerated functional groups such as alkyl, halide, ester and carboxylic acid.

Scheme 3.3. Preparation of aryl-benziodoxolones

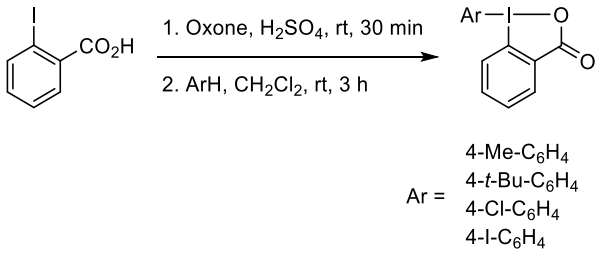

Recently, Yoshikai and coworkers demonstrated a mild and practical approach to access (hetero)aryl-benziodoxoles derivatives via aromatic C–H iodanation.[9] The reaction of Zhdankin's benziodoxole triflate (BXT) with electron-rich (hetero)arenes proceeded at room temperature to form the corresponding (hetero)aryl-benziodoxoles (Scheme 3.4). The reaction displayed site selectivity toward the electron-rich and sterically less hindered position of the aromatic ring. As a limitation, highly electron-rich arenes such as 1,4-dimethoxy benzene and N,N-dimethylaniline failed to participate in the reaction system presumably due to unfavorable oxidation by BXT. Another limitation is the lack of reactivity of electron neutral and electron-poor arenes.

Scheme 3.4. Aryl-benziodoxole synthesis via λ^3-iodanation

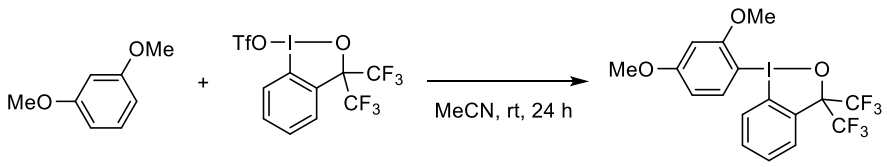

The Waser group reported the first synthesis of heterocycle-based benziodoxolone derivatives from indoles and pyrroles using Lewis acid catalyst ($Zn(OTf)_2$) and acetoxy-benziodoxolone (Scheme 3.5).[10] A good number of indole-BXs containing methoxy, fluoro, chloro, iodo, boryl groups at various positions were

prepared in high yields. Furthermore, thiophene-BX, furan-BX, carbazole-BX were also obtained albeit in low yield. A proposed catalytic cycle involves the activation of acetoxy-benziodoxolone with $Zn(OTf)_2$ and electrophilic attack of the iodonium species **I**, on the indole substrate, followed by deprotonation of the intermediate **II** to afford the indole-BX product and regenerate the zinc catalyst.

Scheme 3.5. Zn-Catalyzed synthesis of indole/pyrrole-benziodoxolones

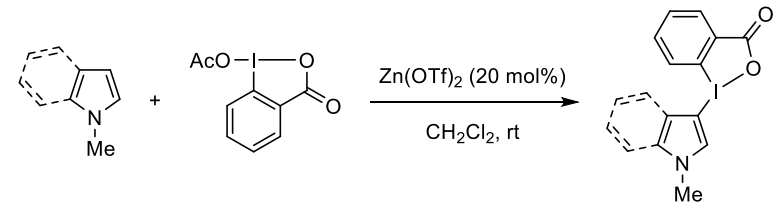

Proposed catalytic cycle

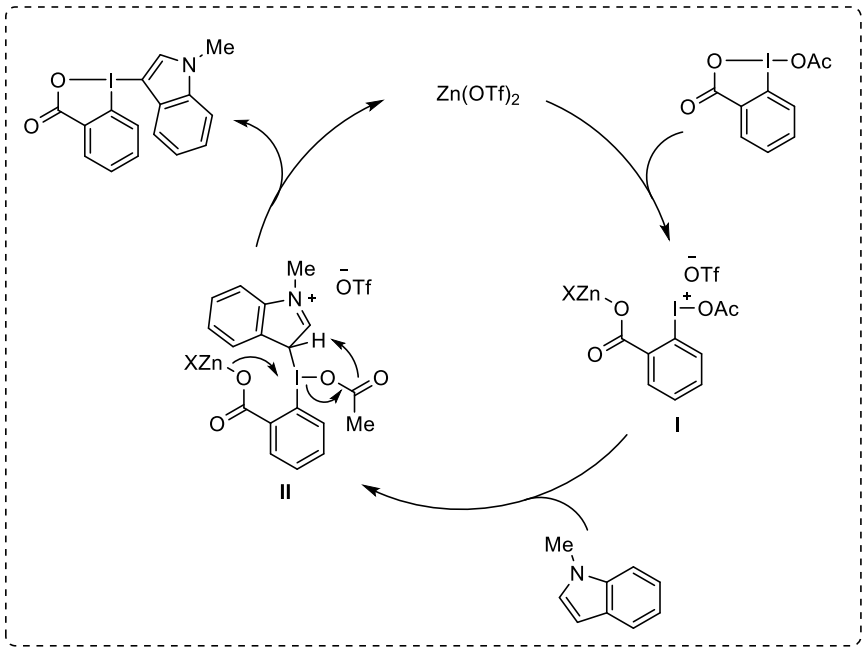

Waser and coworkers demonstrated boron-to-iodine(III) group transfer as a means to synthesize C-2 substituted indole-BXs, which were not accessible using the above $Zn(OTf)_2$-catalyzed method. Thus, the reaction between indole-2-trifluoroborate salts

and fluoro-benziodoxol(on)es in the presence of aqueous $NaBF_4$ afforded the corresponding indole-2-BXs in good yields (Scheme 3.6).[11]

Scheme 3.6. Synthetic protocol to access C2-substituted indole-BX

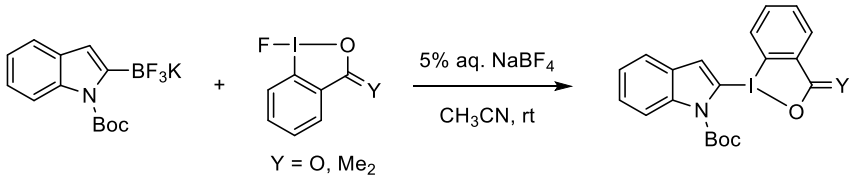

In 2017, Yoshikai group reported the synthesis of heteroaryl-benziodoxoles via electrophilic activation of alkynes with BXT.[12] Thus, alkynylarenes bearing ortho-heteroatom substituents such as methoxy, methylthio, methoxycarbonyl groups, on treatment with BXT, underwent cylcization to afford benzofuran, benzothiophene, and isocoumarin derivatives bearing BX (Scheme 3.7a). Indole-based-BX reagents were also prepared from alkynylarenes bearing ortho-NHTs group and BXT in the presence of Na_2CO_3 (Scheme 3.7b).

Scheme 3.7. Benziodoxole triflate promoted synthesis of heteroaryl-BXs

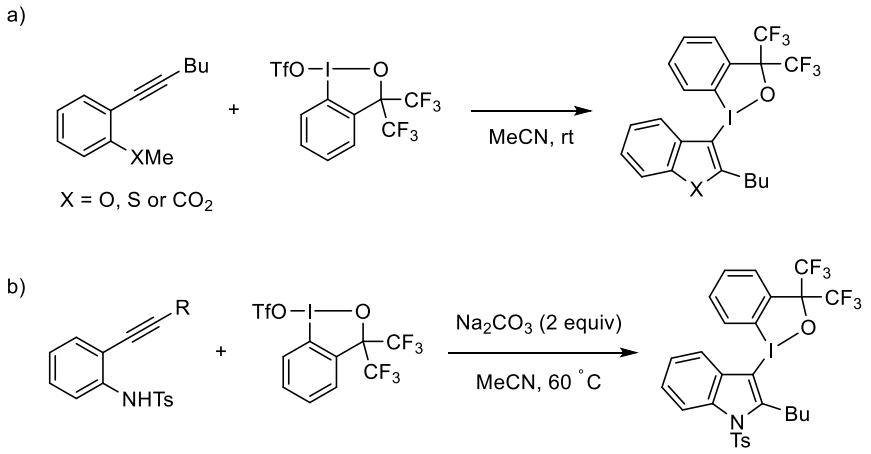

3.2.2. Synthetic Application of Heteroaryl-BX

Heteroaryl-BX reagents have found application in transition metal-catalyzed C–H functionalization reactions. For example, Waser group utilized indole-BXs for ortho-heteroarylation of 2-aryl pyridines and benzamides (Scheme 3.8).[10] In the former case, a catalytic system comprised of [Cp^*RhCl_2], NaOPiv ,and $AgSbF_6$ was found to be optimum to introduce indole or pyrrole groups to the *ortho* position of 2-phenyl pyridine (Scheme 3.8a). On the other hand, a ruthenium-based catalytic system was effective to promote *ortho*-C–H indolation of benzamides (Scheme 3.8b). In both the cases, the scopes of the heteroaryl-BXs and the arene coupling partners are quite broad. Although this work represents a steppingstone towards the utilization of indole- and pyrrole-based electrophilic synthons in synthetic and medicinal chemistry, few aspects demand further discussion. The selectivity of C-2 versus C-3 functionalization of pyrrole is troublesome and requires further optimization whereas yield for furan-, thiophene- and carbazole-BX is on the lower side.

Scheme 3.8. Rh- and Ru-catalyzed C–H indolation

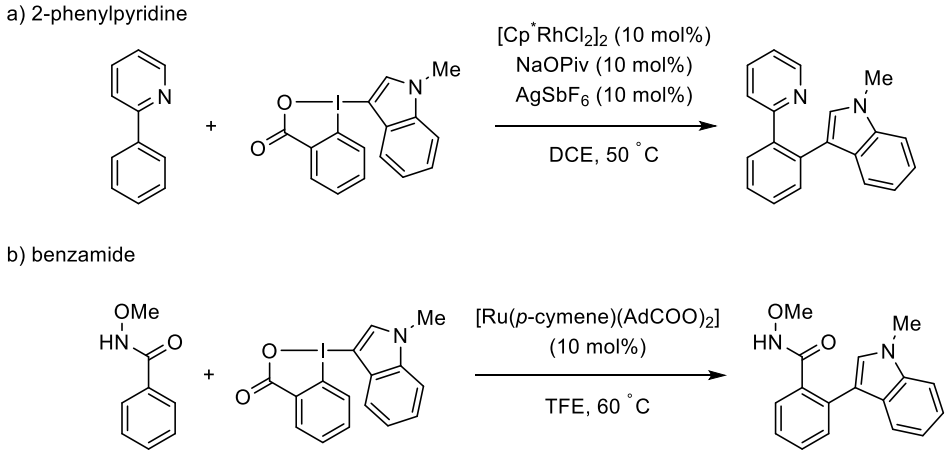

Later on, the same group extended the substrate scope for C–H coupling partners to ortho-hydroxy and ortho-amino benzaldehydes (Scheme 3.9).[13] At room

temperature, chelation-assisted C–H acylation reaction was carried out using iridium(III)-based catalytic system with N-substituted indole-BX, affording a broad range of aryl indolyl ketones in good to moderate yield (Scheme 3.9a). This method is amenable to an electronically diverse range of functional groups such as methoxy, halogen, aldehyde, and nitro, groups. Similar to salicylaldehyde, 2-aminobenzaldehydes bearing N-tosyl directing group also underwent heteroarylation reaction via transition metal-catalyzed C–H functionalization. In this case, of $[Cp^*RhCl_2]_2$ in combination with KOAc in MeOH promoted the coupling between 2-aminobenzaldehydes with indole-BX to give functionalized diaryl ketone in good to excellent yield (Scheme 3.9b).

Scheme 3.9. Directed C–H heteroarylation of benzaldehydes

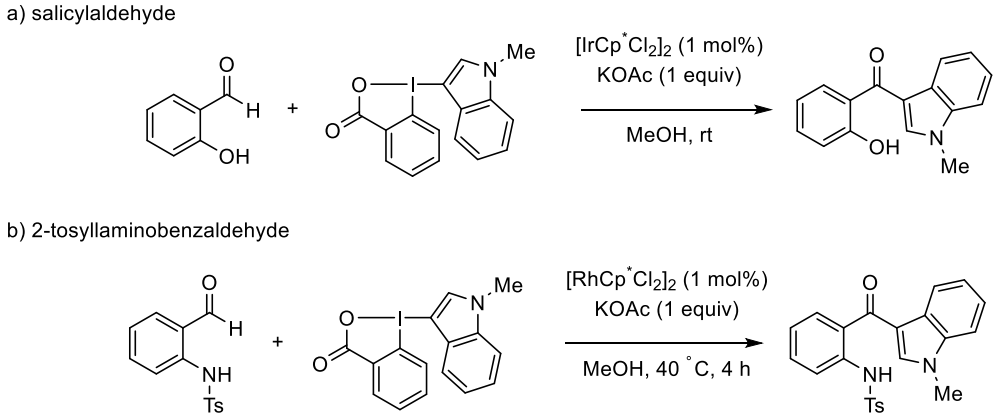

In 2018, Waser group further utilized indole-BX derivatives for regioselective C–H indolation reaction of bipyridinones and quinoline N-oxides a using rhodium based catalytic system (Scheme 3.10).[14] A catalytic system consists of $[Cp^*RhCl_2]_2$, $AgSbF_6$, and $Zn(OTf)_2$ promoted C-6 selective indolation of 2*H*-[1,2'-bipyridin]-2-one derivatives in good to excellent yield (Scheme 3.10a). On the other hand, quinoline N-oxides underwent indolation at the C-8 positions via directed C–H functionalization

(Scheme 3.10b). Notably, Lewis acidic zinc triflate was necessary for the success of this protocol, assuming it coordinates with the I^{III} center and weakens the O–I bond to promote the desired reaction.

Scheme 3.10. Rh-catalyzed regioselective indolation of heteroarenes

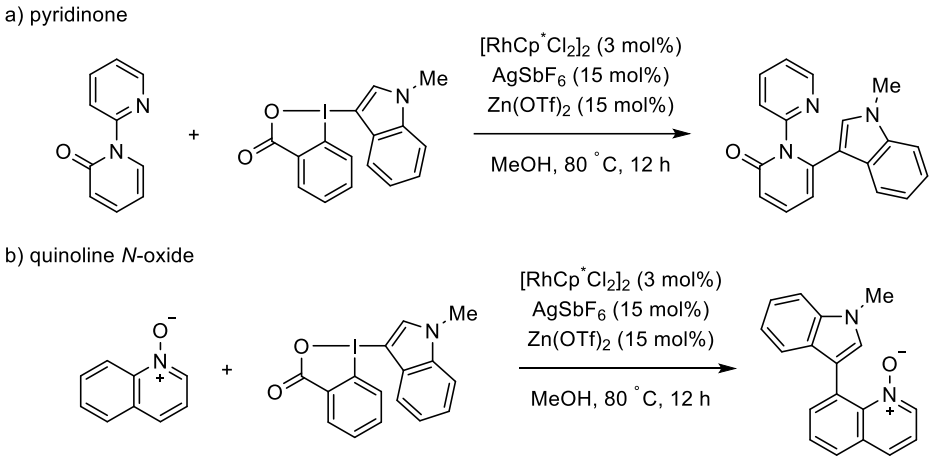

Most of the synthetic protocols utilizing heteroaromatic benziodoxol(one)s have revolved around transition metal-catalyzed C–H functionalization reaction. A synthetic protocol involving indole-BXs under metal-free conditions was demonstrated by Waser group, where they accomplished oxidative cross-coupling between indole-BXs and electron-rich arenes in the presence of Lewis acid (Scheme 3.11).[11]

Scheme 3.11. Metal-free oxidative coupling of heteroarene with indole-BX

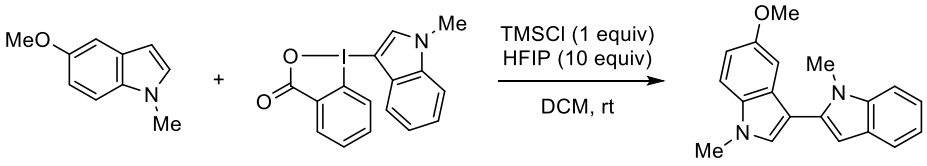

3.3. Vinyl-BX

3.3.1. Synthesis of Vinyl-BX

A selective and multistep method for the preparation of (*E*)-configured aryl-substituted vinyl-benziodoxolones was reported by Olofsson and coworkers.[15] At first, 2-iodobenzoic acid was oxidized with *m*CPBA in the presence of trifluoromethanesulfonic acid (TfOH), and subsequently reacted with (*E*)-styrylboronic acid to form acyclic vinyliodonium salt, which later underwent cyclization in the presence of base to afford phenyl-substituted vinyl-benziodoxolone (Scheme 3.12). The structure of vinyl-benziodoxolone was unambiguously characterized by X-ray crystallography. A variety of vinylboronic acids could be used in one pot manner for the synthesis of the corresponding vinyl-benziodoxolones. Various *para*-substituted Ar-VBX reagents were obtained in moderate yields, while yield of cyclohexyl substituted-VBX was modest.

Scheme 3.12. One-pot synthesis of VBX derivatives

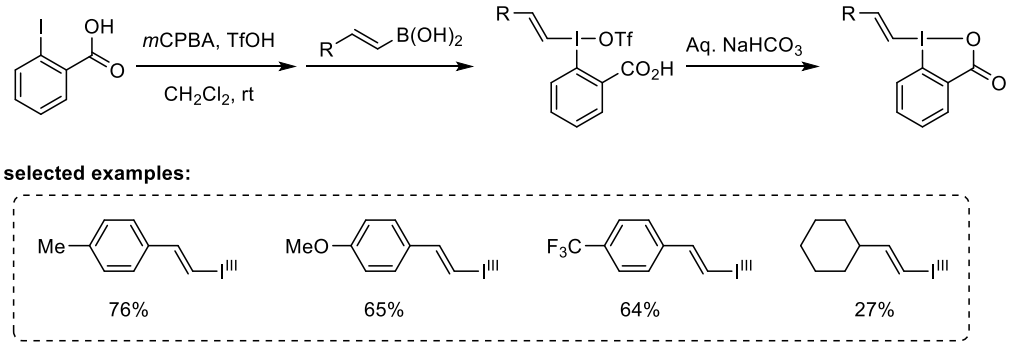

In 2016, Yoshikai and coworkers reported a method to access alkenyl-benziodoxoles from ethynyl-benziodoxoles (EBX) and carboxylic acid using palladium catalyst at room temperature (Scheme 3.13).[16] The reactions follow initial coordination of Pd^{II} center to the triple bond of Ph-EBX to form intermediate **I**, followed by 1,2-I(III)

shift from to generate a vinylidene-palladium intermediate **II**. Migratory insertion of the intermediate **II** and protodemetalation of the vinylpalladium intermediate **III**, would afford the oxygen-substituted vinyl-BX.

Scheme 3.13. Pd-catalyzed synthesis of O-VBX derivatives

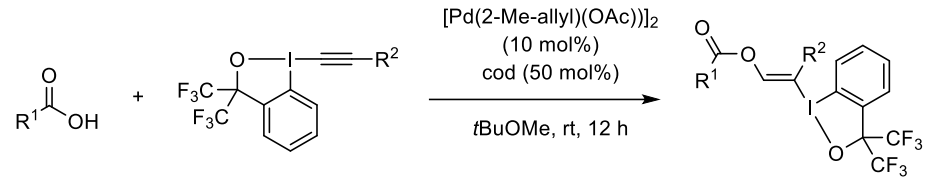

Proposed mechanism:

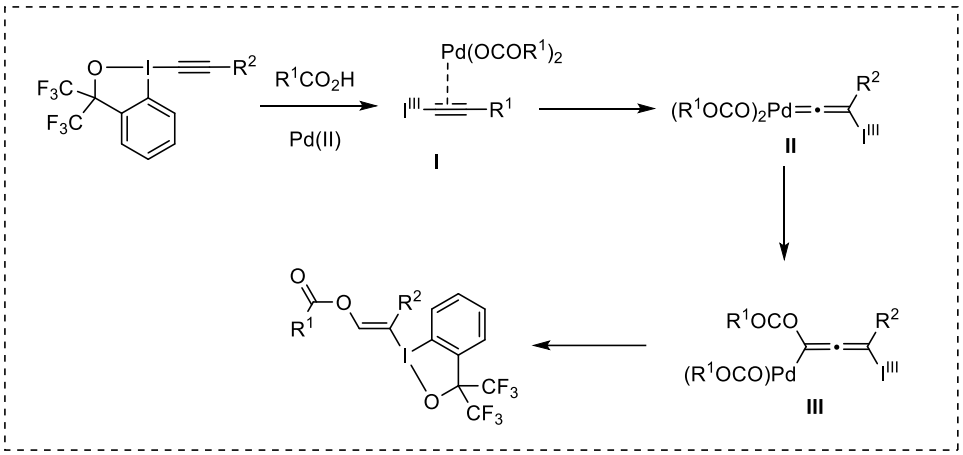

In 2019 Waser and coworkers demonstrated the synthesis of nitrogen-substituted vinyl-benziodoxolone in *Z*-selective fashion.[17] In the presence of a catalytic amount of Cs_2CO_3, para-methoxyphenyl-substituted tosyl amide reacted with EBX to afford nitrogen-substituted VBX derivatives in good to excellent yield (Scheme 3.14). Besides, phenoxy-VBX reagents were also obtained by this protocol by changing the nucleophiles to phenols under the optimized reaction conditions.

Scheme 3.14. Stereoselective synthesis of N-VBX derivatives

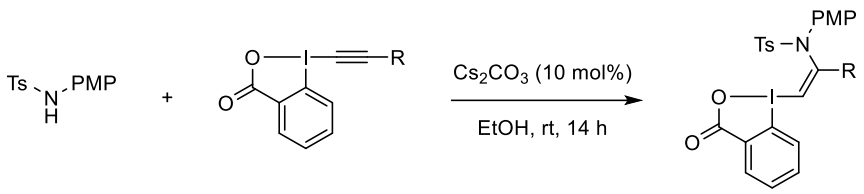

In 2018, Miyake and coworkers reported that 4-hydroxy anisole reacts with Ph-EBX in dark in presence of a stoichiometric amount of base to produce phenoxy-substituted VBX (Scheme 3.15a).[18] More recently, Itoh group demonstrated a straightforward protocol for the synthesis of phenoxy-VBX from unsubstituted EBX-MeCN complex and phenols under ambient reaction conditions (Scheme 3.15b).[19]

Scheme 3.15. Phenoxy-VBX synthesis from EBX and phenols

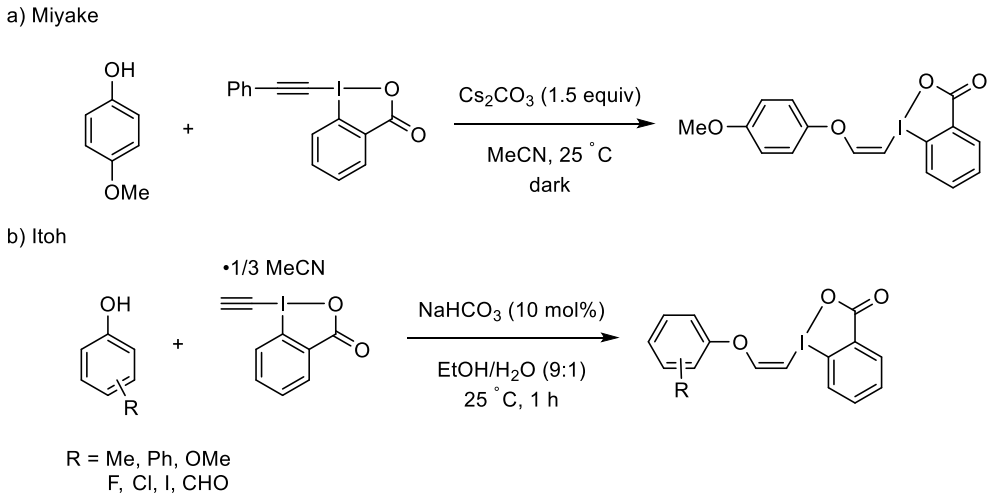

In addition to aryl, nitrogen, and oxygen-substituted VBX, sulfur-substituted VBX have also been reported in the literature. In 2019, Waser and coworkers reported stereoselective synthesis of (*Z*)-S-VBXs from various EBXs and phenyl or benzyl thiols under room-temperature conditions (Scheme 3.16).[20]

Scheme 3.16. Thiophenol-derived VBX synthesis

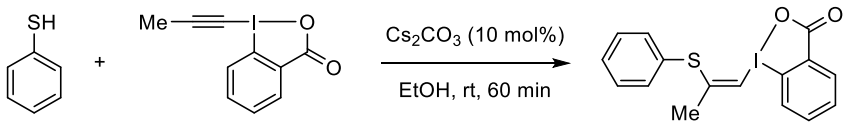

In 2019, Yoshikai et al. developed a stereo-controlled synthesis of halogenated VBX derivatives from EBXs (Scheme 3.17).[21] A stereoselective hydrochlorination of EBX was performed using pyridine hydrochloride to give 2-chloro VBX through an *anti*-addition pathway. On the other hand, iodochlorination of EBX using iodine monochloride followed a syn-addition pathway to afforded the corresponding tetrasubstituted VBXs.

Scheme 3.17. Stereoselective halovinyl-benziodoxoles synthesis

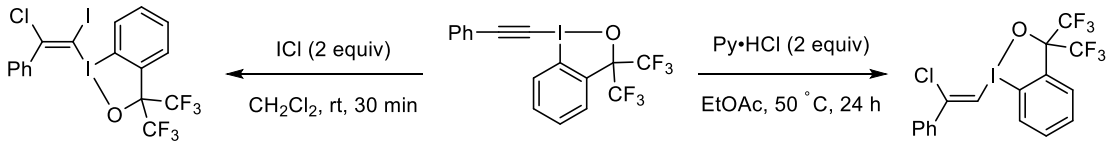

3.3.2. Synthetic Application of Vinyl-BX

Vinylbenziodoxolones have been used as excellent vinylating agents for the construction of carbon-carbon and carbon-heteroatom bonds. For example, Olofsson group reported vinylation of thiols with aryl-VBX reagents using stoichiometric amount *t*BuOK base in THF to afford *E*-alkenyl sulfides (Scheme 3.18).[22] A number of aryl and alkyl thiols were compatible with this reaction system. Thiophenols containing electron-rich and electron-poor aryl ring smoothly could be vinylated with excellent *E*-stereoselectivity. Thiols bearing allyl, furanyl, pyridyl groups were well tolerated. Also, a variety of aryl-VBX containing alkyl, aryl, methoxy, trifluoromethoxy groups reacted

smoothly with thiophenol to give the desired products in high yield and excellent *E/Z* ratio (up to 20:1).

Scheme 3.18. Vinylation of thiols using VBX reagents

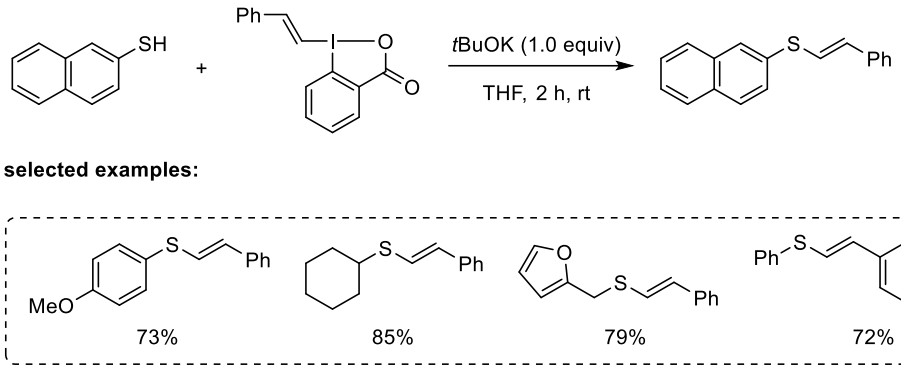

In their latest work, Olofsson and coworkers have developed a method to form carbon-phosphorus bonds using VBX reagents.[23] Ph-VBX in the presence of DBU as organic base selectively vinylated phosphine oxides at room temperature (Scheme 3.19). A broad range of symmetric and unsymmetric diarylphosphine oxides underwent the desired vinylation reaction under the optimized conditions. Importantly, phosphine oxides containing electron-rich aryl rings provided high yields whereas electron-poor counterparts gave low yields. For the scope of VBX reagents, a large number of functional groups such as phenyl, CF_3, and Cl groups at the *para*-position of the aryl ring reacted were tolerated affording the desired vinylated products in good yields. Alkylaryl phosphine oxides and H-phosphinates were also amenable to the present system at an elevated temperature.

Scheme 3.19. Vinylation of phosphine oxides using VBX reagents

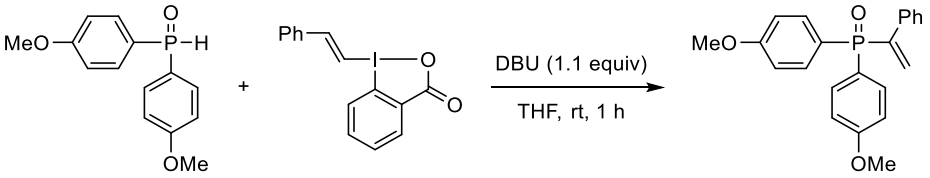

Utilization of vinyl-benziodoxolone as alkenylating reagent in C–H functionalization was developed by Nachtsheim (Scheme 3.20).[24] They accomplished NH_2-directed C–H alkenylation of 2-vinylanilines with Ar-VBXs using a catalytic system consisting of $[IrCp^*Cl_2]_2$ (2.5 mol%) and NaOBz (20 mol%) under ambient conditions. A broad range of α-substituted vinylanilines underwent alkene transfer to form the corresponding 1,3-dienes in good to excellent yield with (*Z*,*E*)-stereoselectivity.

Scheme 3.20. Ir-catalyzed C–H alkenylation of 2-vinylaniline

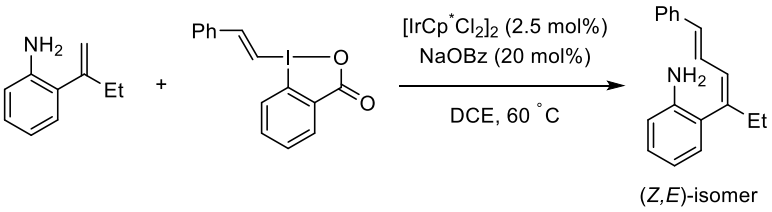

In 2020, Waser group achieved oxy-vinylation of diazo compounds with VBX reagents using a copper-based catalytic system (Scheme 3.21).[25] A cationic copper salt and bis-oxazoline (BOX) ligand-based catalytic system promoted the insertion of diazo compounds into VBX reagent. The reaction tolerated various VBX reagents containing aryl- alkyl-, and π-conjugated scaffolds with high efficiency unharming functional groups such as TIPS, chloro, and ester.The reaction involves *in situ* generations of an electrophilic metal-carbene complex (**B**) from the copper (I) precatalyst and the diazo

compound, followed by 1,1-insertion of the complex **B** into the I–O bond to give an iodonium intermediate **C**, and vinyl transfer, affording the oxyvinylation product.

Scheme 3.21. Oxyvinylation of diazo compound using copper catalyst

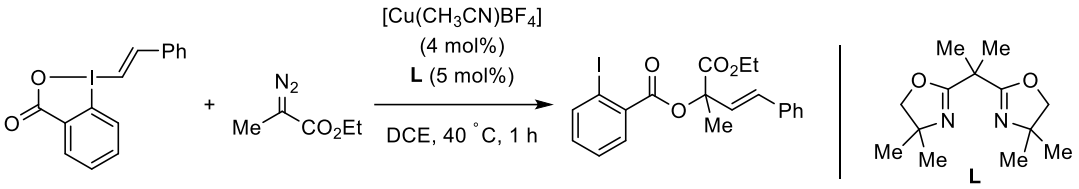

proposed mechanism:

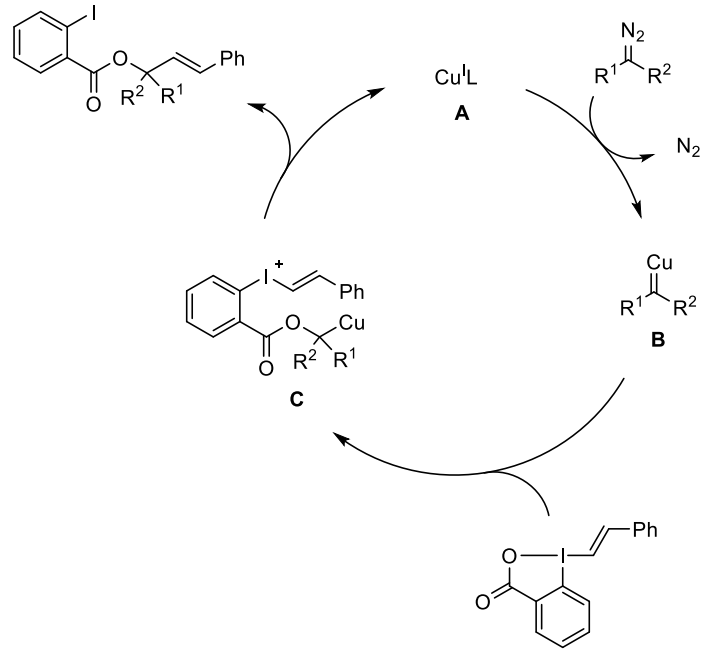

VBX reagents have been found to be good radical acceptors, and several research groups have utilized this property to perform photoredox catalysis. For example, Leonori and coworkers used Ph-VBX reagents for the synthesis of polyfunctionalized nitrogen heterocycles using a light-mediated photocatalytic condition (Scheme 3.22a).[26] In another work, Nemoto group demonstrated visible-light-induced C(sp^3)–H alkenylation of THF with Ar-VBX reagents in the presence of benzophenone promoter (Scheme 3.22b).[27]

Scheme 3.22. Light-induced alkenylation reaction with VBX

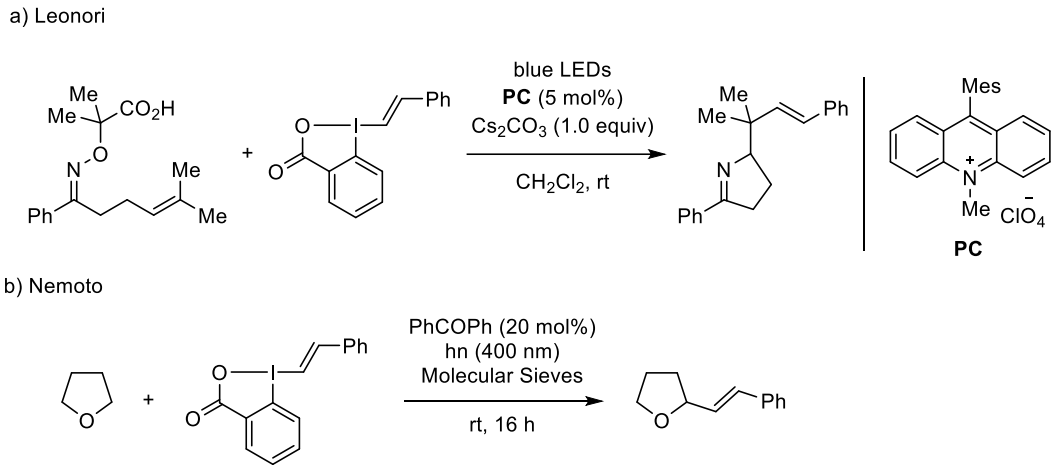

3.4. Future Outlook

In recent years, the synthesis and application of benziodoxol(on)s have been explored by many research groups. BX reagents display efficient group-transfer ability as well as unique reactivity, drawing significant attention from the organic synthetic community. Various approaches have enabled access to a wide range of aryl-, heteroaryl- and vinyl-BX reagents. Despite the significant progress, there remains much room for the development of new BX reagents derived from readily available starting materials. Besides, the application of hetero-aryl or vinyl-BXs is often limited to the protocol using late transition metals or strong bases. Furthermore, mechanistic understanding of the reactions involving BX reagents is sometimes difficult to rationalize.

3.5. References

1. Stang, P. J.; Zhdankin, V. V., *Chem. Rev.* **1996,** *96* (3), 1123-1178.

2. (a) Dess, D. B.; Martin, J. C., *The Journal of Organic Chemistry* **1983,** *48* (22), 4155-4156; (b) Dess, D. B.; Martin, J. C., *J. Am. Chem. Soc.* **1991,** *113* (19), 7277-7287.

3. Frigerio, M.; Santagostino, M.; Sputore, S.; Palmisano, G., *The Journal of Organic Chemistry* **1995,** *60* (22), 7272-7276.

4. Wang, X.; Studer, A., *Acc. Chem. Res.* **2017,** *50* (7), 1712-1724.

5. Charpentier, J.; Früh, N.; Togni, A., *Chem. Rev.* **2015,** *115*, 650.

6. (a) Brand, J. P.; Chevalley, C.; Scopelliti, R.; Waser, J., *Chem.—Eur. J.* **2012,** *18*, 5655; (b) Wodrich, M. D.; Caramenti, P.; Waser, J., *Org. Lett.* **2016,** *18*, 60; (c) Shinde, P. S.; Patil, N. T., *Eur. J. Org. Chem.* **2017**, 3512; (d) González, D. F.; Brand, J. P.; Waser, J., *Chem.—Eur. J.* **2010,** *16*, 9457.

7. Merritt, E. A.; Olofsson, B., *Eur. J. Org. Chem.* **2011,** *2011* (20-21), 3690-3694.

8. Yusubov, M. S.; Yusubova, R. Y.; Nemykin, V. N.; Zhdankin, V. V., *The Journal of Organic Chemistry* **2013,** *78* (8), 3767-3773.

9. Ding, W.; Wang, C.; Tan, J. R.; Ho, C. C.; León, F.; Garcia, F.; Yoshikai, N., *Chemical Science* **2020**.

10. Caramenti, P.; Nicolai, S.; Waser, J., *Chemistry – A European Journal* **2017,** *23* (59), 14702-14706.

11. Caramenti, P.; Nandi, R. K.; Waser, J., *Chemistry – A European Journal* **2018,** *24* (40), 10049-10053.

12. Wu, B.; Wu, J.; Yoshikai, N., *Chemistry – An Asian Journal* **2017,** *12* (24), 3123-3127.

13. Grenet, E.; Waser, J., *Org. Lett.* **2018,** *20* (5), 1473-1476.

14. Grenet, E.; Das, A.; Caramenti, P.; Waser, J., *Beilstein Journal of Organic Chemistry* **2018,** *14*, 1208-1214.

15. Stridfeldt, E.; Seemann, A.; Bouma, M. J.; Dey, C.; Ertan, A.; Olofsson, B., *Chemistry – A European Journal* **2016,** *22* (45), 16066-16070.

16. Wu, J.; Deng, X.; Hirao, H.; Yoshikai, N., *J. Am. Chem. Soc.* **2016,** *138* (29), 9105-9108.

17. Caramenti, P.; Declas, N.; Tessier, R.; Wodrich, M. D.; Waser, J., *Chemical Science* **2019,** *10* (11), 3223-3230.

18. Liu, B.; Lim, C. H.; Miyake, G. M., *J. Am. Chem. Soc.* **2018,** *140*, 12829.

19. Ura, T.; Shimbo, D.; Yudasaka, M.; Tada, N.; Itoh, A., *Chemistry – An Asian Journal* **2020,** *n/a* (n/a).

20. Tessier, R.; Ceballos, J.; Guidotti, N.; Simonet-Davin, R.; Fierz, B.; Waser, J., *Chem* **2019,** *5* (8), 2243-2263.

21. Wu, J.; Deng, X.; Yoshikai, N., *Chemistry – A European Journal* **2019,** *25* (33), 7839-7842.

22. Castoldi, L.; Di Tommaso, E. M.; Reitti, M.; Gräfen, B.; Olofsson, B., *Angew. Chem. Int. Ed.* **2020,** *59* (36), 15512-15516.

23. Castoldi, L.; Rajkiewicz, A. A.; Olofsson, B., *Chem. Commun.* **2020,** *56* (92), 14389-14392.

24. Boelke, A.; Caspers, L. D.; Nachtsheim, B. J., *Org. Lett.* **2017,** *19*, 5344.

25. Pisella, G.; Gagnebin, A.; Waser, J., *Org. Lett.* **2020,** *22* (10), 3884-3889.

26. Davies, J.; Sheikh, N. S.; Leonori, D., *Angew. Chem., Int. Ed.* **2017,** *56*, 13361.

27. Matsumoto, K.; Nakajima, M.; Nemoto, T., *The Journal of Organic Chemistry* **2020,** *85* (18), 11802-11811.

Chapter 4: Iodo(III)-Meyer–Schuster Rearrangement of Propargylic Alcohols Promoted by Benziodoxole Triflate

4.1. Introduction

The Meyer–Schuster (MS) rearrangement is the conversion of propargylic alcohols to α,β-unsaturated carbonyl compounds promoted by acid catalyst.[1] It offers a straightforward and economical method to access enone-type scaffolds from readily available propargyl alcohols which can be typically synthesized by the addition of acetylides to aldehydes or ketones. This reaction involves formal 1,3-hydroxyl migration involving allenyl carbocation generated by the acid activation of the hydroxy group (Scheme 4.1).

Scheme 4.1. Traditional MS rearrangement pathway

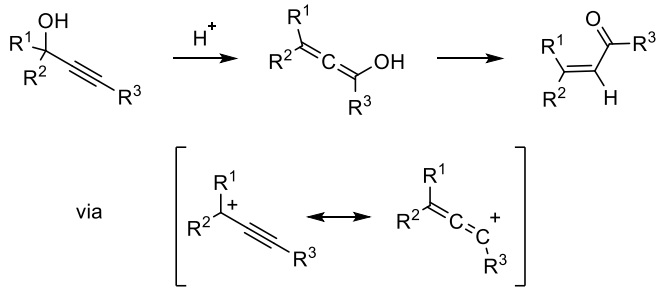

In recent years, MS rearrangement has been extensively studied aiming for milder reaction conditions and, more efficient and regioselective protocols with the aid of acid (Lewis- or Bronsted-acid) or transition-metal catalysts. Soft Lewis acids have played important role in the development of MS rearrangement with their unique mode of alkyne activation, facilitating nucleophilic attack on the alkyne, toward the desired product in favor of other possible pathways. In particular, Dudley group used $AuCl_3$

catalyst for the selective transformation of oxygen-protected propargyl alcohols to α,β-unsaturated ethyl ester (Scheme 4.2a).[2] This reaction system tolerated a broad range of substrates including secondary and tertiary propargyl alcohols under open-air reaction conditions with a catalyst loading as low as 0.1 mol%. However, stereoselectivity for the unsymmetrical propargylic alcohol was low. Later, Akai et al. reported a more general and robust catalytic system comprised of $MoO_2(acac)_2$ (1 mol%), $AuCl(PPh_3)$ (1 mol%), and AgOTf (1 mol%), which promoted the conversion of a broad range of primary, secondary and tertiary propargylic alcohols to the corresponding enones at room temperature (Scheme 4.2b).[3] Notably, the reported reaction protocol displayed with good to excellent *E*-selectivity tolerating sensitive functional groups such as alkoxy and dialkylamide at the acetylenic position. Vidari and coworkers reported that a similar metal-oxo complex of Re(V) alone can serve as a catalyst to promote MS rearrangement of propargylic alcohol the with high *E*-stereoselctivity (Scheme 4.2c).[4] Liu and co-workers reported microwave-assisted, $Sm(OTf)_3$ (1 mol%) and N-fluorobenzenesulfonimide (5 mol%) catalyzed conversion of propargylic alcohols to enones (Scheme 4.2d).[5]

Scheme 4.2. MS rearrangement of propargylic alcohols

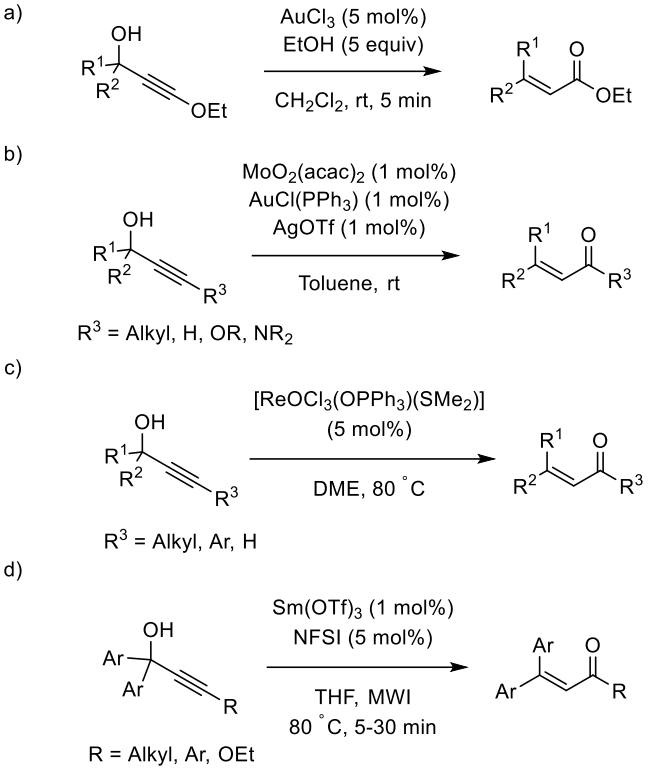

Since the 2000s, electrophile-intercepted MS rearrangement has gained significant attention from the synthetic community because it opens doors to access α-functionalized enones by trapping *in situ* generated allenol intermediate with an electrophile (Scheme 4.3). In the following section, representative examples of electrophile-intercepted MS rearrangement are discussed.

Scheme 4.3. Electrophile-intercepted MS rearrangement

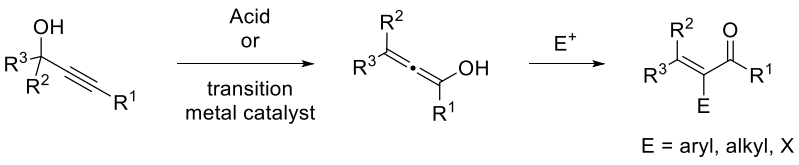

In 2009, Zhang and coworkers described iodo- and bromo-intercepted MS rearrangement to afford α-halo enones (Scheme 4.4a).[6] A catalytic system consisting of

$(Ph_3P)AuNTf_2$ and $MoO_2(acac)_2$ in combination with N-halosuccinimide (NXS) converted primary, secondary, and tertiary propargyl alcohol to the corresponding α-halo enones. In another work, Mohr et al. utilized stoichiometric $VOCl_3$ for halogenative MS rearrangement to give (*Z*)-configured haloenones, where NXS was again used as the halogen source (Scheme 4.4b).[7] Nevado group used a gold-based catalytic system and selectfluor as effective fluorine donor for the fluorinative MS rearrangement of propargylic acetates (Scheme 4.4c).[8]

Scheme 4.4. Halogen-intercepted MS rearrangement using transition metal catalyst

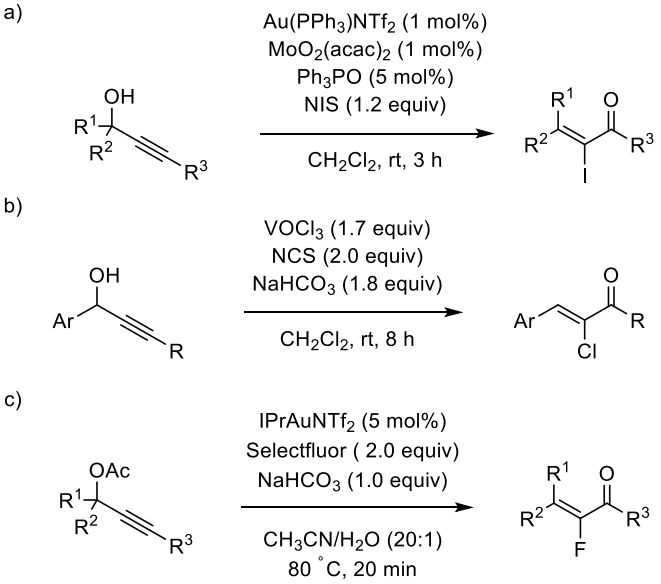

Scheme 4.5 illustrates a plausible catalytic cycle for the cooperative Mo-Au catalyzed halogenative MS rearrangement. At first, an *in situ* generated catalytically active species **A** would react with propargylic alcohol to generate molybdenum-propargylic alkoxide complex **B**, followed by gold-promoted [3,3]-sigmatropic shift to form allenic alkoxide **C**. Interception of NXS electrophile by the intermediate **C** would furnish α-halo-oxonium intermediate **D**, which finally would react with another molecule of

propargylic alcohol to form the halogen-intercepted MS product and regenerates the active catalyst.

Scheme 4.5. Proposed catalytic cycle for cooperative Mo-Au catalyzed α-haloenones synthesis

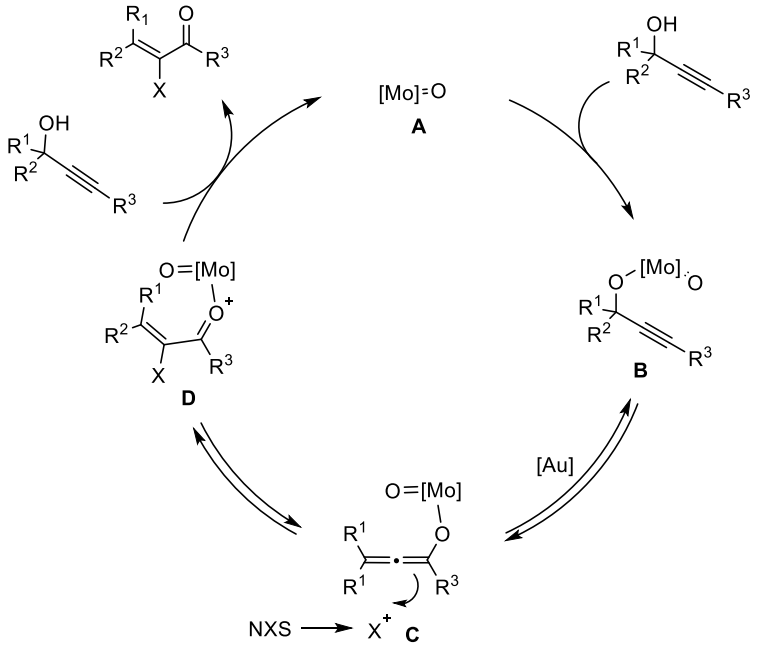

In 2013, Gaunt group achieved arylative MS rearrangement of secondary propargylic alcohol using copper(I) chloride catalyst and a diaryliodonium salt as an electrophile under mild conditions (Scheme 4.6a).[9] Later, Shin et al. developed an alternative protocol for arylative MS rearrangement of both secondary and tertiary propargylic alcohols with aryldiazonium using dual Au(I)-photoredox catalysis (Scheme 4.6b).[10]

Scheme 4.6. Aryl-intercepted MS rearrangement of propargylic alcohol

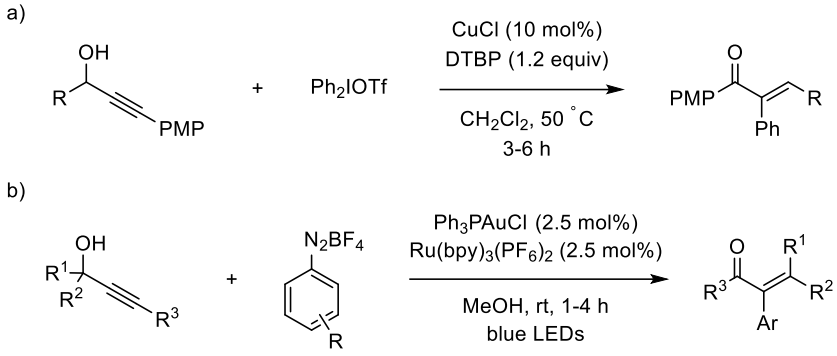

In 2014, Sodeoka and coworkers utilized Togni's reagent[11] as an electrophile for the intercepted MS rearrangement of primary and secondary propargylic alcohol (Scheme 4.7a). Thus, a copper-rhenium based dual catalytic system promoted *Z*-selective trifluoromethylation under ambient reaction conditions.[12] In contrast, Liu et al. reported the use of CuI as the sole catalyst along the Togni reagent resulted in trifluoromethylative MS rearrangement with *E*-selectivity (Scheme 4.7b).[13] Recently, Patil et al. accomplished cationic Au(I)-complex-catalyzed alkynylative MS rearrangement of propargylic alcohols with ethynylbenziodoxolones (EBX) to access (*E*)-enynones (Scheme 4.7c).[14]

Scheme 4.7. Intercepted trifluoromethylation, nitration, and alkynylation of propargylic alcohol

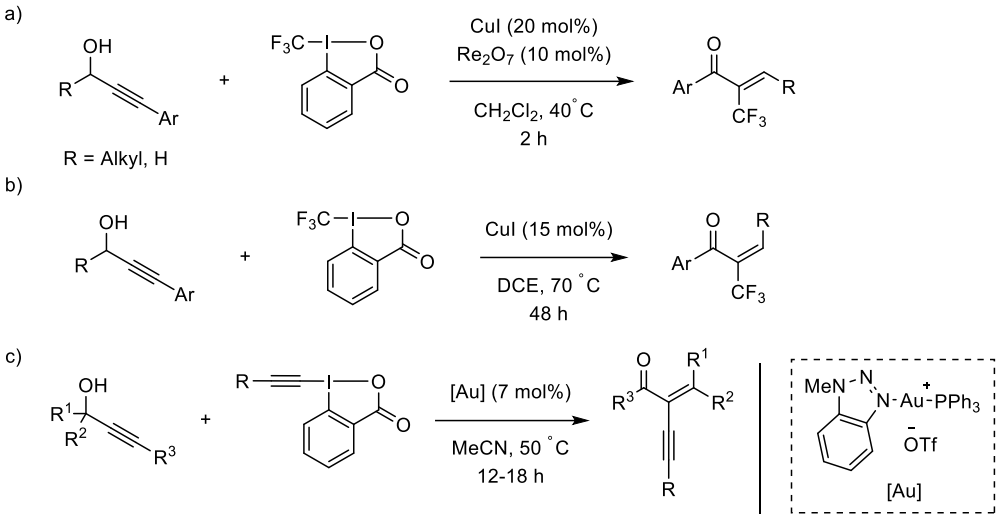

In 2011, Trost group reported allylative MS rearrangement of propargylic alcohol and allylic carbonate utilizing dual vanadium/palladium catalytic system (Scheme 4.8a).[15] In another work, Song and coworkers developed $Pd(OAc)_2$-catalyzed nitro-MS rearrangement of propargylic alcohols with *t*-$BuONO_2$ (Scheme 4.8b).[16]

Scheme 4.8. α-Allylation of propargylic alcohol using V/Pd-based catalyst

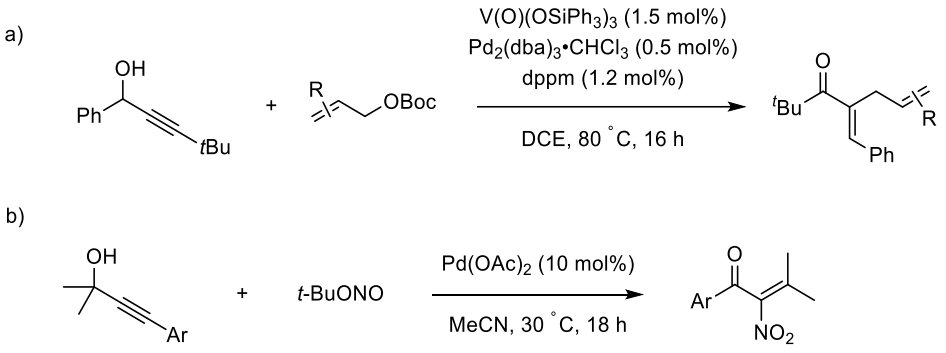

Several metal-free protocols for intercepted-MS rearrangement have been explored using iodine(I) electrophile. Wang et al. first reported metal-free, iodine-intercepted MS rearrangement of secondary propargylic alcohol to α-iodoenal (Scheme 4.9a).[17] In 2012, Moran and Rodriguez developed a protocol to convert tertiary

propargylic alcohol to α-iodo-substituted enone using *m*CPBA, trichloroacetic acid, and sodium iodide-based catalytic system (Scheme 4.9b).[18]

Scheme 4.9. Metal-free α-halogenation of propargylic alcohol

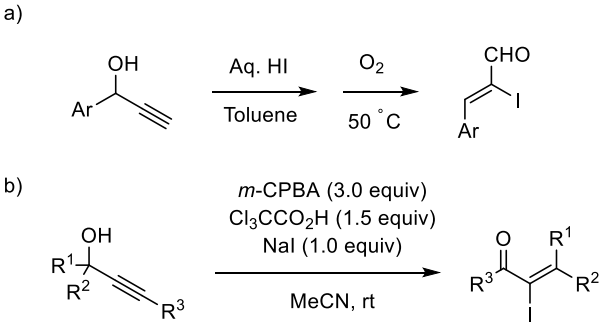

Later, Reddy group developed a method to access α-iodo-α,β-unsaturated esters from 3-alkoxypropargylic alcohols in *Z*-selective manner using iodine or NIS promotes at room temperature (Scheme 4.10).[19] According to the proposed mechanism, the first step is the activation of alkyne with iodonium ion, followed by formation iodo-ketinium intermediate through alkoxy activation, iodo-oxetene ring formation, and finally electrocyclic ring-opening would furnish halogenative MS product.

Scheme 4.10. Iodine-promoted MS rearrangement of alkoxy propargylic alcohol

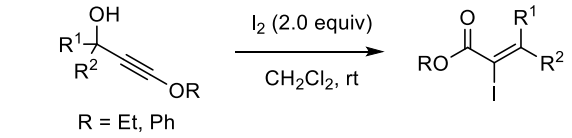

Proposed mechanism:

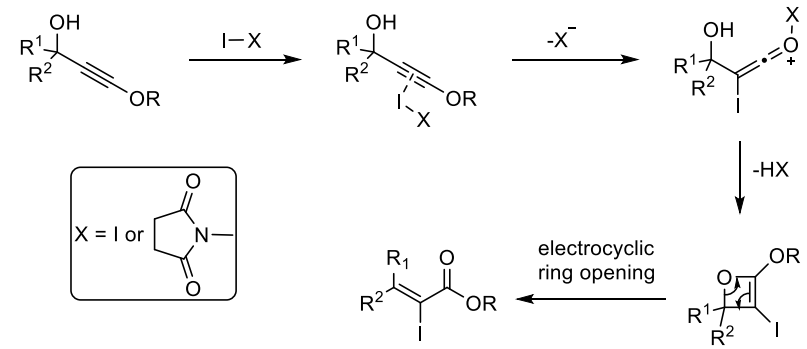

In 2015, Guan and coworkers developed reaction protocols for the synthesis of α-iodo unsaturated ketones from trisubstituted propargylic alcohol in *Z*-selective manner (Scheme 4.11).[20] Mechanism of the reaction follows, a) propargylic alcohol reacts with iodine to generate cationic intermediate **I**, followed by protonation with hypoiodous acid to form allenol intermediate **II**, which finally undergoes iodine-induced isomerization to generate major product **III**. Formation of *Z*-isomer is favoured over *E*-isomer because of the presence of steric hindrance in **IV**.

Scheme 4.11. Iodo-intercepted MS Rearrangement tertiary propargyl alcohol

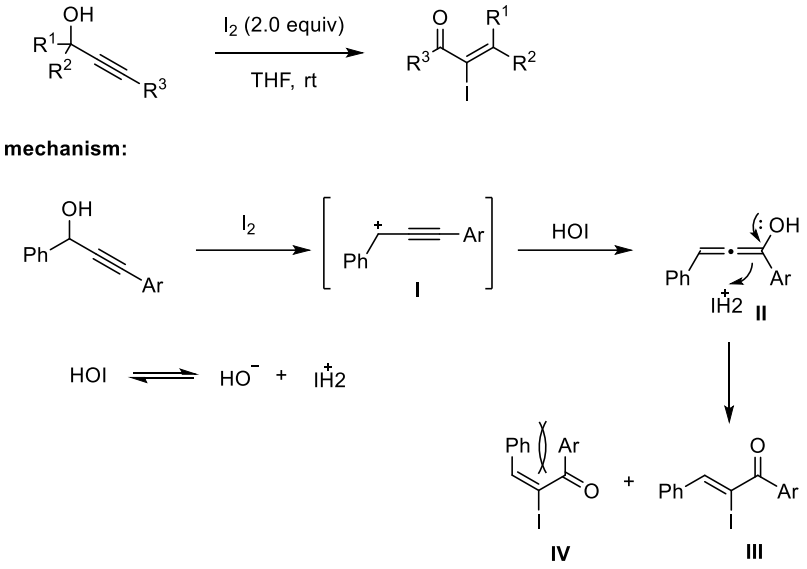

Furthermore, Skrydstrup et al. demonstrated metal-free, halogenative MS rearrangement of ynamides to afford α-iodo, bromo, and chloro acrylamides (Scheme 4.12).[21] A combination of succinimide-based electrophiles (NIS, NBS, and NCS) and $NaHCO_3$ base in MeCN converted ynamides to α-halo acrylamides in high efficiency with *Z*-selectivity. A proposed mechanism involves an initial nucleophillic attack of ynamide to form ketiminium intermediate **I**, followed by an intramolecular shift of acetate to give stable carbenium intermediate **II**. Finally, loss of the acetyl group in the form of AcOH would give the halogenative MS product. The *Z*-selectivity of the reaction can be explained by the stability of the allyl containing cationic intermediate **II** over sterically congested intermediate **III**.

Scheme 4.12. Intercepted MS rearrangement to form α-halo amides

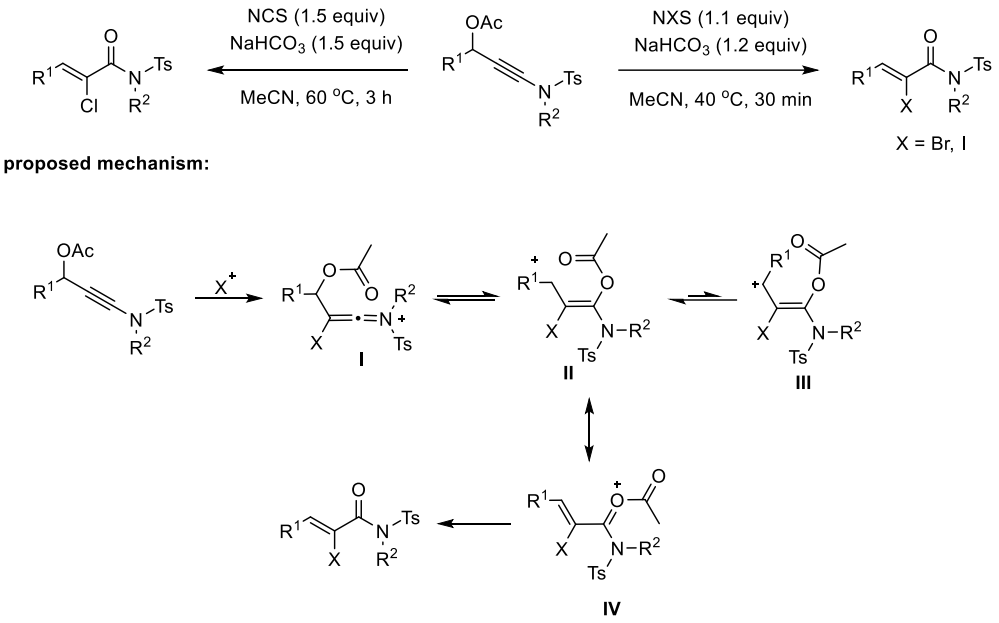

4.1.2. Design of the Work

In light of the above background as well as the background of hypervalent iodine chemistry, we became interested in possible engagement of a cyclic hypervalent iodine electrophile in the intercepted MS rearrangement. Previously, our group reported *trans*-1,2-difunctionalization of alkynes with benziodoxole derivatives and nucleophile via electrophillic π-activation. For example, a iodo(III) etherification of alkynes was accomplished using benziodoxole triflate (BXT) and alcohol nucleophile, affording highly substituted vinyl ether derivatives in high yield (Scheme 4.13a). Later, we also found that fluorobenziodoxole (FBX), in combination with BF_3, can also promote iodo(III) etherification of alkynes with ethereal solvent (Scheme 4.13b). Inspired by these results, we conceived electrophile-intercepted MS rearrangement of propargylic alcohol with such a BX electrophile (Scheme 4.13c). We hypothesized the reaction would follow initial π-activation of the triple bond by the I(III) reagent, which would trigger intramolecular addition of the hydroxy group to form a cyclic four-membered

intermediate. Finally, electrocyclic ring-opening of oxetane-type intermediate would form an λ^3-iodanyl enone product.

Scheme 4.13. I(III)-promoted functionalization reactions

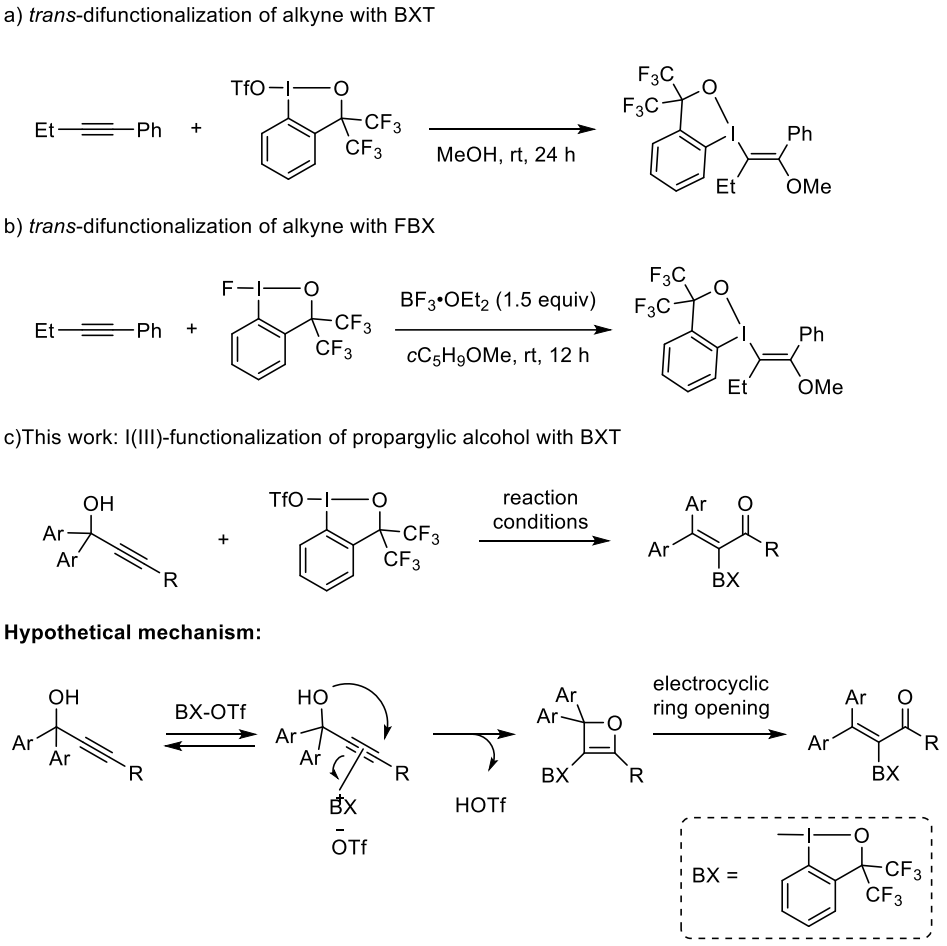

4.2. Result and Discussion

With 1,1,3-triphenylprop-2-yn-1-ol (**2a**, 0.15 mmol) as the model tertiary propargylic alcohol, we examined reaction conditions for iodo(III)- MS rearrangement with benziodoxole triflate (**1**, 0.10 mmol) at room temperature (Table 4.1). Initially, we tested various solvents. To our delight, the desired α-λ^3-iodanylenone **3a** was formed using polar solvents such as DMSO, DMPU, and DMF in good yield (entry 1-3). Performing the reaction in ethereal or halogenated solvent such as THF, DME and

DCE did not improve the reaction efficiency, giving the product in comparable yields (entry 4-6). Other solvents such as toluene and hexane proved to be less efficient, obtaining product in moderate (entry 7-8). Finally, we found Et_2O as the optimal solvent, promoting the desired reaction to 89% of isolated yield. Importantly, reversing the stoichiometry of the substrate **2a** (0.10 mmol) and **1** (0.15 mmol) led to a decrease in the reaction efficiency (entry 10). The structure of the **3a** was characterized using NMR spectroscopy and X-ray crystallographic analysis.

Table 4.1. Optimization of reaction conditions[a]

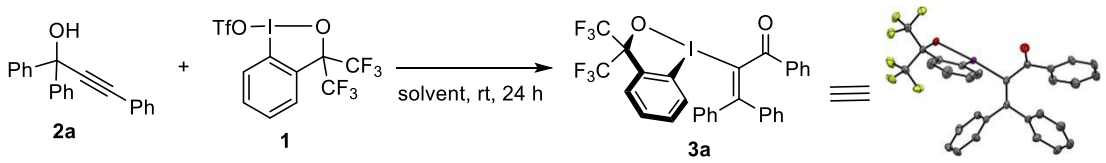

entry	solvent	conv. of **1**	yield (%)[b]
1	DMSO	100	64
2	DMF	100	68
3	DMPU	100	78
4	THF	100	79
5	DME	84	71
6	DCE	100	75
7	hexane	97	57
8	toluene	84	46
9	Et_2O	100	97 (89)[c]
10[d]	Et_2O	100	85

[a] 0.15 mmol of **2a** and 0.2 mmol of 1 was used. [b] Determined by ^{19}F NMR. [c] Isolated yield. [d] 0.1 mmol of **2a** and 0.15 mmol of **1** were used.

After finding optimal reaction conditions, we focused on extending the substrate scope of triaryl propargylic alcohols analogous to **2a** (Table 4.2). Various propargylic alcohols prepared from symmetrical benzophenone and phenylacetylene underwent

smooth reaction to afford corresponding products in high yield tolerating functional groups such as methyl, methoxy, fluoro, and chloro (**3b**, **3d**-**3e**). Propargylic alcohols containing *para*-methoxy and *meta*-nitro group afforded the reaction in somewhat lower yields (**3c** and **3f**). Also, a diverse range of aryl groups at 3-position of propargylic alcohol could be tolerated producing the desired product in 60-94% yield (**3g**-**3r**). Notably, *ortho*-substituted propargylic alcohols were amenable to our reaction system affording excellent yield (**3p**-**3r**). Furthermore, multi-substituted propargylic alcohol **2s** and phenanthrenyl group containing propargylic alcohol **2t** furnished the corresponding products in high yield. Not unexpectedly, an unsymmetrical propargylic alcohol bearing phenyl and *para*-tolyl group afforded a mixture of stereoisomers with low stereoselectivity (1.2:1).

Table 4.2. Scope of 1,1,3-triarylprop-2-yn-1-ols[a]

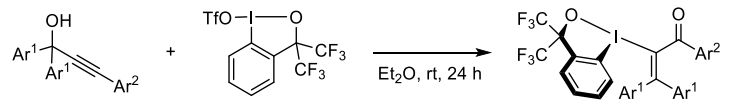

2a-2u **1** **3a-3u**

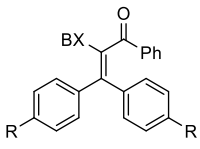

3a (R = H), 89% (83%)[b]
3b (R = Me), 75%
3c (R = OMe), 67%
3d (R = F), 85%
3e (R = Cl), 75%

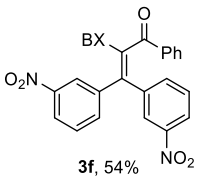

3f, 54%

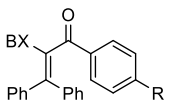

3g (R = Me), 85%
3h (R = Et), 94%
3i (R = OMe), 81%
3j (R = F), 88%
3k (R = Br), 60%
3l (R = CF_3), 77%

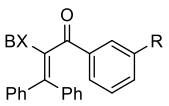

3m (R = Me), 84%
3n (R = F), 85%
3o (R = Cl), 67%

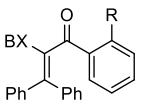

3p (R = Me), 81%
3q (R = OMe), 93%
3r (R = CF_3), 90%

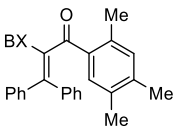

3s, 92%

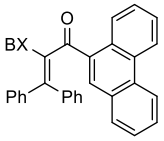

3t, 95%

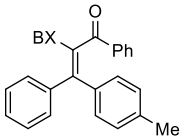

3u, 75% (1.2:1)[c]

[a] 0.3 mmol of **2**, 0.2 mmol of **1**. The benziodoxole moiety is shown by the symbol BX. [b] Performed on a 2 mmol scale. [c] Mixture of stereoisomers was obtained and stereochemistry of each isomer could not be assigned.

Next, we tried to employ propargylic alcohol **2v** to our reaction system but it failed to undergo the desired reaction and decomposed to interactable products. Fortunately, the addition of 2 equivalent of Na_2CO_3 to the reaction mixture suppressed the side reactions, probably caused by TfOH, and afforded the desired iodo-enone product **3v** in 61% yield (Table 4.3). The modified reaction conditions tolerated alkyl-substituted propargylic alcohol bearing primary, secondary, and tertiary alkyl groups to give the desired products in moderate to good yield (**3w**-**3x** and **3z**-**3ab**). Furthermore, chloro-substituted and alkenyl-group containing propargylic alcohol underwent the desired pathway to furnish products in 70% and 66% yield respectively (**3y** and **3ac**).

Table 4.3. Scope of alkyl-substituted propargylic alcohols[a]

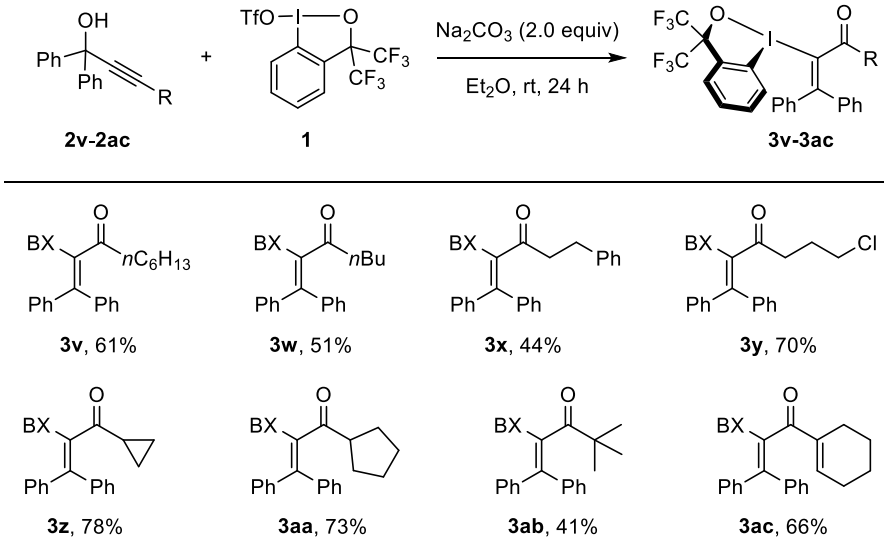

[a] 0.3 mmol of **2**, 0.2 mmol of **1**, and 0.4 mmol of Na_2CO_3. The benziodoxole moiety is shown by the symbol BX.

Table 4.4. summarizes the substrates failed to undergo in our reported method. Cyclohexyl ring containing propargylic alcohol, 1-(phenylethynyl)cyclohexan-1-ol (**2ad**) underwent dehydration reaction under present conditions to afford corresponding enyne product. On the other hand, pyridinyl ring containing propargylic alcohol **2af** did not promoted the desired outcome and largely recovered. Secondary propargylic alcohol **2ag** also decomposed to our reaction system. Other propargylic alcohol such as **2ae**, **2ai**, **2ah,** and **2aj** also failed to participate in iodo(III)- MS rearrangement under optimized reaction conditions.

Table 4.4. Unsuccessful substrates

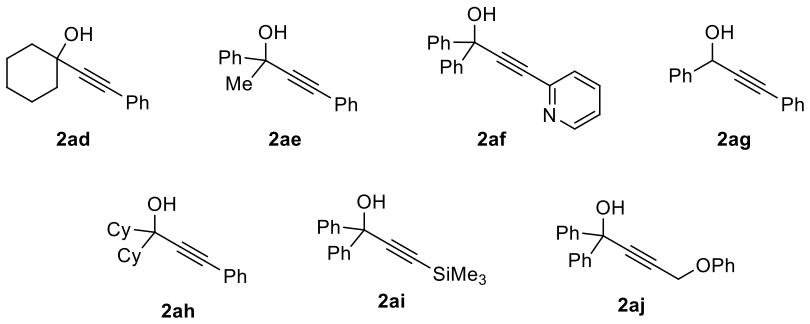

To show the utility of functionalized α-λ^3-iodanylenones, several cross-coupling reactions were performed (Scheme 4.14). The product **3a** was subjected to Suzuki-Miyaura cross-coupling reaction with 4-methoxyphenyl boronic acid, it afforded corresponding tetrasubstituted enone **6** in 63% yield. Next, we performed Sonogashira coupling reaction with product **3a** and **3k**, in both cases C-I(III) bond was cleaved and corresponding coupling products **7** and **8** were formed. Notably, chemoselective cross-coupled product was formed in substrate 3k leaving C-Br bond untouched.

Scheme 4.14. Pd-catalyzed cross-coupling reaction of α-λ^3-iodanylenones

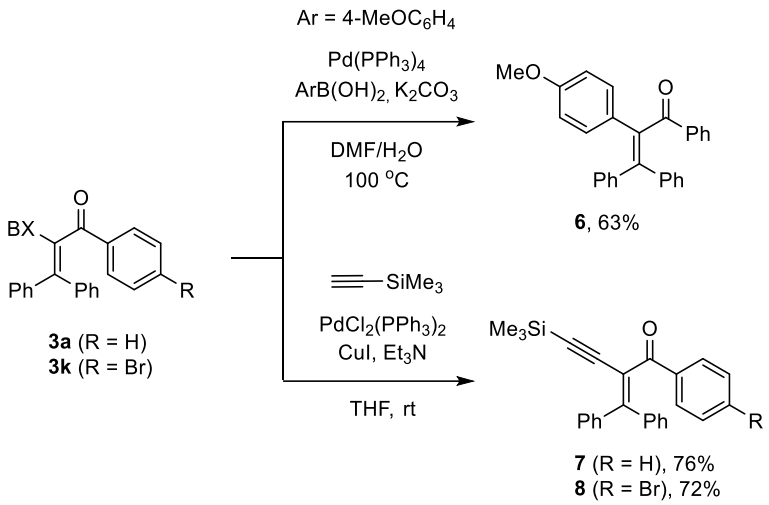

From the observation of dehydration of propargylic alcohol **2ad**, we propose that benziodoxole triflate would act as Lewis acid and prefer to activate hydroxy group over alkyne moiety to form propargylic cation and hydroxybenziodoxole (Scheme 4.15). Next, hydroxy group would be transferred from the water or hydroxybenziodoxole to the 3-position of the alcohol. Finally, allenol intermediate would intercept benziodoxole group to form desired product.

Scheme 4.15. Proposed reaction pathway

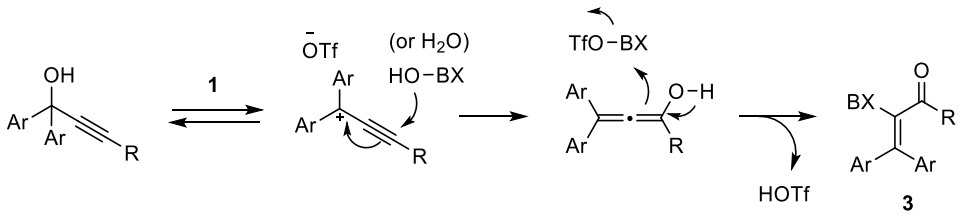

To support the above hypothesis, two control experiments were performed. First, model reaction between propargylic alcohol **2a** and benziodoxole triflate (**1**) in the

presence of 4Å molecular sieves afforded desired iodo(III)-Meyer–Schuster rearrangement product in 95% NMR yield (Scheme 4.16a). It clearly indicates the possible involvement of *in situ* generated hydroxybenziodoxole as nucleophile in this reaction. Next, we tried to prove the involvement of water in the hydroxy transfer process by a simple ^{18}O-labeling experiment, where model reaction was run in the presence of 1 equivalent of ^{18}O-labeled water (Scheme 4.16b). The reaction resulted partial incorporation of ^{18}O isotope in the compound **3a**. Furthermore, we propose that high yield of the 1,1,3-triarylpropargylic alcohols towards intercepted Meyer–Schuster rearrangement strongly suggest that benziodoxole triflate is more efficient over TfOH in both activating the alcohol and intercepting allenol to form the product.

Scheme 4.16. Control experiments

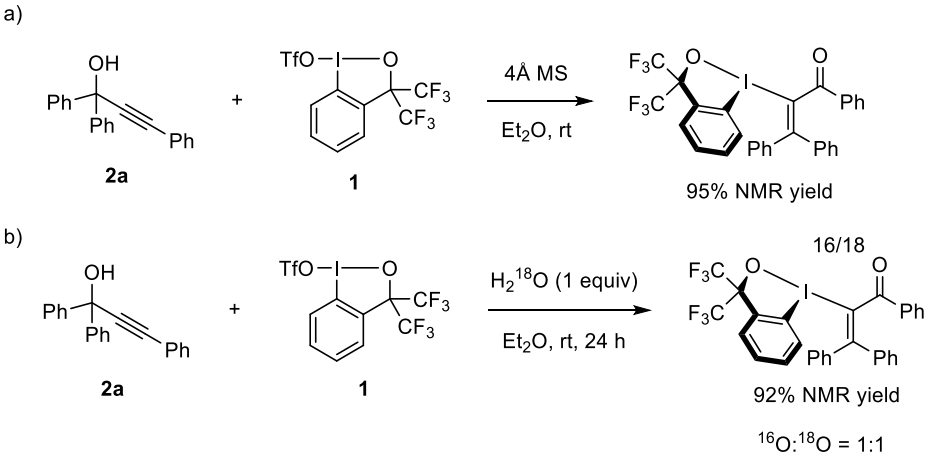

4.3. Conclusion

In summary, we have accomplished iodo(III)-Meyer-Schuster rearrangement of propargylic alcohols using BXT as electrophillic promoter to access α-λ^3-iodanyl enones, which represents another class of vinylbenziodoxo(one)s. A wide variety of functional groups were tolerated under mild reaction conditions. Most of the multi-

substituted α-haloenone scaffolds presented here are new to the literature and hence the reported method may complement previous halogen-intercepted MS rearrangements.

4.4. Experimental Section

Materials. 3,3-bis(trifluoromethyl)-1λ^3-benzo[*d*][1,2]iodaoxol-1(3*H*)-yl trifluoromethanesulfonate (benziodoxole triflate, BXT; 1) was synthesized according to the literature procedure.[22]

Synthesis and Characterization of Propargylic Alcohols

Propargyl alcohols were prepared from the corresponding terminal alkynes and ketones according to the reported literature procedure[2] and purified by flash chromatography on silica gel. The propargylic alcohols (**2a**-**2b**,[23] **2c**,[5] **2d**-**2e**,[23] **2g**,[23] **2h**,[24] **2i**-**j**,[23] **2k**,[24] **2m**-**o**,[24] **2p**,[25] **2q**,[24] **2u**,[25] **2v**,[26] **2w**,[23] **2x**,[27] **2z**,[5] **2ab**,[24] **2ad**,[28] **2ae**,[29] **2af**,[30] and **2ag**[31]) are known compounds and their spectral data showed good agreement with the literature data.

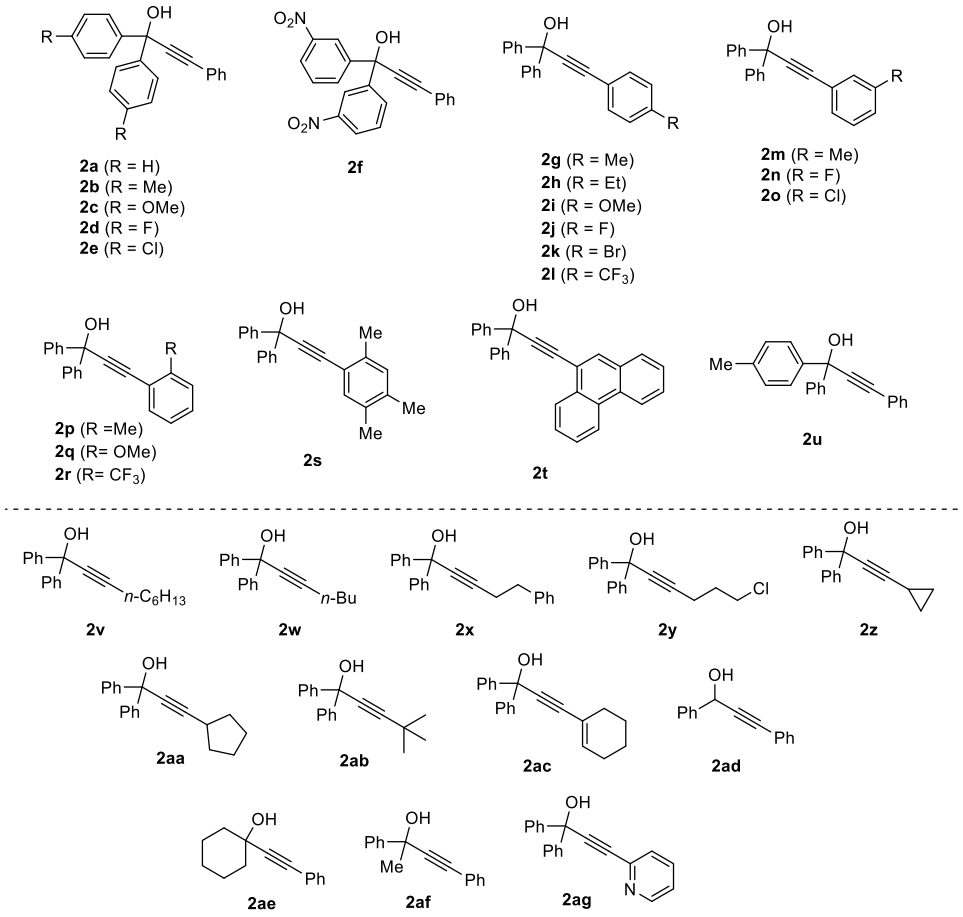

Figure 4.1. Propargylic alcohols used in this study.

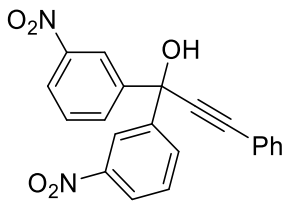

1,1-Bis(3-nitrophenyl)-3-phenylprop-2-yn-1-ol (2f): 4 mmol scale; Brown solid (1.3 g, 87% yield); R_f 0.25 (hexane/EtOAc = 4/1); m.p. 106-108 °C; ^{1}H NMR (500 MHz, $CDCl_3$) δ: 8.59 (t, J = 1.9 Hz, 2H), 8.18-8.16 (m, 2H), 8.00-7.99 (m, 2H), 7.57-7.53 (m, 4H), 7.43-7.35 (m, 3H), 3.43 (s, 1H); ^{13}C NMR (125 MHz, $CDCl_3$) δ: 148.5, 146.4, 132.2, 132.0, 129.9, 129.7, 128.7, 123.4, 121.19, 121.16, 89.6, 89.1, 73.7; HRMS (ESI) m/z: $[M + H]^+$ Calcd for $C_{21}H_{15}N_2O_5$ 375.0981; Found 375.0973.

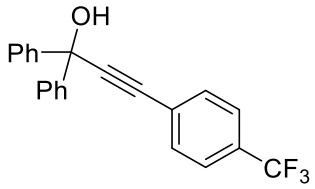

1,1-Diphenyl-3-(4-(trifluoromethyl)phenyl)prop-2-yn-1-ol (2l): 6 mmol scale; Colorless solid (1.5 g, 71% yield); R_f 0.45 (hexane/EtOAc = 9/1); m.p. 63-65 °C; ^{1}H NMR (400 MHz, $CDCl_3$) δ: 7.70-7.68 (m, 4H), 7.64-7.59 (m, 4H), 7.41-7.37 (m, 4H), 7.34-7.30 (m, 2H), 3.01 (s, 1H); ^{13}C NMR (100 MHz, $CDCl_3$) δ: 144.7, 132.2, 130.6 (q, $^2J_{C\text{-}F}$ = 32.7 Hz), 128.5, 128.1, 126.4, 126.2, 125.4 (q, $^3J_{C\text{-}F}$ = 3.7 Hz), 124.0 (q, $^1J_{C\text{-}F}$ = 270.6 Hz), 94.3, 85.9, 75.0; ^{19}F NMR (376 MHz, $CDCl_3$) δ: -62.8; HRMS (ESI) m/z: $[M + H]^+$ Calcd for $C_{22}H_{16}F_3O$ 353.1153; Found 353.1147.

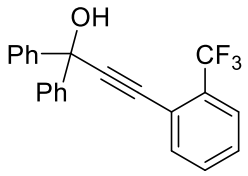

1,1-Diphenyl-3-(2-(trifluoromethyl)phenyl)prop-2-yn-1-ol (2r): 4 mmol scale; Yellow oil (1.1 g, 78% yield); R_f 0.37 (hexane/EtOAc = 9/1); ^{1}H NMR (400 MHz, $CDCl_3$) δ: 7.74-7.69 (m, 5H), 7.65 (d, J = 7.6 Hz, 1H), 7.50 (t, J = 7.4 Hz, 1H), 7.46-7.37 (m, 5H), 7.34-7.29 (m, 2H), 3.07 (s, 1H); ^{13}C NMR (100 MHz, $CDCl_3$) δ: 144.7, 134.3, 131.5 (q, $^2J_{C\text{-}F}$ = 30.5 Hz), 131.6, 128.5, 128.4, 127.9, 126.2, 125.9 (q, $^3J_{C\text{-}F}$ = 5.2 Hz), 123.7 (q, $^1J_{C\text{-}F}$ = 271.9 Hz), 120.8 (q, $^3J_{C\text{-}F}$ = 1.6 Hz), 97.4, 83.2, 75.1; ^{19}F NMR (282 MHz, $CDCl_3$) δ: -61.9; HRMS (ESI) m/z: $[M + H]^+$ Calcd for $C_{22}H_{16}F_3O$ 353.1153; Found 353.1149.

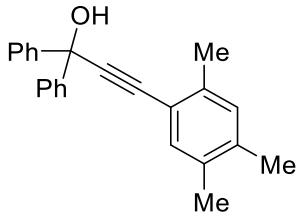

1,1-Diphenyl-3-(2,4,5-trimethylphenyl)prop-2-yn-1-ol (2s): 3 mmol scale; White solid (0.69 g, 70% yield); R_f 0.48 (hexane/EtOAc = 9/1); m.p. 76-78 °C; ^{1}H NMR (500 MHz, $CDCl_3$) δ: 7.98-7.97 (m, 4H), 7.63-7.60 (m, 4H), 7.56-7.52 (m, 3H), 3.17 (s, 1H), 2.66 (s, 3H), 2.51 (s, 3H), 2.47 (s, 3H); ^{13}C NMR (100 MHz, $CDCl_3$) δ: 145.5, 137.9, 137.7, 133.9, 133.2, 131.0, 128.4, 127.8, 126.2, 119.5, 94.8, 86.8, 75.2, 20.4, 19.8, 19.1; HRMS (ESI) m/z: $[M + H]^+$ Calcd for $C_{24}H_{23}O$ 327.1749; Found 327.1744.

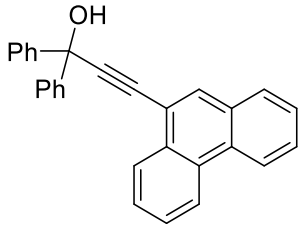

3-(Phenanthren-9-yl)-1,1-diphenylprop-2-yn-1-ol (2t): 2 mmol scale; White solid (0.45 g, 57% yield); R_f 0.3 (hexane/EtOAc = 9/1); m.p. 114-116 °C; ^{1}H NMR (400 MHz, $CDCl_3$) δ: 8.68 (dd, J = 12.4, 8.1 Hz, 2H), 8.41 (dd, J = 7.8, 0.9 Hz, 1H), 8.08 (s, 1H), 7.86 (d, J = 7.6 Hz, 1H), 7.82-7.80 (m, 4H), 7.72-7.59 (m, 4H), 7.44-7.40 (m, 4H), 7.36-7.31 (m, 2H), 3.09 (s, 1H); ^{13}C NMR (100 MHz, $CDCl_3$) δ: 145.2, 132.5, 131.3, 131.2, 130.5, 130.2, 128.7, 128.6, 128.0, 127.8, 127.3, 127.2, 127.1, 127.0, 126.3, 122.9, 122.8, 118.9, 96.3, 85.8, 75.4; HRMS (ESI) m/z: $[M + H]^+$ Calcd for $C_{29}H_{21}O$ 385.1592; Found 385.1593.

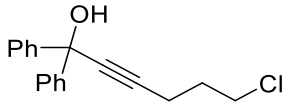

6-Chloro-1,1-diphenylhex-2-yn-1-ol (2x): 6 mmol scale; Colourless oil (1.40 g, 82% yield); R_f 0.25 (hexane/EtOAc = 9/1); ^{1}H NMR (300 MHz, $CDCl_3$) δ: 7.69 (d, *J* = 7.8 Hz, 4H), 7.43-7.30 (m, 6H), 3.69 (t, *J* = 6.3 Hz, 2H), 3.11 (s, 1H), 2.59 (t, *J* = 6.8 Hz, 2H), 2.10-2.01 (m, 2H); ^{13}C NMR (100 MHz, $CDCl_3$) δ: 145.4, 128.4, 127.7, 126.1, 86.2, 84.3, 74.6, 43.8, 31.3, 16.5; HRMS (ESI) m/z: $[M + H]^+$ Calcd for $C_{18}H_{18}ClO$ 285.1046; Found 285.1040.

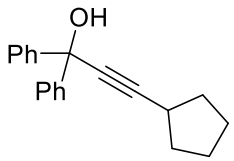

3-Cyclopentyl-1,1-diphenylprop-2-yn-1-ol (2z): 10 mmol scale; Colourless oil (1.6 g, 58% yield); R_f 0.4 (hexane/EtOAc = 9/1); ^{1}H NMR (400 MHz, $CDCl_3$) δ: 7.61 (d, *J* = 7.9 Hz, 4H), 7.32 (t, *J* = 7.8 Hz, 4H), 7.26-7.22 (m, 2H), 2.81-2.76 (m, 1H), 2.75-2.73 (m, 1H), 2.00-1.94 (m, 2H), 1.80-1.67 (m, 4H), 1.63-1.57 (m, 2H); ^{13}C NMR (100 MHz, $CDCl_3$) δ: 145.8, 128.2, 127.5, 126.1, 92.6, 82.7, 74.5, 33.9, 30.4, 25.1; HRMS (ESI) m/z: $[M + H]^+$ Calcd for $C_{20}H_{21}O$ 277.1592; Found 277.1583.

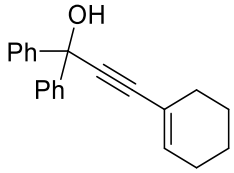

3-(Cyclohex-1-en-1-yl)-1,1-diphenylprop-2-yn-1-ol (2ab): 6 mmol scale; Yellow oil (1.17 g, 68% yield); R_f 0.25 (hexane/EtOAc = 9/1); ^{1}H NMR (400 MHz, $CDCl_3$) δ: 7.67-7.65 (m, 4H), 7.35 (t, *J* = 7.2 Hz, 4H), 7.30-7.25 (m, 2H), 6.25-6.23 (m, 1H), 2.92 (s, 1H), 2.26-2.21 (m, 2H), 2.17-2.12 (m, 2H), 1.72-1.60 (m, 4H); ^{13}C NMR (100 MHz, $CDCl_3$) δ: 145.4, 135.8, 128.3, 127.6, 126.1, 120.2, 89.2, 74.8, 29.2, 25.7, 22.3, 21.5; HRMS (ESI) m/z: $[M + H]^+$ Calcd for $C_{21}H_{21}O$ 289.1592; Found 289.1587.

General procedures for the iodo(III)-MS rearrangement of propargylic alcohols with benziodoxole triflate

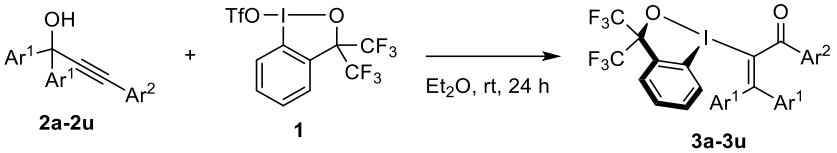

Procedure A: An oven-dried 4 mL vial equipped with a magnetic stir bar was charged sequentially with propargylic alcohol (**2**, 0.30 mmol) and Et_2O (1 mL), followed by the addition of benziodoxole triflate (**1**, 103.6 mg, 0.20 mmol). The resulting mixture was stirred at room temperature for 24 h. The reaction mixture was then diluted with EtOAc (10 mL) and quenched with saturated Na_2CO_3 solution (5 mL), followed by extraction with EtOAc (5 mL x 3). The combined organic layer was washed with water (10 mL) and brine (10 mL), dried over Na_2SO_4, and concentrated under reduced pressure. The residue was purified by flash column chromatography on silica gel to afford the desired product **3**.

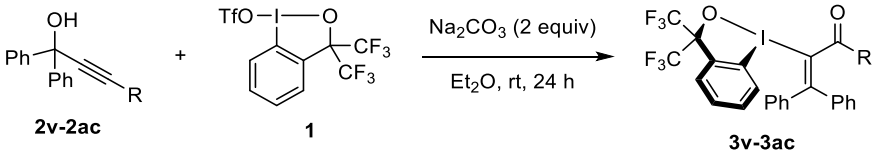

Procedure B: An oven dried 4 mL vial equipped with a magnetic stir bar was charged sequentially with Na_2CO_3 (42.4 mg, 0.40 mmol), propargylic alcohol (**2**, 0.30 mmol), and Et_2O (1 mL), followed by the addition of benziodoxole triflate (**1**, 103.6 mg, 0.20 mmol). The resulting mixture was stirred at room temperature for 24 h. The reaction mixture was then diluted with EtOAc (10 mL) and treated with saturated Na_2CO_3 solution (5 mL), followed by extraction with EtOAc (5 mL x 3). The combined organic layer was washed with water (10 mL) and brine (10 mL), dried over Na_2SO_4, and

concentrated under reduced pressure. The residue was purified by flash column chromatography on silica gel to afford desired product **3**.

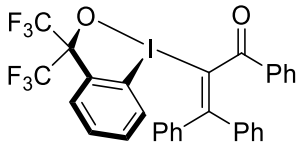

2-(3,3-Bis(trifluoromethyl)-1λ^3-benzo[*d*][1,2]iodaoxol-1(3*H*)-yl)-1,3,3-triphenylprop-2-en-1-one (3a): Procedure A; Yellow solid (116 mg, 89% yield); R_f 0.33 (hexane/EtOAc = 7/3); m.p. 185-187 °C; ^{1}H NMR (400 MHz, $CDCl_3$) δ: 8.09-8.05 (m, 1H), 7.89-7.87 (m, 2H), 7.77 (s, 1H), 7.60-7.56 (m, 2H), 7.48-7.43 (m, 1H), 7.37-7.26 (m, 5H), 7.21-7.11 (m, 7H); ^{13}C NMR (100 MHz, $CDCl_3$) δ: 194.8, 162.0, 141.5, 138.7, 134.7, 133.8, 132.6, 131.7, 130.6, 130.1, 130.0, 129.6, 128.9, 128.7, 128.5, 128.2, 127.0, 123.8 (q, $^1J_{C\text{-}F}$ = 289.7 Hz), 113.8, 81.8-80.9 (m); ^{19}F NMR (376 MHz, $CDCl_3$) δ: -76.0; HRMS (ESI) m/z: $[M + H]^+$ Calcd for $C_{30}H_{20}F_6IO_2$ 653.0412; Found 653.0406.

Recrystallization from DCM/hexane using liquid diffusion method afforded single crystals suitable for X-ray diffraction analysis. A colorless plate-like specimen of $C_{30}H_{19}F_6IO_2$, with approximate dimensions of 0.020 mm x 0.200 mm x 0.280 mm was used for the X-ray crystallographic analysis, which unambiguously confirmed the molecular structure of **3a** and its s-trans configuration in the solid state (Figure 4.2 and Table 4.5).[32]

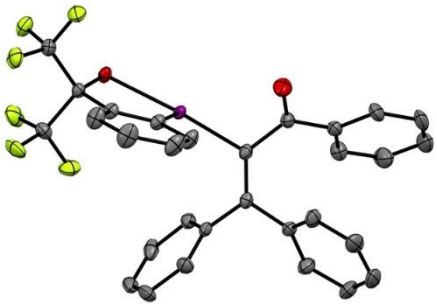

Figure 4.2. ORTEP drawing of **3a** (thermal ellipsoids set as 50% probability)

Table 4.5. Crystal data and structure refinement for yoshi94m_0m_5 (3a)

Identification code	Yoshi94m_0m_5	
Chemical formula	$C_{30}H_{19}F_6IO_2$	
Formula weight	652.35 g/mol	
Temperature	100(2) K	
Wavelength	0.71073 Å	
Crystal size	0.020 x 0.200 x 0.280 mm	
Crystal habit	colorless plate	
Crystal system	monoclinic	
Space group	P 1 21/n 1	
Unit cell dimensions	a = 15.9593(6) Å	α = 90°
	b = 8.8250(4) Å	β = 101.0454(16)°
	c = 19.0109(7) Å	γ = 90°
Volume	2627.91(18) $Å^3$	
Z	4	
Density (calculated)	1.649 g/cm^3	
Absorption coefficient	1.288 mm^{-1}	
F(000)	1288	
Theta range for data	2.55 to 37.85°	
Reflections collected	13622	
Independent reflections	9873 [R(int) = 0.0575]	
Coverage independent	97.3%	
Absorption correction	Multi-Scan	
Max. and min. transmission	0.9750 and 0.7140	
Structure solution technique	direct methods	
Structure solution program	XT, VERSION 2014/5	
Refinement method	Full-matrix least-squares on F^2	
Refinement program	SHELXL-2018/3 (Sheldrick, 2018)	
Function minimized	$\Sigma w(F_o^2 - F_c^2)^2$	
Data / restraints / parameters	13622 / 0 / 353	
Goodness-of-fit on F^2	1.044	
Δ/σ_{max}	0.001	
Final R indices	9739 data;	R1 = 0.0574, wR2
	all data	R1 = 0.0998, wR2
Weighting scheme	$w=1/[\sigma^2(F_o^2)+(0.0814P)^2+1.5676P]$ where	
Largest diff. peak and hole	0.582 and -0.626 $eÅ^{-3}$	
R.M.S. deviation from mean	0.245 $eÅ^{-3}$	

Procedure for 2 mmol-scale reaction: A 25 mL Schlenk tube equipped with a magnetic stir bar was charged sequentially with 1,1,3-triphenylprop-2-yn-1-ol (**2a**, 0.85 g, 3.0 mmol) and Et_2O (10 mL), followed by the addition of BXT (**1**, 1.04 g, 2.0 mmol). The resulting mixture was stirred at room temperature for 24 h. The reaction mixture was then diluted with EtOAc (50 mL) and quenched with saturated Na_2CO_3 solution (50 mL), followed by extraction with EtOAc (20 mL x 3). The combined organic layer was washed with water (50 mL) and brine (50 mL), dried over Na_2SO_4, and concentrated under reduced pressure. The residue was purified by flash column chromatography on silica gel to afford desired product **3a** (1.08 g, 83% yield).

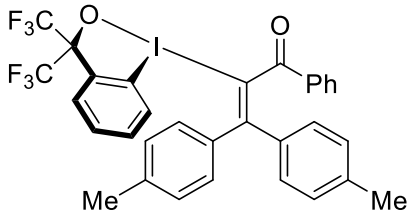

2-(3,3-Bis(trifluoromethyl)-1λ^3-benzo[*d*][1,2]iodaoxol-1(3*H*)-yl)-1-phenyl-3,3-di-*p*-tolylprop-2-en-1-one (3b): Procedure A; Yellow solid (102 mg, 75% yield); R_f 0.2 (hexane/EtOAc = 4/1); m.p. 182-184 °C; ^{1}H NMR (500 MHz, $CDCl_3$) δ: 8.02-8.00 (m, 1H), 7.87-7.85 (m, 2H), 7.77 (d, *J* = 7.0 Hz, 1H), 7.60-7.54 (m, 2H), 7.46 (t, *J* = 7.4 Hz, 1H), 7.34 (t, *J* = 7.9 Hz, 2H), 7.11-7.05 (m, 6H), 6.94 (d, *J* = 8.1 Hz, 2H), 2.34 (s, 3H), 2.20 (s, 3H); ^{13}C NMR (100 MHz, $CDCl_3$) δ: 194.9, 162.7, 140.7, 140.4, 139.0, 136.2, 134.9, 133.6, 132.5, 131.8, 130.5, 130.23, 130.19, 129.6, 129.3, 129.2, 129.1, 128.9, 128.5, 125.7, 123.9 (q, $^1J_{C\text{-}F}$ = 290.0 Hz), 113.9, 81.6-81.0 (m), 21.33, 21.30; ^{19}F NMR (282 MHz, $CDCl_3$) δ: -76.0 Hz; HRMS (ESI) m/z: $[M + H]^+$ Calcd for $C_{32}H_{24}F_6IO_2$ 681.0725; Found 681.0733.

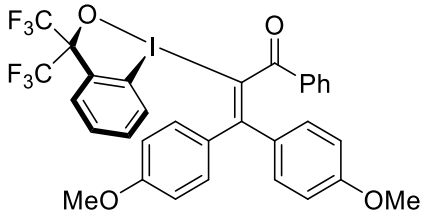

2-(3,3-bis(trifluoromethyl)-1λ^3-benzo[*d*][1,2]iodaoxol-1(3*H*)-yl)-3,3-bis(4-methoxyphenyl)-1-phenylprop-2-en-1-one (3c): Procedure A; Yellow solid (96 mg, 67% yield); R_f 0.2 (hexane/EtOAc = 4/1); m.p. 180-182 °C; ^{1}H NMR (400 MHz, $CDCl_3$) δ: 7.92 (dd, *J* = 8.0, 0.8 Hz, 1H), 7.84-7.82 (m, 2H), 7.76 (d, *J* = 7.4 Hz, 1H), 7.57-7.48 (m, 2H), 7.42-7.39 (m, 1H), 7.31-7.26 (m, 2H), 7.14 (d, *J* = 8.7 Hz, 2H), 7.08 (d, *J* = 8.8 Hz, 2H), 6.80 (d, *J* = 8.7 Hz, 2H), 6.63 (d, *J* = 8.8 Hz, 2H), 3.77 (s, 3H), 3.66 (s, 3H); ^{13}C NMR (100 MHz, $CDCl_3$) δ: 194.8, 163.2, 161.35, 161.34, 135.1, 134.2, 133.3, 132.4, 132.40, 131.9, 131.8, 131.1, 130.5, 130.2, 129.6, 128.7, 128.2, 124.4, 124.0 (q, $^1J_{C\text{-}F}$ = 290.0 Hz), 114.0, 113.9, 81.9-80.7 (m), 55.4, 55.3; ^{19}F NMR (282 MHz, $CDCl_3$) δ: -70.0; HRMS (ESI) m/z: $[M + H]^+$ Calcd for $C_{32}H_{24}F_6IO_4$ 713.0623; Found 713.0630.

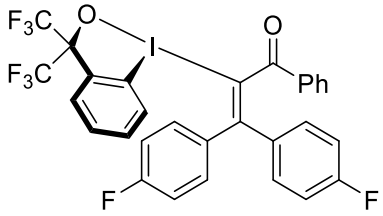

2-(3,3-Bis(trifluoromethyl)-1λ^3-benzo[*d*][1,2]iodaoxol-1(3*H*)-yl)-3,3-bis(4-fluorophenyl)-1-phenylprop-2-en-1-one (3d): Procedure A; White solid (117 mg, 85% yield); R_f 0.15 (hexane/EtOAc = 4/1); m.p. 185-187 °C; ^{1}H NMR (300 MHz, $CDCl_3$) δ: 8.00-7.98 (m, 1H), 7.85 (d, *J* = 7.5 Hz, 2H), 7.76 (s, 1H), 7.63-7.56 (m, 2H), 7.48 (t, *J* = 7.2 Hz, 1H), 7.36 (t, *J* = 7.8 Hz, 2H), 7.21-7.13 (m, 4H), 6.98 (t, *J* = 8.4 Hz, 2H), 6.83 (t, *J* = 8.5 Hz, 2H); ^{13}C NMR (100 MHz, $CDCl_3$) δ: 194.7, 163.6 (d, $^1J_{C\text{-}F}$ = 250.1 Hz), 163.5 (d, $^1J_{C\text{-}F}$ = 251.2 Hz), 159.5, 137.5, 137.4, 134.8, 134.7, 134.5, 134.1, 132.7, 132.1

(d, $^{3}J_{C\text{-}F}$ = 8.6 Hz), 131.7, 131.1 (d, $^{3}J_{C\text{-}F}$ = 8.5 Hz), 130.8, 130.3, 129.6, 129.0, 128.4, 127.9, 123.8 (q, $^{1}J_{C\text{-}F}$ = 289.6 Hz), 116.0 (d, $^{2}J_{C\text{-}F}$ = 22.0 Hz), 115.9 (d, $^{2}J_{C\text{-}F}$ = 21.9 Hz), 113.7, 81.8-80.7 (m); ^{19}F NMR (282 MHz, $CDCl_3$) δ: -76.0, -109.0, -109.6; HRMS (ESI) m/z: $[M + H]^+$ Calcd for $C_{30}H_{18}F_8IO_2$ 689.0224; Found 689.0234.

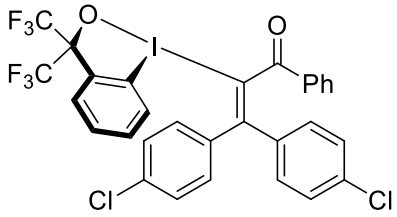

2-(3,3-Bis(trifluoromethyl)-1λ^3-benzo[*d*][1,2]iodaoxol-1(3*H*)-yl)-3,3-bis(4-chlorophenyl)-1-phenylprop-2-en-1-one (3e): Procedure A; White solid (108 mg, 75% yield); R_f 0.2 (hexane/EtOAc = 4/1); m.p. 208-210 °C; ^{1}H NMR (400 MHz, $CDCl_3$) δ: 7.98-7.96 (m, 1H), 7.84-7.82 (m, 2H), 7.75 (bd, *J* = 6.2 Hz, 1H), 7.61-7.55 (m, 2H), 7.51-7.46 (m, 1H), 7.38-7.33 (m, 2H), 7.26-7.23 (m, 2H), 7.11-7.05 (m, 6H); ^{13}C NMR (100 MHz, $CDCl_3$) δ: 194.6, 158.6, 158.5, 139.5, 136.7, 136.5, 134.4, 134.3, 132.8, 131.6, 131.1, 130.9, 130.3, 129.6, 129.2, 129.1, 129.0, 128.5, 128.4, 123.8 (q, $^{1}J_{C\text{-}F}$ = 289.3 Hz), 113.8, 81.5-80.9 (m); ^{19}F NMR (282 MHz, $CDCl_3$) δ: -75.8; HRMS (ESI) m/z: $[M + H]^+$ Calcd for $C_{30}H_{18}Cl_2F_6IO_2$ 720.9633; Found 720.9633.

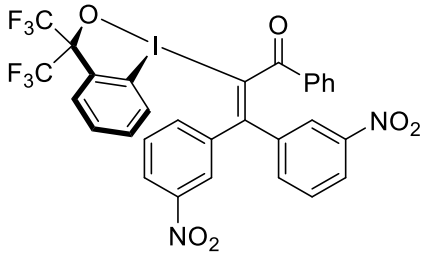

2-(3,3-Bis(trifluoromethyl)-1λ^3-benzo[*d*][1,2]iodaoxol-1(3*H*)-yl)-3,3-bis(3-nitrophenyl)-1-phenylprop-2-en-1-one (3f): Procedure A; Yellow solid (64 mg, 54% yield); R_f 0.37 (hexane/EtOAc = 3/2); m.p. 199-201 °C; ^{1}H NMR (400 MHz, DMSO-

d_6) δ: 8.39 (s, 1H), 8.25 (dd, *J* = 8.2, 1.4 Hz, 1H), 8.10 (d, *J* = 8.0 Hz, 1H), 8.06-8.00 (m, 2H), 7.97 (d, *J* = 7.4 Hz, 2H), 7.84-7.62 (m, 6H), 7.52-7.47 (m, 2H), 7.35 (t, *J* =7.8 Hz, 2H); ^{13}C NMR (100 MHz, DMSO-d_6) δ: 194.6, 155.4, 147.24, 147.17, 141.9, 138.8, 135.9, 135.4, 134.3, 133.8, 133.2, 132.0, 131.9, 130.8, 130.2, 130.1, 129.82, 129.79, 129.1, 128.5, 124.31, 124.26, 123.8 (q, $^1J_{C\text{-}F}$ = 289.8 Hz), 113.4, 81.6-81.1 (m), 79.1; ^{19}F NMR (376 MHz, DMSO-d_6) δ: -76.1; HRMS (ESI) m/z: $[M + H]^+$ Calcd for $C_{30}H_{18}F_6IN_2O_6$ 743.0114; Found 743.0123.

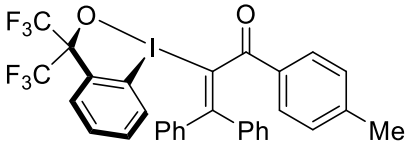

2-(3,3-Bis(trifluoromethyl)-1λ^3-benzo[*d*][1,2]iodaoxol-1(3*H*)-yl)-3,3-diphenyl-1-(*p*-tolyl)prop-2-en-1-one (3g): Procedure A; Yellow solid (113 mg, 85% yield); R_f 0.25 (hexane/EtOAc = 4/1); m.p. 187-189 °C; ^{1}H NMR (400 MHz, $CDCl_3$) δ: 8.14-8.12 (m, 1H), 7.83-7.78 (m, 3H), 7.63-7.59 (m, 2H), 7.38-7.17 (m, 12H), 2.35 (s, 3H); ^{13}C NMR (100 MHz, $CDCl_3$) δ: 194.4, 161.2, 145.0, 141.6, 138.6, 132.6, 132.1, 131.6, 130.5, 130.1, 130.0, 129.8, 129.78, 129.73, 129.6, 128.8, 128.64, 128.60, 128.5, 126.9, 123.8 (q, $^1J_{C\text{-}F}$ = 289.9 Hz), 113.8, 81.5-80.6 (m), 21.7; ^{19}F NMR (376 MHz, $CDCl_3$) δ: -76.0; HRMS (ESI) m/z: $[M + H]^+$ Calcd for $C_{31}H_{22}F_6IO_2$ 667.0569; Found 667.0573.

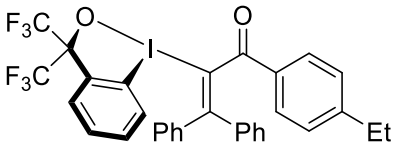

2-(3,3-Bis(trifluoromethyl)-1λ^3-benzo[*d*][1,2]iodaoxol-1(3*H*)-yl)-1-(4-ethylphenyl)-3,3-diphenylprop-2-en-1-one (3h): Procedure A; Yellow solid (127 mg, 94% yield); R_f 0.3 (hexane/EtOAc = 4/1); m.p. 157-159 °C; ^{1}H NMR (400 MHz, $CDCl_3$)

δ: 8.13 (d, *J* = 8.7 Hz, 1H), 7.83-7.76 (m, 3H), 7.61-7.55 (m, 2H), 7.36-7.13 (m, 12 H), 2.64 (q, *J* = 7.6 Hz, 2H), 1.20 (t, *J* = 7.6 Hz, 3H); ^{13}C NMR (100 MHz, $CDCl_3$) δ: 194.4, 161.0, 151.1, 141.6, 138.6, 132.6, 132.4, 131.6, 130.5, 130.1, 129.9, 129.85, 129.83, 129.7, 128.8, 128.7, 128.6, 128.51, 128.49, 127.1, 123.9 (q, $^1J_{C\text{-}F}$ = 289.9 Hz), 113.9, 81.8-80.7 (m), 29.0, 14.9; ^{19}F NMR (376 MHz, $CDCl_3$) δ: -76.0; HRMS (ESI) m/z: $[M + H]^+$ Calcd for $C_{32}H_{24}F_6IO_2$ 681.0725; Found 681.0729.

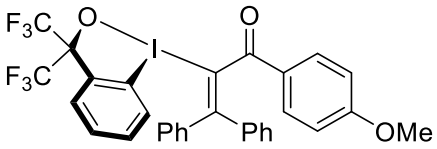

2-(3,3-Bis(trifluoromethyl)-1λ^3-benzo[*d*][1,2]iodaoxol-1(3*H*)-yl)-1-(4-methoxyphenyl)-3,3-diphenylprop-2-en-1-one (3i): Procedure A; Yellow solid (110 mg, 81%); R_f 0.12 (hexane/EtOAc = 4/1); m.p. 164-166 °C; ^{1}H NMR (400 MHz, $CDCl_3$) δ: 8.14-8.10 (m, 1H), 7.89-7.86 (m, 2H), 7.77-7.75 (bs, 1H), 7.61-7.56 (m, 2H), 7.36-7.13 (m, 10H), 6.84 (d, *J* = 8.9 Hz, 2H), 3.80 (s, 3H); ^{13}C NMR (125 MHz, $CDCl_3$) δ: 193.3, 164.1, 160.7, 141.7, 138.6, 132.6, 132.1, 131.6, 130.6, 130.1, 130.0, 129.84, 129.77, 128.8, 128.7, 128.6, 128.5, 127.5, 127.3, 126.8, 123.9 (q, $^1J_{C\text{-}F}$ = 290.0 Hz), 114.3, 113.9, 81.4-81.0 (m), 55.6; ^{19}F NMR (376 MHz, $CDCl_3$) δ: -76.0; HRMS (ESI) m/z: $[M + H]^+$ Calcd for $C_{31}H_{22}F_6IO_3$ 683.0518; Found 683.0524.

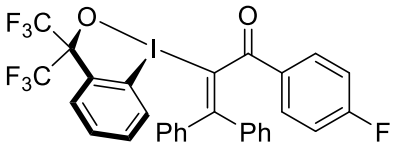

2-(3,3-Bis(trifluoromethyl)-1λ^3-benzo[*d*][1,2]iodaoxol-1(3*H*)-yl)-1-(4-fluorophenyl)-3,3-diphenylprop-2-en-1-one (3j): Procedure A; Yellow solid (118 mg, 88% yield); R_f 0.2 (hexane/EtOAc = 4/1); m.p. 201-203 °C; ^{1}H NMR (300 MHz, $CDCl_3$)

δ: 8.02-7.99 (m, 1H), 7.91-7.86 (m, 2H), 7.76 (brs, 1H), 7.60-7.57 (m, 2H), 7.38-7.16 (m, 10H), 7.00 (t, J = 8.5 Hz, 2H); ^{13}C NMR (75 MHz, $CDCl_3$) δ: 193.3, 165.8 (d, $^1J_{C-F}$ = 255.4), 162.3, 141.4, 138.7, 132.5, 132.2 (d, $^3J_{C-F}$ = 12.7 Hz), 131.7, 131.11, 131.07, 130.6, 130.3, 130.2, 130.02, 129.93, 128.9, 128.7, 128.6, 128.4, 126.8, 123.8 (q, $^1J_{C-F}$ = 292.5 Hz), 116.0 (d, $^2J_{C-F}$ = 22.0 Hz), 113.7, 81.6-80.8 (m); ^{19}F NMR (282 MHz, $CDCl_3$) δ: -76.0, -103.2; HRMS (ESI) m/z: $[M + H]^+$ Calcd for $C_{30}H_{19}F_7IO_2$ 671.0318; Found 671.0317.

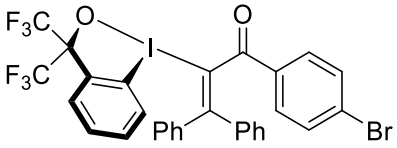

2-(3,3-Bis(trifluoromethyl)-1λ^3-benzo[*d*][1,2]iodaoxol-1(3*H*)-yl)-1-(4-bromophenyl)-3,3-diphenylprop-2-en-1-one (3k): Procedure A; Orange solid (88 mg, 60% yield); R_f 0.25 (hexane/EtOAc = 4/1); m.p. 208-210 °C; ^{1}H NMR (400 MHz, $CDCl_3$) δ: 7.97-7.95 (m, 1H), 7.77 (d, J = 7.0 Hz, 1H), 7.73-7.69 (m, 2H), 7.63-7.56 (m, 2H), 7.50-7.46 (m, 2H), 7.40-7.36 (m, 1H), 7.33-7.29 (m, 2H), 7.24-7.13 (m, 7H); ^{13}C NMR (100 MHz, $CDCl_3$) δ: 193.9, 162.6, 141.4, 138.7, 133.6, 132.6, 132.3, 131.8, 131.0, 130.7, 130.5, 130.4, 130.2, 130.1, 129.1, 129.0, 128.8, 128.7, 128.4, 126.9, 123.8 (q, $^1J_{C-F}$ = 289.7 Hz), 113.8, 81.6-81.0 (m); ^{19}F NMR (376 MHz, $CDCl_3$) δ: -76.1; HRMS (ESI) m/z: $[M + H]^+$ Calcd for $C_{30}H_{19}BrF_6IO_2$ 730.9517; Found 730.9521.

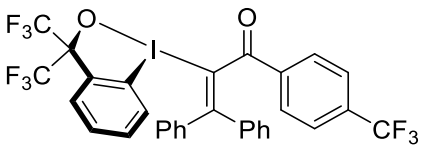

2-(3,3-Bis(trifluoromethyl)-1λ^3-benzo[*d*][1,2]iodaoxol-1(3*H*)-yl)-3,3-diphenyl-1-(4-(trifluoromethyl)phenyl)prop-2-en-1-one (3l): Procedure A; Yellow solid (111

mg, 77% yield); R_f 0.4 (hexane/EtOAc = 3/1); m.p. 205-207 °C; ^{1}H NMR (500 MHz, $CDCl_3$) δ: 7.93 (d, J = 8.1 Hz, 3H), 7.78 (d, J = 6.7 Hz, 1H), 7.62-7.55 (m, 4H), 7.40-7.36 (m, 1H), 7.33-7.30 (m, 2H), 7.22-7.14 (m, 7H); ^{13}C NMR (100 MHz, $CDCl_3$) δ: 194.0, 163.9, 141.3, 138.8, 137.7, 134.6 (q, $^2J_{C\text{-}F}$ = 32.5 Hz), 132.6, 131.9, 130.8, 130.7, 130.4, 130.2, 129.8, 129.1, 128.79, 128.75, 128.2, 127.0, 125.8 (q, $^3J_{C\text{-}F}$ = 3.5 Hz), 123.9 (q, $^1J_{C\text{-}F}$ = 289.6 Hz), 123.4 (q, $^1J_{C\text{-}F}$ = 271.5 Hz), 113.6, 81.6-81.0 (m); ^{19}F NMR (282 MHz, $CDCl_3$) δ: -63.3, -76.0; HRMS (ESI) m/z: $[M + H]^+$ Calcd for $C_{31}H_{19}F_9IO_2$ 721.0286; Found 721.0280.

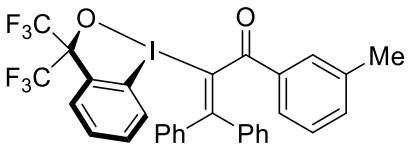

2-(3,3-Bis(trifluoromethyl)-1λ^3-benzo[*d*][1,2]iodaoxol-1(3*H*)-yl)-3,3-diphenyl-1-(*m*-tolyl)prop-2-en-1-one (3m): Procedure A; Yellow solid (112 mg, 84% yield); R_f 0.25 (hexane/EtOAc = 4/1); m.p. 146-148 °C; ^{1}H NMR (400 MHz, $CDCl_3$) δ: 8.10-8.08 (m, 1H), 7.77-7.58 (m, 5H), 7.37-7.14 (m, 12H), 2.33 (s, 3H); ^{13}C NMR (75 MHz, $CDCl_3$) δ: 194.9, 161.5, 141.6, 138.9, 138.7, 134.72, 134.69, 132.6, 131.6, 130.6, 130.2, 130.05, 130.02, 129.9, 128.9, 128.8, 128.7, 128.6, 128.5, 127.2, 127.0, 123.9 (q, $^1J_{C\text{-}F}$ = 289.7 Hz), 114.0, 81.6-80.9 (m), 21.3; ^{19}F NMR (282 MHz, $CDCl_3$) δ: -72.2; HRMS (ESI) m/z: $[M + H]^+$ Calcd for $C_{31}H_{22}F_6IO_2$ 667.0569; Found 667.0574.

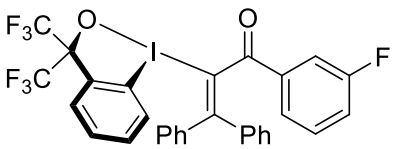

2-(3,3-Bis(trifluoromethyl)-1λ^3-benzo[*d*][1,2]iodaoxol-1(3*H*)-yl)-1-(3-fluorophenyl)-3,3-diphenylprop-2-en-1-one (3n): Procedure A; Yellow solid (114

mg, 85% yield); R_f 0.33 (hexane/EtOAc = 4/1); m.p. 208-210 °C; ^{1}H NMR (300 MHz, $CDCl_3$) δ: 8.02-7.99 (m, 1H), 7.82 (d, J = 6.0 Hz, 1H), 7.68-7.56 (m, 4H), 7.46-7.20 (m, 12H); ^{13}C NMR (100 MHz, $CDCl_3$) δ: 193.7, 163.0, 162.8 (d, $^1J_{C\text{-}F}$ = 247.7 Hz), 141.4, 138.8, 137.0 (d, $^3J_{C\text{-}F}$ = 6.4 Hz), 132.6, 131.8, 130.8, 130.6, 130.53, 130.46, 130.3, 130.2, 130.1, 129.0, 128.8, 128.7, 128.4, 126.9, 125.4 (d, $^3J_{C\text{-}F}$ = 2.8 Hz), 123.9 (q, $^1J_{C\text{-}F}$ = 289.6 Hz), 120.8 (d, $^2J_{C\text{-}F}$ = 21.4 Hz), 116.1 (d, $^2J_{C\text{-}F}$ = 22.7 Hz), 113.8, 81.6-81.0 (m); ^{19}F NMR (282 MHz, $CDCl_3$) δ: -76.1, -110.9; HRMS (ESI) m/z: $[M + H]^+$ Calcd for $C_{30}H_{19}F_7IO_2$ 671.0318; Found 671.0317.

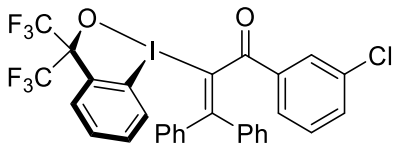

2-(3,3-Bis(trifluoromethyl)-1λ^3-benzo[*d*][1,2]iodaoxol-1(3*H*)-yl)-1-(3-chlorophenyl)-3,3-diphenylprop-2-en-1-one (3o): Procedure A; Yellow solid (92 mg, 67% yield); R_f 0.33 (hexane/EtOAc = 4/1); m.p. 129-131 °C; ^{1}H NMR (300 MHz, $CDCl_3$) δ: 7.98-7.95 (m, 1H), 7.82-7.71 (m, 3H), 7.65-7.58 (m, 2H), 7.44-7.18 (m, 12H); ^{13}C NMR (75 MHz, $CDCl_3$) δ: 193.5, 163.2, 141.4, 138.8, 136.4, 135.2, 133.6, 132.6, 131.9, 130.7, 130.5, 130.3, 130.2, 130.1, 129.5, 129.0, 128.8, 128.7, 128.3, 127.7, 127.0, 123.7 (q, $^1J_{C\text{-}F}$ = 289.9 Hz), 113.8, 82.1-80.5 (m); ^{19}F NMR (282 MHz, $CDCl_3$) δ: -76.0; HRMS (ESI) m/z: $[M + H]^+$ Calcd for $C_{30}H_{19}ClF_6IO_2$ 687.0022; Found 687.0023.

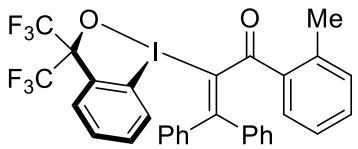

2-(3,3-Bis(trifluoromethyl)-1λ^3-benzo[*d*][1,2]iodaoxol-1(3*H*)-yl)-3,3-diphenyl-1-(*o*-tolyl)prop-2-en-1-one (3p): Procedure A; Yellow solid (108 mg, 81% yield); R_f

0.25 (hexane/EtOAc = 4/1); m.p. 189-191 °C; ^{1}H NMR (300 MHz, $CDCl_3$) δ: 8.00-7.97 (m, 1H), 7.74 (d, *J* = 6.7 Hz, 1H), 7.66 (d, *J* = 7.7 Hz, 1H), 7.62-7.53 (m, 2H), 7.34-7.20 (m, 4H), 7.16-7.07 (m, 9H), 2.41 (s, 3H); ^{13}C NMR (100 MHz, $CDCl_3$) δ: 196.5, 162.8, 141.6, 140.4, 139.0, 135.0, 132.5, 132.48, 132.44, 131.8, 130.6, 130.2, 130.04, 130.00, 129.64, 129.59, 128.9, 128.7, 128.43, 128.41, 125.7, 123.9 (q, $^{1}J_{C\text{-}F}$ = 289.9 Hz), 113.6, 81.6-81.0 (m), 21.5; ^{19}F NMR (282 MHz, $CDCl_3$) δ: -76.0; HRMS (ESI) m/z: $[M + H]^+$ Calcd for $C_{31}H_{22}F_6IO_2$ 667.0569; Found 667.0571.

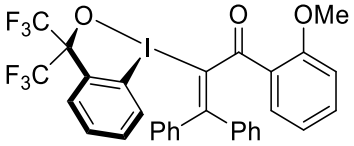

2-(3,3-Bis(trifluoromethyl)-1λ^3-benzo[*d*][1,2]iodaoxol-1(3*H*)-yl)-1-(2-methoxyphenyl)-3,3-diphenylprop-2-en-1-one (3q): Procedure A; Yellow solid (127 mg, 93% yield); R_f 0.3 (hexane/EtOAc = 4/1); m.p. 122-124 °C; ^{1}H NMR (400 MHz, $CDCl_3$) δ: 8.20 (d, *J* = 8.0 Hz, 1H), 7.80-7.76 (m, 2H), 7.67-7.58 (m, 2H), 7.52-7.48 (m, 1H), 7.34-7.09 (m, 10H), 7.00-6.99 (m, 2H), 4.00 (s, 3H); ^{13}C NMR (100 MHz, $CDCl_3$) δ: 193.1, 158.1, 156.39, 156.36, 142.1, 138.8, 135.7, 132.7, 131.9, 131.7, 130.5, 130.4, 130.0, 129.8, 129.4, 129.35, 129.28, 128.6, 128.5, 128.4, 125.1, 123.9 (q, $^{1}J_{C\text{-}F}$ = 289.8 Hz), 121.7, 114.0, 111.8, 81.6-81.1 (m); 56.1; ^{19}F NMR (376 MHz, $CDCl_3$) δ: -76.1; HRMS (ESI) m/z: $[M + H]^+$ Calcd for $C_{31}H_{22}F_6IO_3$ 683.0518; Found 683.0518.

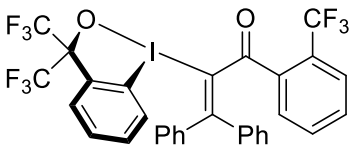

2-(3,3-Bis(trifluoromethyl)-1λ^3-benzo[*d*][1,2]iodaoxol-1(3*H*)-yl)-3,3-diphenyl-1-(2-(trifluoromethyl)phenyl)prop-2-en-1-one (3r): Procedure A; White solid (130 mg,

90% yield); R_f 0.12 (hexane/EtOAc = 4/1); m.p. 183-185 °C; ^{1}H NMR (400 MHz, $CDCl_3$) δ: 7.82 (d, *J* = 8.0 Hz, 1H), 7.77 (d, *J* = 7.1 Hz, 1H), 7.65-7.56 (m, 2H), 7.50 (dd, J = 20.0, 7.3 Hz, 2H), 7.37-7.25 (m, 5H), 7.18-7.08 (m, 7H); ^{13}C NMR (100 MHz, $CDCl_3$) δ: 194.6, 167.5, 141.5, 138.9, 136.5, 132.3, 131.9, 131.5, 131.2, 130.5, 130.43, 130.39, 130.3, 130.1, 129.8, 129.7, 128.8, 128.6, 128.5, 127.9, 127.6, 127.3, 126.9 (q, $^3J_{C\text{-}F}$ = 5.4 Hz), 123.7 (q, $^1J_{C\text{-}F}$ = 272.1 Hz), 123.9 (q, $^1J_{C\text{-}F}$ = 289.7 Hz), 113.3, 82.0-80.8 (m); ^{19}F NMR (282 MHz, $CDCl_3$) δ: -57.1, -76.0; HRMS (ESI) m/z: $[M + H]^+$ Calcd for $C_{31}H_{19}F_9IO_2$ 721.0286; Found 721.0287.

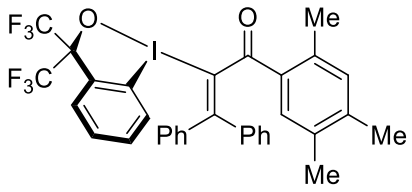

2-(3,3-Bis(trifluoromethyl)-1λ^3-benzo[*d*][1,2]iodaoxol-1(3*H*)-yl)-3,3-diphenyl-1-(2,4,5-trimethylphenyl)prop-2-en-1-one (3s): Procedure A; Yellow solid (128 mg, 92% yield); R_f 0.2 (hexane/EtOAc = 4/1); m.p. 190-192 °C; ^{1}H NMR (300 MHz, $CDCl_3$) δ: 8.09 (d, *J* = 7.9 Hz, 1H), 7.75 (d, *J* = 6.9 Hz, 1H), 7.61-7.53 (m, 2H), 7.45 (s, 1H), 7.34-7.17 (m, 10H), 6.91 (s, 1H), 2.39 (s, 3H), 2.19 (s, 3H), 2.18 (s, 3H); ^{13}C NMR (75 MHz, $CDCl_3$) δ: 196.1, 161.1, 142.2, 141.7, 138.9, 138.3, 134.1, 133.9, 132.5, 132.1, 131.9, 131.6, 130.5, 130.1, 129.7, 129.4, 129.3, 128.8, 128.6, 128.4, 123.9 (q, $^1J_{C\text{-}F}$ = 289.6 Hz), 113.9, 81.6-80.9 (m), 21.1, 19.7, 19.4; ^{19}F NMR (282 MHz, $CDCl_3$) δ: -76.0; HRMS (ESI) m/z: $[M + H]^+$ Calcd for $C_{33}H_{26}F_6IO_2$ 695.0882; Found 695.0882.

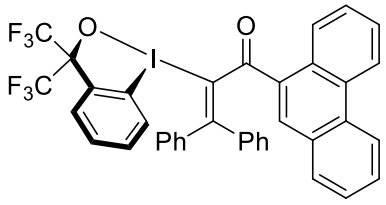

2-(3,3-Bis(trifluoromethyl)-1λ^3-benzo[*d*][1,2]iodaoxol-1(3*H*)-yl)-1-(phenanthren-9-yl)-3,3-diphenylprop-2-en-1-one (3t): Procedure A; Yellow solid (140 mg, 95% yield); R_f 0.2 (hexane/EtOAc = 4/1); m.p. 154-156 °C; ^{1}H NMR (300 MHz, DMSO-d_6) δ: 8.71-8.64 (m, 4H), 8.12 (dd, *J* = 23.0, 8.2 Hz, 2H), 7.91-7.86 (m, 1H), 7.75-7.64 (m, 6H), 7.48-7.38 (m, 5H), 7.14-7.12 (m, 2H), 6.81-6.76 (m, 3H); ^{13}C NMR (100 MHz, DMSO-d_6) δ: 196.1, 164.6, 141.9, 139.5, 132.7, 132.5, 132.4, 131.2, 130.3, 130.04, 129.95, 129.6, 129.5, 129.3, 129.2, 129.1, 129.0, 128.4, 128.2, 128.0, 127.3, 127.22, 127.18, 124.1 (q, $^1J_{C\text{-}F}$ = 290.2 Hz), 122.9, 122.8, 113.9, 82.3-81.1 (m); ^{19}F NMR (282 MHz, DMSO-d_6) δ: -75.2; HRMS (ESI) m/z: $[M + H]^+$ Calcd for $C_{38}H_{24}F_6IO_2$ 753.0725; Found 753.0726.

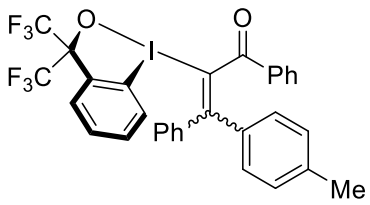

2-(3,3-Bis(trifluoromethyl)-1λ^3-benzo[*d*][1,2]iodaoxol-1(3*H*)-yl)-1,3-diphenyl-3-(*p*-tolyl)prop-2-en-1-one (3u): Procedure A. Obtained as a mixture of stereoisomers, whose ratio was determined to be 1.2:1 by the ^{1}H NMR integrations of the characteristic methyl groups. The *E/Z* stereochemistry of each isomer could not be determined; Yellow oil (100 mg, 75% yield); R_f 0.25 (hexane/EtOAc = 4/1); ^{1}H NMR (400 MHz, $CDCl_3$, *E/Z* mixture) δ: 8.06-8.00 (both isomers, m, 1.87H), 7.89-7.85 (both isomers, m, 3.65H), 7.79-7.75 (both isomers, m, 1.90H), 7.62-7.55 (both isomers, m, 3.73H), 7.51-7.45 (both isomers, m, 1.90H), 7.39-7.28 (both isomers, m, 6.81H), 7.19-7.05 (both isomers, m, 11.56H), 6.96 (d, *J* = 8.0 Hz, 1.96H), 2.35 (minor isomer, s, 2.51H), 2.22 (major isomer, s, 3H). ^{13}C NMR (100 MHz, $CDCl_3$, *E/Z* mixture) δ: 195.0, 194.8, 162.3, 162.0, 141.8, 140.7, 140.5, 139.0, 138.8, 135.9, 134.90, 134.88, 133.79, 133.75,

132.6, 131.81, 131.77, 130.6, 130.3, 130.13, 130.11, 130.0, 129.68, 129.66, 129.4, 129.3, 129.06, 128.98, 128.92, 128.7, 128.56, 128.54, 126.7, 126.3, 123.9 (q, $^{1}J_{C\text{-}F}$ = 289.7 Hz), 114.03, 113.96, 81.9-80.7 (m), 21.40, 21.36; ^{19}F NMR (376 MHz, $CDCl_3$, E/Z mixture) δ: -76.06, -76.07; HRMS (ESI) m/z: $[M + H]^+$ Calcd for $C_{31}H_{22}F_6IO_2$ 667.0569; Found 667.0566.

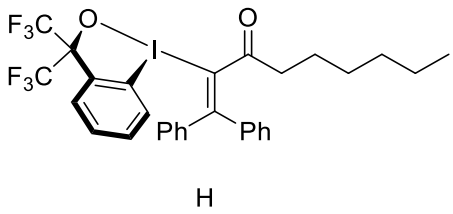

2-(3,3-Bis(trifluoromethyl)-1λ^3-benzo[*d*][1,2]iodaoxol-1(3*H*)-yl)-1,1-diphenylnon-1-en-3-one (3v): Procedure B; Orange solid (81 mg, 61% yield); R_f 0.25 (hexane/EtOAc = 4/1); m.p. 129-131 °C; ^{1}H NMR (400 MHz, $CDCl_3$) δ: 7.81-7.75 (m, 2H), 7.65-7.60 (m, 2H), 7.47-7.38 (m, 3H), 7.35-7.31 (m, 1H), 7.28-7.22 (m, 4H), 7.09-7.07 (m, 2H), 2.30 (t, *J* = 7.3 Hz, 2H), 1.48-1.41 (m, 2H), 1.22-1.15 (m, 2H), 1.12-1.02 (m, 4H), 0.81 (t, *J* = 7.3 Hz, 3H); ^{13}C NMR (100 MHz, $CDCl_3$) δ: 204.3, 161.9, 141.6, 139.1, 132.3, 132.1, 130.6, 130.5, 130.4, 130.0, 129.8, 129.0, 128.74, 128.67, 128.1, 124.0 (q, $^{1}J_{C\text{-}F}$ = 289.8 Hz), 113.2, 81.9-80.7 (m), 42.4, 31.4, 28.7, 24.7, 22.4, 14.0; ^{19}F NMR (376 MHz, $CDCl_3$) δ: -76.0; HRMS (ESI) m/z: $[M + H]^+$ Calcd for $C_{30}H_{28}F_6IO_2$ 661.1038; Found 661.1044.

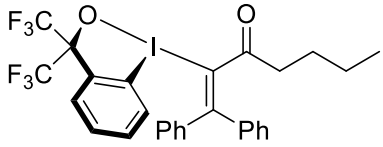

2-(3,3-Bis(trifluoromethyl)-1λ^3-benzo[*d*][1,2]iodaoxol-1(3*H*)-yl)-1,1-diphenylhept-1-en-3-one (3w): Procedure B; Yellow solid (65 mg, 51% yield); R_f 0.25

(hexane/EtOAc = 4/1); m.p. 194-196 °C; ^{1}H NMR (400 MHz, $CDCl_3$) δ: 7.80-7.73 (m, 2H), 7.65-7.60 (m, 2H), 7.47-7.37 (m, 3H), 7.36-7.32 (m, 1H), 7.28-7.21 (m, 4H), 7.09-7.06 (m, 2H), 2.30 (t, *J* = 7.4 Hz, 2H), 1.46-1.39 (m, 2H), 1.14-1.04 (m, 2H), 0.73 (t, *J* = 7.3 Hz, 3H); ^{13}C NMR (100 MHz, $CDCl_3$) δ: 204.4, 162.1, 141.6, 139.1, 132.4, 132.0, 130.7, 130.6, 130.4, 130.3, 130.1, 129.9, 129.0, 128.8, 128.7, 128.1, 123.9 (q, $^{1}J_{C\text{-}F}$ = 289.8 Hz), 113.2, 81.5-80.7 (m), 42.1, 26.9, 22.2, 13.7; ^{19}F NMR (376 MHz, $CDCl_3$) δ: -76.0; HRMS (ESI) m/z: $[M + H]^+$ Calcd for $C_{28}H_{24}F_6IO_2$ 633.0725; Found 633.0721.

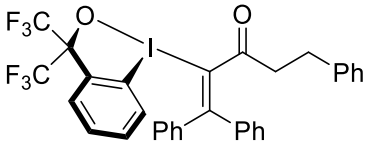

2-(3,3-Bis(trifluoromethyl)-1λ^3-benzo[*d*][1,2]iodaoxol-1(3*H*)-yl)-1,1,5-triphenylpent-1-en-3-one (3x): Procedure B; Orange solid (60 mg, 44% yield); R_f 0.25 (hexane/EtOAc = 4/1); m.p. 143-145 °C; ^{1}H NMR (400 MHz, $CDCl_3$) δ: 7.81 (d, J = 7.2 Hz, 1H), 7.69 (d, *J* = 7.9 Hz, 1H), 7.64-7.52 (m, 3H), 7.44 (t, *J* = 7.7 Hz, 2H), 7.38-7.20 (m, 8H), 6.99 (dd, *J* = 20.1, 7.5 Hz, 4H), 2.79 (t, *J* = 7.4 Hz, 2H), 2.61 (t, *J* = 7.4 Hz, 2H); ^{13}C NMR (100 MHz, $CDCl_3$) δ: 203.6, 162.96, 162.93, 141.4, 140.2, 139.1, 132.3, 131.9, 130.8, 130.6, 130.3, 130.2, 130.0, 129.1, 128.8, 128.7, 128.6, 128.5, 127.8, 126.5, 123.9 (q, $^{1}J_{C\text{-}F}$ = 289.9 Hz), 113.2, 81.5-80.9 (m), 44.2, 31.5; ^{19}F NMR (376 MHz, $CDCl_3$) δ: -75.9; HRMS (ESI) m/z: $[M + H]^+$ Calcd for $C_{32}H_{24}F_6IO_2$ 681.0725; Found 681.0726.

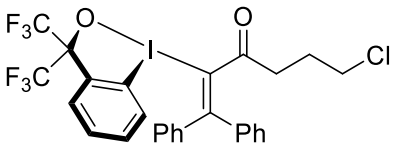

2-(3,3-Bis(trifluoromethyl)-1λ^3-benzo[*d*][1,2]iodaoxol-1(3*H*)-yl)-6-chloro-1,1-diphenylhex-1-en-3-one (3y): Procedure B; Orange solid (92 mg, 70% yield); R_f 0.35 (hexane/EtOAc = 7/3); m.p. 177-179 °C; ^{1}H NMR (400 MHz, $CDCl_3$) δ: 7.81-7.77 (m, 1H), 7.74-7.70 (m, 1H), 7.67-7.61 (m, 2H), 7.49-7.32 (m, 4H), 7.28-7.22 (m, 4H), 7.10-7.08 (m, 2H), 3.34 (t, *J* = 6.2 Hz, 2H), 2.48 (t, *J* = 7.0 Hz, 2H), 1.93-1.86 (m, 2H); ^{13}C NMR (100 MHz, $CDCl_3$) δ: 202.9, 163.1, 141.5, 139.2, 132.6, 132.0, 130.9, 130.8, 130.5, 130.3, 130.0, 129.9, 129.2, 128.8, 128.7, 127.9, 123.9 (q, $^1J_{C\text{-}F}$ = 289.8 Hz), 113.1, 81.5-80.9 (m), 44.2, 39.0, 27.4; ^{19}F NMR (376 MHz, $CDCl_3$) δ: -76.0; HRMS (ESI) m/z: $[M + H]^+$ Calcd for $C_{27}H_{21}ClF_6IO_2$ 653.0179; Found 653.0178.

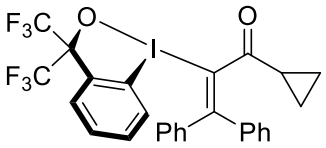

2-(3,3-Bis(trifluoromethyl)-1λ^3-benzo[*d*][1,2]iodaoxol-1(3*H*)-yl)-1-cyclopropyl-3,3-diphenylprop-2-en-1-one (3z): Procedure B; Yellow solid (96 mg, 78% yield); R_f 0.2 (hexane/EtOAc = 7/3); m.p. 191-193 °C; ^{1}H NMR (500 MHz, $CDCl_3$) δ: 7.83 (d, *J* = 7.4 Hz, 1H), 7.75 (dd, J = 8.0, 1.0 Hz, 1H), 7.65-7.58 (m, 2H), 7.47-7.44 (m, 1H), 7.41-7.35 (m, 3H), 7.30-7.26 (m, 4H), 7.13-7.11 (m, 2H), 1.83-1.78 (m, 1H), 1.06-1.03 (m, 2H), 0.76-0.72 (m, 2H); ^{13}C NMR (100 MHz, $CDCl_3$) δ: 203.1, 163.0, 141.8, 139.3, 132.3, 131.9, 131.2, 130.63, 130.61, 130.5, 130.4, 130.2, 128.9, 128.7, 128.6, 127.9, 123.9 (q, $^1J_{C\text{-}F}$ = 290.5 Hz), 112.9, 81.4-80.8 (m), 22.3, 14.1; ^{19}F NMR (282 MHz, $CDCl_3$) δ: -76.0; HRMS (ESI) m/z: $[M + H]^+$ Calcd for $C_{27}H_{20}F_6IO_2$ 617.0412; Found 617.0411.

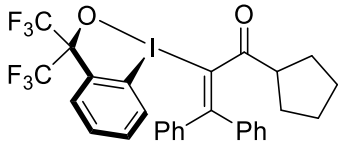

2-(3,3-Bis(trifluoromethyl)-1λ^3-benzo[*d*][1,2]iodaoxol-1(3*H*)-yl)-1-cyclopentyl-3,3-diphenylprop-2-en-1-one (3aa): Procedure B; Yellow solid (94 mg, 73% yield); R_f 0.25 (hexane/EtOAc = 4/1); m.p. 205-207 °C; ^{1}H NMR (400 MHz, $CDCl_3$) δ: 7.85-7.82 (m, 1H), 7.79-7.77 (brs, 1H), 7.64-7.59 (m, 2H), 7.43-7.37 (m, 3H), 7.36-7.31 (m, 1H), 7.28-7.21 (m, 4H), 7.08-7.06 (m, 2H), 2.83-2.76 (m, 1H), 1.68-1.53 (m, 6H), 1.49-1.40 (m, 2H); ^{13}C NMR (100 MHz, $CDCl_3$) δ: 208.7, 161.8, 141.6, 139.0, 132.3, 131.9, 130.7, 130.5, 130.3, 130.1, 130.0, 129.8, 129.0, 128.8, 128.7, 128.3, 123.9 (q, $^1J_{C\text{-}F}$ = 289.6 Hz), 113.2, 81.8-80.7 (m), 51.2, 31.9, 26.5; ^{19}F NMR (376 MHz, $CDCl_3$) δ: -76.0; HRMS (ESI) m/z: $[M + H]^+$ Calcd for $C_{29}H_{24}F_6IO_2$ 645.0725; Found 645.0725.

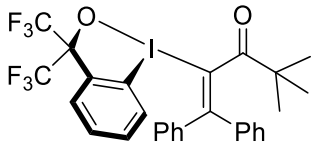

2-(3,3-Bis(trifluoromethyl)-1λ^3-benzo[*d*][1,2]iodaoxol-1(3*H*)-yl)-4,4-dimethyl-1,1-diphenylpent-1-en-3-one (3ab): Procedure B; Yellow solid (52 mg, 41% yield); R_f 0.2 (hexane/EtOAc = 4/1); m.p. 205-207 °C; ^{1}H NMR (400 MHz, $CDCl_3$) δ: 8.24 (d, J = 8.2 Hz, 1H), 7.70-7.63 (m, 2H), 7.56 (t, J = 7.1 Hz, 1H), 7.37-7.23 (m, 8H), 7.08-7.06 (m, 2H), 1.02 (s, 9H); ^{13}C NMR (100 MHz, $CDCl_3$) δ: 212.1, 156.6, 140.9, 138.9, 132.3, 131.7, 130.4, 130.0, 129.9, 129.8, 129.2, 128.8, 128.7, 128.62, 128.58, 124.3, 123.7 (q, $^1J_{C\text{-}F}$ = 289.3 Hz), 113.0, 81.6-80.5 (m), 45.2, 27.7; ^{19}F NMR (376 MHz, $CDCl_3$) δ: -76.1; HRMS (ESI) m/z: $[M + H]^+$ Calcd for $C_{28}H_{24}F_6IO_2$ 633.0725; Found 633.0728.

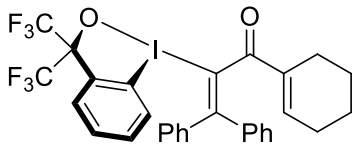

2-(3,3-Bis(trifluoromethyl)-1λ^3-benzo[*d*][1,2]iodaoxol-1(3*H*)-yl)-1-(cyclohex-1-en-1-yl)-3,3-diphenylprop-2-en-1-one (3ac): Procedure B; Yellow solid (86 mg, 66% yield); R_f 0.15 (hexane/EtOAc = 4/1); m.p. 179-181 °C; ^{1}H NMR (400 MHz, $CDCl_3$) δ: 8.00-7.95 (m, 1H), 7.76-7.74 (m, 1H), 7.62-7.56 (m, 2H), 7.36-7.24 (m, 6H), 7.17-7.09 (m, 4H), 6.84-6.82 (m, 1H), 2.12-2.04 (m, 4H), 1.48-1.38 (m, 4H); ^{13}C NMR (100 MHz, $CDCl_3$) δ: 196.1, 161.5, 144.7, 141.4, 139.7, 138.4, 132.4, 131.9, 130.5, 130.1, 129.8, 129.5, 128.9, 128.7, 128.68, 128.64, 126.7, 123.9 (q, $^1J_{C\text{-}F}$ = 289.7 Hz), 113.8, 81.5-81.0 (m), 26.5, 23.6, 21.8, 21.4; ^{19}F NMR (376 MHz, $CDCl_3$) δ: -76.1; HRMS (ESI) m/z: $[M + H]^+$ Calcd for $C_{30}H_{24}F_6IO_2$ 657.0725; Found 657.0727.

Product Transformations

Suzuki–Miyaura coupling reaction

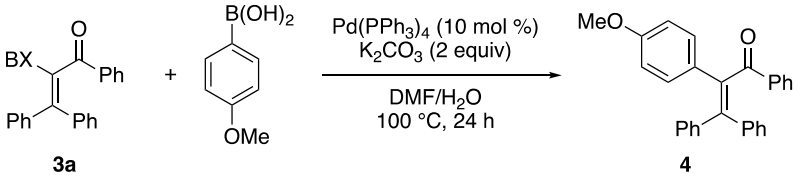

2-(4-Methoxyphenyl)-1,3,3-triphenylprop-2-en-1-one (4): Under argon atmosphere, a 10 mL Schlenk tube equipped with a stir bar was charged with **3a** (130.5 mg, 0.20 mmol), 4-methoxyphenylboronic acid (45.6 mg, 0.30 mmol), $Pd(PPh_3)_4$ (11.6 mg, 0.010 mmol), and an aqueous solution of K_2CO_3 (1 M, 0.40 mL, 0.40 mmol), followed by the addition of DMF (2 mL). The resulting mixture was stirred in an oil bath at 100 °C (bath temperature) for 24 h. The mixture was cooled to room temperature, diluted with Et_2O (20 mL), and washed with H_2O (10 mL) and brine (10 mL). The organic layer was dried over $MgSO_4$ and concentrated under reduced pressure. The

residue was purified by flash column chromatography on silica gel (eluent: hexane/Et_2O = 50/1) to afford the title compound (**4**) as a yellow oil (49 mg, 63% yield); R_f 0.67 (hexane/EtOAc = 4/1); ^1H NMR (500 MHz, $CDCl_3$) δ: 7.92 (d, *J* = 7.5 Hz, 2H), 7.40 (t, *J* = 7.3 Hz, 1H), 7.31 (t, *J* = 7.7 Hz, 2H), 7.21-7.07 (m, 10H), 7.01 (d, *J* = 8.7 Hz, 2H), 6.67 (d, *J* = 8.7 Hz, 2H), 3.72 (s, 3H); ^{13}C NMR (125 MHz, $CDCl_3$) δ: 199.4, 158.8, 143.9, 142.0, 141.3, 139.3, 138.0, 132.7, 131.4, 131.25, 131.20, 130.15, 129.8, 128.4, 128.14, 128.10, 128.0, 127.6, 114.0, 55.2; HRMS (ESI) m/z: $[M + H]^+$ Calcd for $C_{28}H_{23}O_2$ 391.1698; Found 391.1698.

Sonogashira coupling reaction

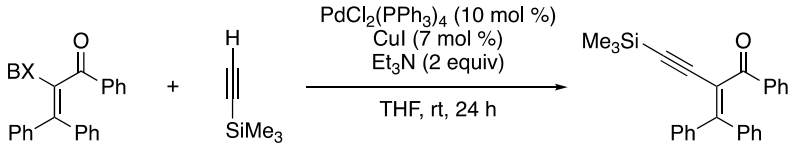

2-(Diphenylmethylene)-1-phenyl-4-(trimethylsilyl)but-3-yn-1-one (5): Under argon atmosphere, a 10 mL Schlenk tube equipped with a stir bar was charged with **3a** (130.5 mg, 0.20 mmol), $PdCl_2(PPh_3)_2$ (14 mg, 0.020 mmol), CuI (2.7 mg, 0.014 mmol), and THF (1 mL). Trimethylsilylacetylene (39.5 mg, 0.40 mmol) and Et_3N (40.5 mg, 0.40 mmol) were added, and the resulting mixture was stirred at room temperature for 24 h. The reaction mixture was diluted with Et_2O (20 mL) and washed with H_2O (10 mL) and brine (10 mL). The organic layer was dried over $MgSO_4$ and concentrated under reduced pressure. The residue was purified by flash column chromatography on silica gel (eluent: hexane/EtOAc = 100/1) to afford the title compound (5) as a yellow oil (58 mg, 76% yield); R_f 0.37 (hexane/EtOAc = 20/1); ^1H NMR (400 MHz, $CDCl_3$) δ: 7.96-7.94 (m, 2H), 7.62-7.59 (m, 2H), 7.48-7.44 (m, 1H), 7.39-7.33 (m, 5H), 7.16-7.05 (m, 5H), 0.08 (s, 9H); ^{13}C NMR (100 MHz, $CDCl_3$) δ: 194.2, 154.3, 139.9, 139.8, 136.3,

133.2, 130.5, 130.1, 129.9, 129.1, 128.7, 128.3, 128.1, 127.8, 121.3, 103.8, 102.9, -0.4; HRMS (ESI) m/z: $[M + H]^+$ Calcd for $C_{26}H_{25}OSi$ 381.1675; Found 381.1674.

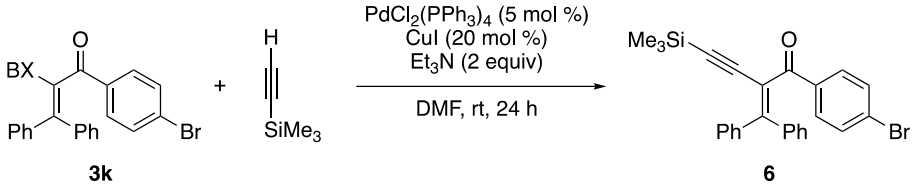

3k **6**

1-(4-Bromophenyl)-2-(diphenylmethylene)-4-(trimethylsilyl)but-3-yn-1-one (6): The reaction of **3k** (160.9 mg, 0.22 mmol) and trimethylsilylacetylene (0.40 mmol) was performed with modification of the above procedure with respect to the catalyst loadings and the solvent (DMF in place of THF). Purification of the crude product by flash column chromatography on silica gel (eluent: hexane) afforded the title compound (**6**) as a yellow oil (66 mg, 72% yield); R_f 0.75 (hexane/EtOAc = 10/1); ^{1}H NMR (500 MHz, $CDCl_3$) δ: 7.83-7.80 (m, 2H), 7.60-7.58 (m, 2H), 7.50-7.48 (m, 2H), 7.38-7.36 (m, 3H), 7.19-7.11 (m, 3H), 7.05-7.03 (m, 2H), 0.09 (s, 9H); ^{13}C NMR (100 MHz, $CDCl_3$) δ: 193.1, 154.8, 139.62, 139.60, 135.1, 131.7, 131.3, 130.5, 130.0, 129.2, 128.9, 128.4, 128.2, 127.8, 120.7, 104.1, 102.6, -0.4; HRMS (ESI) m/z: $[M + H]^+$ Calcd for $C_{26}H_{24}BrOSi$ 459.0780; Found 459.0773.

4.5. References

1. (a) Engel, D. A.; Dudley, G. B., *Organic & Biomolecular Chemistry* **2009,** *7* (20), 4149-4158; (b) Cadierno, V.; Crochet, P.; García-Garrido, S. E.; Gimeno, J., *Dalton Transactions* **2010,** *39* (17), 4015-4031; (c) Justaud, F.; Hachem, A.; Gree, R., *Eur. J. Org. Chem.* **2020,** *n/a* (n/a); (d) Swaminathan, S.; Narayanan, K. V., *Chem. Rev.* **1971,** *71* (5), 429-438.

2. Engel, D. A.; Dudley, G. B., *Org. Lett.* **2006,** *8* (18), 4027-4029.

3. Egi, M.; Yamaguchi, Y.; Fujiwara, N.; Akai, S., *Org. Lett.* **2008,** *10* (9), 1867-1870.

4. Stefanoni, M.; Luparia, M.; Porta, A.; Zanoni, G.; Vidari, G., *Chemistry – A European Journal* **2009,** *15* (16), 3940-3944.

5. Du, C.; Wang, X.; Jin, S.; Shi, H.; Li, Y.; Pang, Y.; Liu, Y.; Cheng, M.; Guo, C.; Liu, Y., *Asian Journal of Organic Chemistry* **2016,** *5* (6), 755-762.

6. Ye, L.; Zhang, L., *Org. Lett.* **2009,** *11* (16), 3646-3649.

7. Zhao, M.; Mohr, J. T., *Tetrahedron* **2017,** *73* (29), 4115-4124.

8. de Haro, T.; Nevado, C., *Chem. Commun.* **2011,** *47* (1), 248-249.

9. Collins, B. S. L.; Suero, M. G.; Gaunt, M. J., *Angew. Chem. Int. Ed.* **2013,** *52* (22), 5799-5802.

10. Um, J.; Yun, H.; Shin, S., *Org. Lett.* **2016,** *18* (3), 484-487.

11. (a) Eisenberger, P.; Gischig, S.; Togni, A., *Chemistry – A European Journal* **2006,** *12* (9), 2579-2586; (b) Kieltsch, I.; Eisenberger, P.; Togni, A., *Angew. Chem. Int. Ed.* **2007,** *46* (5), 754-757.

12. Egami, H.; Ide, T.; Fujita, M.; Tojo, T.; Hamashima, Y.; Sodeoka, M., *Chemistry – A European Journal* **2014,** *20* (38), 12061-12065.

13. Xiong, Y.-P.; Wu, M.-Y.; Zhang, X.-Y.; Ma, C.-L.; Huang, L.; Zhao, L.-J.; Tan, B.; Liu, X.-Y., *Org. Lett.* **2014,** *16* (3), 1000-1003.

14. Banerjee, S.; Ambegave, S. B.; Mule, R. D.; Senthilkumar, B.; Patil, N. T., *Org. Lett.* **2020,** *22* (12), 4792-4796.

15. Trost, B. M.; Luan, X., *J. Am. Chem. Soc.* **2011,** *133* (6), 1706-1709.

16. Lin, Y.; Kong, W.; Song, Q., *Org. Lett.* **2016,** *18* (15), 3702-3705.

17. Chen, S.; Wang, J., *The Journal of organic chemistry* **2007,** *72* (13), 4993-4996.

18. Moran, W. J.; Rodríguez, A., *Organic & Biomolecular Chemistry* **2012,** *10* (43), 8590-8592.

19. Puri, S.; Thirupathi, N.; Sridhar Reddy, M., *Org. Lett.* **2014,** *16* (20), 5246-5249.

20. Zhu, H.-T.; Fan, M.-J.; Yang, D.-S.; Wang, X.-L.; Ke, S.; Zhang, C.-Y.; Guan, Z.-H., *Organic Chemistry Frontiers* **2015,** *2* (5), 506-509.

21. Kramer, S.; Friis, S. D.; Xin, Z.; Odabachian, Y.; Skrydstrup, T., *Org. Lett.* **2011,** *13* (7), 1750-1753.

22. Ding, W.; Chai, J.; Wang, C.; Wu, J.; Yoshikai, N., *J. Am. Chem. Soc.* **2020,** *142* (19), 8619-8624.

23. Zhang, X.; Teo, W. T.; Chan, P. W. H., *Org. Lett.* **2009,** *11* (21), 4990-4993.

24. Song, X.-R.; Song, B.; Qiu, Y.-F.; Han, Y.-P.; Qiu, Z.-H.; Hao, X.-H.; Liu, X.-Y.; Liang, Y.-M., *The Journal of Organic Chemistry* **2014,** *79* (16), 7616-7625.

25. Song, X.-R.; Han, Y.-P.; Qiu, Y.-F.; Qiu, Z.-H.; Liu, X.-Y.; Xu, P.-F.; Liang, Y.-M., *Chemistry – A European Journal* **2014,** *20* (38), 12046-12050.

26. Zheng, H.; Lejkowski, M.; Hall, D. G., *Chemical Science* **2011,** *2* (7), 1305-1310.

27. Cheng, X.; Wang, Z.; Quintanilla, C. D.; Zhang, L., *J. Am. Chem. Soc.* **2019,** *141* (9), 3787-3791.

28. Kitazawa, T.; Minowa, T.; Mukaiyama, T., *Chem. Lett.* **2006,** *35* (9), 1002-1003.

29. Yoshida, M.; Hayashi, M.; Shishido, K., *Org. Lett.* **2007,** *9* (9), 1643-1646.

30. Kotani, S.; Kukita, K.; Tanaka, K.; Ichibakase, T.; Nakajima, M., *The Journal of Organic Chemistry* **2014,** *79* (11), 4817-4825.

31. Dong, Y.-W.; Wang, G.-W.; Wang, L., *Tetrahedron* **2008,** *64* (44), 10148-10154.

32. CCDC 2046320 (**3a**) provides supplementary crystallographic data for this paper. These data can be obtained free of charge from The Cambridge Crystallographic Data Centre

List of Publications

1. **Laskar, R. A.**, Yoshikai, N. Cobalt-Catalyzed N–H Imine-Directed Arene C–H Benzylation with Benzyl Phosphates. *The Journal of Organic Chemistry* **2019**, *84*, 13172-13178**.** DOI: 10.1021/acs.joc.9b01775.

2. **Laskar, R. A.**, Ding, W.; Yoshikai, N. Iodo(III)-Meyer–Schuster Rearrangement of Propargylic Alcohols Promoted by Benziodoxole Triflate. *Org. Lett.* **2021**, 23, 1113–1117. DOI: 10.1021/acs.orglett.1c00039.